195

NUREG/CR-4541

Experimental Assessment of the Sealing Effectiveness of Rock Fracture Grouting

Prepared by A. Schaffer, J. J. K. Daemen

Department of Mining and Geological Engineering
University of Arizona

Prepared for
U.S. Nuclear Regulatory
Commission

BEST COPY AVAILABLE

NOTICE

This report was prepared as an account of work sponsored by an agency of the United States Government. Neither the United States Government nor any agency thereof, or any of their employees, makes any warranty, expressed or implied, or assumes any legal liability of responsibility for any third party's use, or the results of such use, of any information, apparatus, product or process disclosed in this report, or represents that its use by such third party would not infringe privately owned rights.

NOTICE

Availability of Reference Materials Cited in NRC Publications

Most documents cited in NRC publications will be available from one of the following sources:

1. The NRC Public Document Room, 1717 H Street, N.W.
   Washington, DC 20555
2. The Superintendent of Documents, U.S. Government Printing Office, Post Office Box 37082, Washington, DC 20013-7082
3. The National Technical Information Service, Springfield, VA 22161

Although the listing that follows represents the majority of documents cited in NRC publications, it is not intended to be exhaustive.

Referenced documents available for inspection and copying for a fee from the NRC Public Document Room include NRC correspondence and internal NRC memoranda; NRC Office of Inspection and Enforcement bulletins, circulars, information notices, inspection and investigation notices; Licensee Event Reports; vendor reports and correspondence; Commission papers; and applicant and licensee documents and correspondence.

The following documents in the NUREG series are available for purchase from the GPO Sales Program: formal NRC staff and contractor reports, NRC sponsored conference proceedings, and NRC booklets and brochures. Also available are Regulatory Guides, NRC regulations in the *Code of Federal Regulations*, and *Nuclear Regulatory Commission Issuances*.

Documents available from the National Technical Information Service include NUREG series reports and technical reports prepared by other federal agencies and reports prepared by the Atomic Energy Commission, forerunner agency to the Nuclear Regulatory Commission.

Documents available from public and special technical libraries include all open literature items, such as books, journal and periodical articles, and transactions. *Federal Register* notices, federal and state legislation, and congressional reports can usually be obtained from these libraries.

Documents such as theses, dissertations, foreign reports and translations, and non-NRC conference proceedings are available for purchase from the organization sponsoring the publication cited.

Single copies of NRC draft reports are available free, to the extent of supply, upon written request to the Division of Technical Information and Document Control, U.S. Nuclear Regulatory Commission, Washington, DC 20555.

Copies of industry codes and standards used in a substantive manner in the NRC regulatory process are maintained at the NRC Library, 7920 Norfolk Avenue, Bethesda, Maryland, and are available there for reference use by the public. Codes and standards are usually copyrighted and may be purchased from the originating organization or, if they are American National Standards, from the American National Standards Institute, 1430 Broadway, New York, NY 10018.

BEST COPY AVAILABLE

NUREG/CR-4541

Experimental Assessment of the Sealing Effectiveness of Rock Fracture Grouting

Manuscript Completed: December 1986
Date Published: March 1987

Prepared by
A. Schaffer, J. J. K. Daemen

Department of Mining and Geological Engineering
University of Arizona
Tucson, AZ 85721

Prepared for
Division of Engineering Safety
Office of Nuclear Regulatory Research
U.S. Nuclear Regulatory Commission
Washington, DC 20555
NRC FIN B6627
Under Contract No. NRC-04-78-271

BEST COPY AVAILABLE

ABSTRACT

The objective of this investigation is to determine the effectiveness of cement grouts as sealants of fractures in rock. Laboratory experiments have been conducted on seven 15-cm granite cubes containing saw cuts, three 23-cm diameter andesite cores containing induced tension cracks, and one 15-cm diameter marble core containing a natural fracture. Prior to grouting, the hydraulic conductivity of the fractures is determined under a range of normal stresses, applied in loading and unloading cycles, from 0 to 14 MPa (2000 psi). Grout is injected through an axial borehole, at a pressure of 1.2 to 8.3 MPa (180 to 1200 psi), pressure selected to provide a likely groutable fracture aperture, while the fracture is stressed at a constant normal stress. The fracture permeability is measured after grouting.

Flow tests on the ungrouted samples confirm the inverse relation between normal stress and fracture permeability. The equivalent aperture determined by these tests is a reliable indicator of groutability. Postgrouting permeability measurements as performed here, and frequently in practice, can be misleading, since incomplete grouting of fractures can result in major apparent reductions in permeability. The apparent permeability reduction is caused by grouting of a small area of a highly preferential flowpath directly adjacent to the hole used for grouting and for permeability testing. Experimental results confirm claims in the literature that ordinary portland cement inadequately penetrates fine fractures.

BEST COPY AVAILABLE

BLANK PAGE

TABLE OF CONTENTS

	Page
ABSTRACT	iii
LIST OF FIGURES	viii
LIST OF TABLES	x
ACKNOLEDGMENTS	xi
LIST OF SYMBOLS	xiii
EXECUTIVE SUMMARY	1
1. Introduction	1
2. Procedures	3
2.1. Cement Grout Selection, Preparation and Uniaxial Compression Strength Testing	3
2.2. Bleed Testing	3
2.3. Rock Samples and Their Preparation	3
2.4. Determination of Hydraulic Conductivity	4
2.5. Fracture Grouting	4
3. Experimental Results	4
3.1. Uniaxial Testing	4
3.2. Bleed Testing	4
3.3. Rock Sample 1 Testing	4
3.4. Rock Sample 3 Testing	5
3.5. Rock Sample 4 Testing	5
3.6. Rock Sample 5 Testing	5
3.7. Rock Sample 6 Testing	5
3.8. Rock Sample 8 Testing	6
3.9. Rock Sample 9 Testing	6
3.10. Rock Sample 10 Testing	6
3.11. Rock Sample 10 Testing	6
4. Conclusions	6
5. Research Recommendations	8
CHAPTER ONE: INTRODUCTION	11
1.1 Objective	11
1.2 Scope and Limitations	12
1.3 Organization	12
1.4 Rock Mass Sealing Contract No. NRC-04-78-271 - Reports Issued	12
CHAPTER TWO: FLUID FLOW THROUGH ROCK FRACTURES	16
2.1 Fracture Flow Theory and Experiments	16
2.2 Laboratory Studies of Fluid Flow Through a Single Fracture	19

BEST COPY AVAILABLE

TABLE OF CONTENTS--Continued

		Page
2.3	Field Permeability Tests Used in Grouting	27
	2.3.1 Lugeon Test	27
	2.3.2 Other Field Permeability Test Methods	31
	2.3.3 Assessment of Grouting	31
CHAPTER THREE:	ROCK FRACTURE GROUTING	34
3.1	Introduction	34
3.2	Grout Mix Selection	38
3.3	Cement-Bentonite Grout Mixes	41
3.4	Grout Quality	44
3.5	Filter Blockage of Cement Based Grouts	45
3.6	Grouting Pressures	49
3.7	Fracture Grout Penetration Model Studies and Analyses	50
CHAPTER FOUR:	EXPERIMENTAL APPARATUS AND PROCEDURES	55
4.1	Apparatus	55
4.2	Cement Preparation and Uniaxial Compressive Strength Testing	55
4.3	Bleed Testing	61
4.4	Rock Sample Preparation	61
4.5	Determination of Hydraulic Conductivity	62
4.6	Fracture Grouting	64
CHAPTER FIVE:	EXPERIMENTAL RESULTS	66
5.1	Uniaxial Compressive Strength Testing of Cement Grouts	66
5.2	Bleed Testing	66
5.3	Fracture Flow and Grouting Tests	68
	5.3.1 Sample 1	68
	5.3.2 Sample 2	70
	5.3.3 Sample 3	70
	5.3.4 Sample 4	73
	5.3.5 Sample 5	73
	5.3.6 Sample 6	77
	5.3.7 Sample 7	77
	5.3.8 Sample 8	81
	5.3.9 Sample 9	81
	5.3.10 Sample 10	81
	5.3.11 Sample 11	85
5.4	Influence of Normal Stress on Fracture Flow	85
CHAPTER SIX:	CONCLUSIONS AND FURTHER RESEARCH RECOMMENDATIONS	90
6.1	Conclusions	90
	6.1.1 Grout Characterization Testing	90
	6.1.2 Fracture Permeability Testing	91
	6.1.3 Grouting Implicaitons	91
6.2	Research Recommendations	93

COPY AVAILABLE

TABLE OF CONTENTS--Continued

		Page
REFERENCES		97
APPENDIX A:	GROUT COMPOSITION AND UNIAXIAL COMPRESSIVE STRENGTH TEST RESULTS	115
APPENDIX B:	BLEED TEST RESULTS	127
APPENDIX C:	FRACTURE FLOW STRESS-PERMEABILITY TEST RESULTS	135
APPENDIX D:	BIBLIOGRAPHIES, TEXTBOOKS, AND PROCEDDINGS OF MEETINGS ON GROUTING	177

BEST COPY AVAILABLE

LIST OF FIGURES

Figure		Page
2.1	Range of validity of flow laws proposed by Louis	21
2.2	Typical results of field water test	28
3.1	Effect of water-cement ratio on grout properties	39
3.2	Relationship between bleeding and water-cement ratio	42
3.3	Effects of water-cement ratio on Marsh funnel viscosity	43
3.4	Grain size distributions for three types of cement	46
4.1	Schematic drawing of equipment used for permeability testing and fracture grouting	56
4.2	Laboratory set-up for permeability testing of rock fracture	57
4.3	Laboratory set-up for rock fracture grouting	58
4.4	Cutaway platens used to transmit load	59
4.5	Lower platen and grout tube	60
4.6	A 222 mm (9 inch) diameter core sample of Grande Basaltic Andesite ready for point loading	63
5.1	Sample 1 (Charcoal granite) after grouting	69
5.2	Sample 2 (Charcoal granite) after grouting	71
5.3	Loss of grout through an induced tension crack, sample 3, Charcoal granite	74
5.4	Close-up of extended tension crack	74
5.5	Sample 4 (Oracle Ridge Marble) after grouting	75
5.6	Sample 5 (Grande basaltic andesite) after grouting	76
5.7	Sample 6 (Grande basaltic andesite) after grouting	78
5.8	Sample 7 (Grande basaltic andesite) after second grouting	80
5.9	Close-up of sample 7 showing minor shrinkage cracks in large voids	80

BEST COPY AVAILABLE

LIST OF FIGURES--Continued

Figure		Page
5.10	Sample 8 (Charcoal granite) after grouting	82
5.11	Sample 9 (Charcoal granite) after grouting	83
5.12	Sample 10 (Charcoal granite) after grouting	84
5.13	Sample 11 (Charcoal granite) after grouting	86

BEST COPY AVAILABLE

LIST OF TABLES

Table		Page
2.1	Degree of Contact Area for Fractures in Granite and Marble	22
2.2	Typical Lugeon Values and Joint Thicknesses	30
5.1	Uniaxial Compressive Strengths and Total Bleed Capacities of Grout Mixes	67
5.2	Permeability Test Results Before and After Grouting for Sample 1, Charcoal Granite	69
5.3	Permeability Test Results Before and After Grouting for Sample 2, Charcoal Granite	71
5.4	Permeability Test Results Before and After Grouting for Sample 3, Charcoal Granite	72
5.5	Permeability Test Results Before and After Grouting for Sample 4, Oracle Ridge Marble	75
5.6	Permeability Test Results Before and After Grouting for Sample 5, Grande Basaltic Andesite	76
5.7	Permeability Test Results Before and After Grouting for Sample 6, Grande Basaltic Andesite	78
5.8	Permeability Test Results Before and After Grouting for Sample 7, Grande Basaltic Andesite	79
5.9	Permeability Test Results Before and After Grouting for Sample 8, Charcoal Granite	82
5.10	Permeability Test Results Before and After Grouting for Sample 9, Charcoal Granite	83
5.11	Permeability Test Results Before and After Grouting for Sample 10, Charcoal Granite	84
5.12	Permeability Test Results Before and After Grouting for Sample 11, Charcoal Granite	86

BEST COPY AVAILABLE

ACKNOWLEDGMENTS

The research reported on has been performed by the University of Arizona, Department of Mining and Geological Engineering, for the U.S. Nuclear Regulatory Commission (NRC). Project monitor for the NRC is Mr. Jacob Philip. The project is under Mr. Leon L. Beratan, Chief, Earth Sciences Branch, Division of Radiation Programs and Earth Sciences, Office of Nuclear Regulatory Research.

Dr. Jaak J.K. Daemen, Associate Professor, Department of Mining and Geological Engineering, University of Arizona, is the Principal Investigator. Dr. James G. McCray, Acting Director, Nuclear Fuel Cycle Research Program, Department of Nuclear and Energy Engineering, University of Arizona, has provided project management assistance. Andrew Schaffer has performed the experimental and theoretical work as part of his M.S. Degree requirements. Experimental assistance has been provided by laboratory technicians Jon W. Graham, Warren T. Lewis and Vince Realmuto. Michael Porter has assembled, typed and produced the report.

We gratefully acknowledge the assistance of the Dowell Division of Dow Chemical, U.S.A., in providing cement and additives, and especially the technical advice provided by Erik B. Nelson.

American Colloid Company supplied C/S Granular bentonite.

BEST COPY AVAILABLE

BLANK PAGE

LIST OF SYMBOLS

A - rate of change of the contact area, as a function of normal stress P

b - mean joint spacing

C - constant used in cubic law

e - equivalent parallel plate (fracture) aperture

e_m - fracture aperture at the reference normal stress P_m

f - flow reduction factor used in cubic law

h - hydraulic head

H - root mean square value of the asperity height distribution

H_1, H_2 - excess pressure head at beginning and end of falling head test

K_1 - fracture hydraulic conductivity at unit normal stress

K_f - fracture hydraulic conductivity

K_j - hydraulic conductivity through smooth, parallel plates

K_m - fracture hydraulic conductivity at minimum or at reference normal stress P_m

K_o - fracture hydraulic conductivity at zero normal stress

K_s - hydraulic conductivity parallel to joint set

L - length of fracture (flowpath)

P - normal stress across fracture

P_m - minimum (reference) fracture normal stress

P_{max} - the "healing" normal stress, at which the fracture permeability reduces to zero

Q - fluid flow rate

R, r - outer and inner radius of a radial flowpath

r - correlation coefficient

r_b - buret radius

R_e - Reynolds number

S - surface roughness index

t_1, t_2 - time at beginning and end of test

W - width of fracture (flowpath)

Y - mean height of fracture asperities

$\alpha, \alpha_1, \alpha_2$ - slope of log (conductivity) vs. log (pressure) diagrams

ϵ, ϵ_1 - slope of log (conductivity) vs. fracture stress

γ - unit fluid weight

μ - kinematic viscosity

BEST COPY AVAILABLE

EXECUTIVE SUMMARY

1. Introduction

Current plans for the disposal of high-level nuclear waste call for its isolation in underground repositories. Fractures in the rock mass surrounding a repository and its shafts, access drifts, emplacement rooms and holes, and exploratory holes, may provide preferential flowpaths for the seepage of groundwater. In order to reduce their permeability, such cracks may have to be sealed. The likelihood that extensive or at least local grouting will be required as part of repository sealing has been noted in numerous publications addressing high level waste repository closing (e.g. Koplick et al., 1979; Gyenge, 1980a,b; Yuen and Boyd, 1982; Kelsall et al., 1982; Kelsall et al., 1983; Mott, Hay & Anderson, 1983; Kelsall et al., 1985a,b,c), as well as in studies dealing more specifically with grouting performance (e.g. Crawford and Groskopf, 1984; Lau and Crawford, 1986). The most explicit and detailed use of fracture grouting for repository sealing probably is given in the conceptual seal designs for the Nevada Nuclear Waste Storage Investigations Project (Fernandez and Freshley, 1984; Fernandez, 1985).

Rule 10 CFR 60 (U.S. Nuclear Regulatory Commission, 1983, 1985) requires, in addition to the seals for shafts and boreholes (§60.134), that "the design of the underground facility shall provide for control of water or gas intrusion" (§60.133,d) and that "the design of the underground facility shall incorporate excavation methods that will limit the potential for creating a preferential pathway for groundwater or radioactive waste migration to the accessible environment" (§60.133,f, U.S. Nuclear Regulatory Commission, 1983), or "... that will limit the potential for creating a preferential pathway for groundwater to contact the waste packages or radionuclide migration to the accessible environment" (unsaturated zone amendment, §60.133,f, U.S. Nuclear Regulatory Commission, 1985).

Of particular concern within the context of repository sealing are fractures within the damaged zone directly adjacent to excavations, especially shafts and access drifts, at locations where primary seals or plugs are to be installed.* A fractured zone in the rock surrounding main seals can readily provide a dominant bypass flowpath

---

*It is recognized that the most severe environmental conditions of the type referenced here are most likely to be encountered around the HLW package emplacement holes, especially if a swelling packing were to be used, or if pressurized steam or gas were generated. The contract under which this work is performed does not address that rock barrier, and it is uncertain whether any performance will be expected of that barrier, or whether grouting in that area would be considered.

BEST COPY AVAILABLE

around the seals, thereby negating the effectiveness of the plug. The concern about bypass flowpaths is the main reason why grouting of the rock surrounding seals is virtually always required in underground mining and construction (e.g. Garrett and Campbell Pitt, 1961; Wittke, 1973; Loofbourow, 1973; National Coal Board, 1982; Moller et al., 1983; Chamber of Mines of South Africa, 1983; Auld, 1983). Considerable uncertainty remains about the optimum grouting conditions, especially with regard to the preferable injection pressures. A controversy about grouting pressures has persisted for a long time, not only in deep underground grouting, but possibly even more pronounced in conventional surface dam foundation grouting. Deere (1982) lists numerous references on this topic, particularly with regard to high-pressure European grouting practice vs. American low-pressure grouting practice, although he also argues that the differences might be less pronounced than commonly perceived. The closely related topic as to whether to use thick or thin grout mixes has been discussed by Deere and Lombardi (1985).

The experimental work reported on here addresses primarily the issues of grout distribution along a fracture perpendicular to an applied stress, and the influence of grout injection pressure (relative to the applied pressure) on penetration and sealing effectiveness of the grout. The main objective of this investigation is to assess the watertightness of grouted fractures in rock, using permeability measurements. Ordinary portland cement grout has been chosen as a grouting material since it is commonly used. It is widely accepted to be a durable sealant, although, with the cumulation of decades of experience, serious concerns about cement grout stability have been expersed (e.g. Rissler, as quoted by Gale and Reardon, 1984; Osende, 1985, who identifies deterioration of high quality cement grouts in dam foundations within a decade after installation). Rock samples containing a single fracture have been subjected to a normal stress and pressure-grouted. Permeability measurements taken before and after grouting assess the reduction in permeability due to grouting. All experiments have been performed in the laboratory.

This research includes the characterization of cement-based grouts. Two sedimentation stable cement-bentonite mixes and three neat cement mixes have been designed. Uniaxial testing has been performed to determine the effect of bentonite on the grout compressive strength. Bleed testing has been performed to verify that the stable mixes were properly designed and prepared.

The relation between normal stress and permeability has been determined for the fractures to be grouted. The fractures are loaded, unloaded, and reloaded incrementally to obtain the dependence of permeability on normal stress and fracture deformation. This is illustrated with graphs of hydraulic conductivity versus normal stress.

The experimental apparatus has been designed to allow maintaining a constant normal stress across the fracture while permeability measurements and grouting are performed. Also important is the capability to vary the normal stress so that cyclic stress-permeability measurements can be obtained. A grout pump capable of

BEST COPY AVAILABLE

delivering small quantities of cement at high pressures is used to grout tight, laboratory-scale size fractures. It deserves pointing out that the system is stress-controlled, and that only an indirect assessment of the (average) fracture aperture is possible.

Normal loads are applied to the rock fracture using a 100 ton (90.7 metric ton) loading frame and hydraulic jacking system. The hydraulic system consists of a hand pump a shut-off valve, pressure gage, and either a 50 ton (45.4 metric ton) or 100 ton (90.7 metric ton) cylinder. Permeability testing is accomplished with a falling head permeameter.

The grout pump is a positive displacement piston pump with a capacity of 200 cc (12.2 cu in) and can pump at pressures in excess of 13.8 MPa (2000 psi).

2. Procedures

2.1. Cement Grout Selection, Preparation and Uniaxial Compression Strength Testing

Initially, two grout mixes were selected. Grout mix 1 has a 0.64 water-cement ratio by weight. Grout mix 2 has a water-cement ratio equal to 1.33 plus 2% bentonite by weight of water to keep it stable. Because of the difficulties encountered when attempting to grout the first four rock samples, a thinner grout mix was used in later samples. Grout mix 3 has a water-cement ratio of 2.0 plus 2.5% bentonite by weight of water to keep it stable. (Unstable) grout mix 4 has a water-cement ratio of 1.33 and (unstable) grout mix 5 a water-cement ratio of 2.0, corresponding to (stable) grout mixes 2 and 3, respectively. The uniaxial compressive strength of grout mix specimens was tested after 8 and 28 day curing.

2.2. Bleed Testing

Bleed testing of the stable mixes was performed to allow a comparison with their unstable counterparts.

2.3. Rock Samples and Their Preparation

The first three and the last four samples were 15 cm (6 in) cubes of Charcoal granite obtained from the Charcoal Black Quarry, St. Cloud, Minnesota. The specimens were cut in half. Sawcuts served as "fractures" to be grouted. The fourth sample was a 15 cm (6 in) diameter core of marblized limestone containing a natural fracture perpendicular to the cylinder axis. The fifth, sixth and seventh samples were 22.5 cm (9 in) diameter cores of Grande basaltic andesite. A single fracture normal to the cylinder axis was created in these samples by point loading. The top half of each sample then had a 2.5 cm (1 in) diameter hole drilled through it to allow for the placement of the grout tube.

BEST COPY AVAILABLE

2.4. Determination of Hydraulic Conductivity

A falling head permeameter is used to determine the hydraulic conductivity of the fractures. Each fracture is initially saturated and then incrementally loaded, unloaded, and reloaded to determine the dependence of permeability on normal stress. The hydraulic conductivity is calculated assuming smooth, parallel surfaces and laminar parallel fluid flow. The hydraulic conductivity and the parallel plate aperture are presented in tables. A semi-log plot of hydraulic conductivity versus normal stress illustrates their dependence. Best fit parameters are presented for various lows that have been proposed to express the dependency of hydraulic conductivity on normal stress.

2.5. Fracture Grouting

Upon completion of the permeability testing, each sample is grouted. A normal stress of 6.9 MPa (1000 psi) across the rock fracture was used for the first two samples. It was planned to grout at high normal stresses to simulate at-depth grouting conditions. However, the fracture apertures obtained under such stresses were too small to allow grouting.

Once the aperture to be grouted was determined, a grout mix was chosen. During grouting, the pressure was slowly increased to the desired maximum in order to avoid surges in the grout flow. The maximum pressure was then maintained for a period of 5 to 10 minutes. When grouting was completed the grout tube was removed and the borehole thoroughly cleaned. After two or more days curing, permeability measurements assess the effectiveness of the cement grout seal.

3. Experimental Results

3.1. Uniaxial Testing

The average uniaxial compressive strengths of all five grout mixes are given in Table 5.1.

3.2. Bleed Testing

The summary of the total bleed capacities (Table 5.1) reveals that bleeding is somewhat less than reported by others.

3.3. Rock Sample 1 Testing

Grouting was performed on sample 1 at a normal stress of 6.9 MPa (1000 psi) and a grout injection pressure of 2.76 MPa (400 psi) with grout mix 1. The rock fracture did accept grout over limited portions of its area. This fracture had an equivalent aperture of 69 μm. Permeability measurements to assess the effectiveness of the cement grout seal were not successful.

BEST COPY AVAILABLE

3.4. Rock Sample 3 Testing

The permeability testing shows the decrease in permeability with increasing normal stress and the irreversible decrease in permeability due to fracture deformation. Upon completion of permeability testing the normal stress on the fracture was reduced to 1.38 MPa (200 psi). Grout mix 2 was injected at a pressure of 1.24 MPa (180 psi). At this maximum injection pressure, a vertical crack developed through the upper half of the sample. This new crack filled well with grout. Water flowed through the crack at the rate of 30 ml in 26 seconds. No grout was taken by the original fracture. The only thing accomplished by grouting was damaging the rock by inducing a hydraulic fracture at a pressure of 1.24 MPa (180 psi), indicating a surprisingly small tensile strength for this (Charcoal granite) rock sample.

3.5. Rock Sample 4 Testing

Grouting for sample 4 was performed at a normal stress of 1.38 MPa (200 psi) and a grout injection pressure of 1.24 MPa (180 psi) with grout mix 2. A substantial decrease in hydraulic conductivity occurred. However, sample inspection revealed that only a small spot of cement had been emplaced.

3.6. Rock Sample 5 Testing

Grouting of sample 5 was performed with mix 1 at an injection pressure of 3.45 MPa (500 psi). The crack in the upper half of the sample filled well with grout, while no grout flowed through the crack in the lower half. Permeability measurements before and after grouting reveal a marked decrease in the rate of head drop.

3.7. Rock Sample 6 Testing

Permeability test results for a natural fracture in Grande basaltic andesite clearly show the decrease in permeability with increasing normal stress and the irreversible decrease in permeability due to fracture deformation. The normal stress on the fracture was reduced until only a slight, unmeasurable holding pressure was applied to the fracture in order to obtain the widest possible aperture for grouting. Grout mix 3 was chosen and a grout injection pressure of 2.07 MPa (300 psi) was used.

The fracture is well filled with grout. This was unexpected for a 16μm crack. Apparently, the rubber pad between the loading platen and the top of the sample was too deformable, and the true fracture aperture probably unknown, but substantially larger than the one determined from the falling head (very low injection pressure) test.

Severe grout shrinkage occurred in the large voids around the periphery of the sample after one day exposure to room conditions.

BEST COPY AVAILABLE

3.8. Rock Sample 8 Testing

Samples 8 through 11 were 15 cm (6 in) cubes of Charcoal granite containing a sawcut. These samples were prepared similarly in order to allow making a comparison of the minimum equivalent aperture that can be grouted and of the performance of different mixes on similar crack widths.

Since grout was accepted by the 69 μm fracture of sample 1, it was decided to attempt to grout sample 8 at a 51 μm aperture. Grout mix 2 was injected at a pressure of 6.21 MPa (900 psi). A marked decrease in single fracture hydraulic conductivity was obtained. However, visual observation showed that only a negligible amount of cement had been emplaced.

3.9. Rock Sample 9 Testing

For sample 9, it was attempted to grout a fracture with a similar aperture as sample 8, but with a thinner mix. A marked decrease in single fracture hydraulic conductivity was obtained, but only a negligible amount of cement had been accepted by the fracture.

3.10. Rock Sample 10 Testing

For sample 10, a 68 μm aperture was obtained using a normal stress of 13.8 MPa (2000 psi). The sample was grouted with mix 4 at an injection pressure of 5.52 MPa (800 psi). A seven-fold decrease in the rate of head drop was obtained. A significant amount of grout was injected. The flow is not radially symmetric, but is limited to two linear flowpaths.

3.11. Rock Sample 11 Testing

An aperture of 66 μm was obtained at a normal stress of 1.38 MPa (200 psi). Grout mix 3 was injected at 2.07 MPa (300 psi).

It appears possible that a cement-bentonite mix behaves as a better sealant than a neat cement mix when kept saturated. A somewhat greater quantity of grout was injected into sample 11 than into either samples 1 or 10.

4. Conclusions

A comparison of the uniaxial test results for the stable cement-bentonite mixes with their unstable counterparts reveals that the stable mixes are stronger. This contradicts the accepted belief that bentonite weakens a grout mix. Unstable mixes cured in cylinders were more variable in composition than stable mixes. This led to lower compressive strengths, despite the fact that their final water-cement ratios after bleeding were lower. Unit weight and compressive strength results for unstable mixes also were more erratic. In the field, the sedimentation process is more complicated and is affected by such factors as the dip of the grouted fractures, the flow conditions encountered, the magnitude and duration of the applied

BEST COPY AVAILABLE

pumping pressure, the mixing, pumping and flow shear. Therefore, for an unstable mix, the final composition and properties of the hardened cement sheet emplaced in the fracture remain rather unpredictable. On the other hand, a stable mix would have properties that are more predictable because of its uniform composition before and after emplacement. Thus, their use in grouting seems preferable.

Fracture permeability testing confirms the dependence of permeability on normal stress. The greatest change in permeability occurs at low stresses. During unloading and reloading an irreversible decrease in permeability occurs due to the permanent deformation of asperities resulting in a better mated fracture surface.

These stress-permeability test results show that the zone around repository openings subject to stress relaxation might increase in permeability because of fracture widening. If these zones of increased permeability result in significant flowpaths, fracture grouting might be needed. Because stress relaxation is time-dependent, the decision as to when to grout becomes important.

The falling head permeameter performed well for most of the permeability testing program. There were problems in saturating some of the samples. In particular, some of the tests performed for the stress-permeability curves of sample 4 are suspected of being unsaturated. Two of the samples containing tension cracks, samples 5 and 6, were difficult to saturate while initially unloaded. A large number of tests were required before a steady rate of head drop could be obtained. It seems that a constant head permeameter with a large capacity or a recirculating capability would have been preferable to the falling head apparatus used here. Similarly, it would be preferable to determine the fracture permeability at the same injection pressure used for grouting.

The permeability measurements taken after the grouting of samples 4, 8 and 9 indicate that such measurements can be misleading. Ineffective grouting of the samples resulted in major reductions in apparent permeability. A radial, divergent flow can be heavily influenced by conditions close to the borehole. It is thus recommended that a radial, convergent or a linear flow, e.g. from a different hole, be used to assess the effectiveness of a grout seal.

The question as to whether displacement grouting is beneficial or detrimental to the sealing of rock fractures can not be adequately answered on the basis of this very preliminary set of experiments. This is in part because the stiffness of the test apparatus is unknown when compared to that of an actual rock mass. With the exception of sample 6, which was tested in an unloaded state, it is assumed that fracture displacements were negligible. The test results for sample 6 did show that the fracture hydraulic conductivity was unchanged by grouting despite the fact that the fracture was well filled with grout. This evidence is inconclusive, however, since it is based on only one sample and it is not known how much actual fracture displacement occurred.

BEST COPY AVAILABLE

The use of high grouting pressures to increase the flow rate and penetration distance of a grout could not be investigated. The small rock sample size limited the volumes of grout that could be injected. For the samples and conditions used, a 1.38 to 2.07 MPa (200 to 300 psi) injection pressure was sufficient for grout emplacement.

The problem of grout mix durability should be of great concern when large voids are grouted. The severe shrinkage of cement-bentonite grout in the large voids of sample 6 points to a potential shortcoming of such a mix. It seems that the addition of bentonite in a cement grout can lead to a nondurable mix if it does not remain saturated. However, shrinkage cracking was not noticed in any of the tighter fractures grouted with these mixes, but neither was it investigated in great detail.

The determination of the equivalent aperture of a fracture may be a viable means for developing a criterion governing the use of cement for fracture grouting, although the instrumentation used here, particularly the lack of aperture monitoring during grouting, is insufficient to provide conclusive evidence. It can also be an aid in the selection of a starting grout mix. The practicality of its use will depend on the feasibility of obtaining fracture information for the intervals of rock that are to be water tested.

The failure to inject any grout into the finer cracks, in addition to reported claims regarding the limitations of cement based grouts, confirm the impossibility of injecting ordinary portland cement into fine fractures. Such fractures may result in significant rock mass permeabilities if they occur in sufficient numbers. More physical and chemical testing of alternative grouting materials is needed to evaluate substitutes for ordinary portland cement.

Visual observations during grouting (i.e. fracture outflows) as well as inspections of the grout distributions typically show a highly non-uniform flowpath, i.e. strongly preferential channel of fingering type flow.

5. Research Recommendations

These grouting experiments present a scouting investigation of a few of the many aspects that will influence the sealing performance that can be accomplished by grouting the rock directly adjacent to various repository openings, and in particular at permanent seal locations.

The most apparent needs from the results obtained thus far appear to be for experiments on larger size "fractures", i.e. fractures with longer flowpaths. This unfortunately is difficult to perform at stress levels even approximating repository conditions, due to the large load requirements. However, even experiments over relatively short flowpaths can be highly revealing, as illustrated here.

Recommended further experimentation along the lines introduced would include experiments on natural joints and experiments on artificial joints. Natural joint experiments, almost certainly supplemented with

BEST COPY AVAILABLE

artificial joints, i.e. induced tensile fractures, should focus on a detailed study of the joint morphology and grout distribution. Virtually all experiments performed here confirm the frequent observation in fracture flow studies of a highly nonuniform flow, i.e. pronounced fingering. Fracture grout studies can provide considerable insight into fracture flow mechanics, because they allow direct observation and mapping of the preferred flowpaths, as well as a wide range of viscosity control. Therefore, a detailed comparison of fracture morphology and flowpath would allow a much more realistic assessment of fracture flow, in addition to the immediate objective of obtaining an improved understanding of grout flow and grouting sealing performance. An essential prerequisite for achieving the maximum possible benefits from such a study would be considerably improved instrumentation during fracture grouting. Particularly desirable would be displacement monitoring at multiple positions along and across the fracture, as well as acoustic emission monitoring of the grouting progress. A precise control and measurement of grout viscosity is needed. The experiments need to be performed under a range of external and injection pressures, as well as for a range of fracture orientations with respect to the stressfield.

The experiments on "artificial" fractures identified earlier would consist of grouting experiments in gaps between parallel plates with carefully designed and controlled apertures and rugosities. In this testing configuration, it is possible to vary the surface morphology, and thus establish a much better controlled investigation of the relation between flowpaths, injection parameters (e.g. pressure, rate, pump shear), grout characteristics (e.g. viscosity, particle size), sealing effectiveness, and fracture characteristics. Such investigations also would be particularly appropriate to study the effectiveness of a wide range of group mixes.

As in all aspects of HLW repository performance, longevity or durability of any barrier component will be a major concern. Several tests suggest themselves naturally: extended time flow testing of grouted fractures; experiments to identify flow conditions resulting in grout damage, e.g. piping or channeling through grout; accelerated aging experiments by means of thermal and load cycling (e.g. both normal and shear); drying experiments.

All the previously proposed work is aimed exclusively at the study of single fracture grouting. Field situations involve grouting fracture networks, and, from a research point of view, in particular the mechanics of grout flow from one fracture into an intersecting one. Although experimental complications, especially the need for adequate sample preparation and test instrumentation, increase significantly, a conceptual experimental program can readily be visualized. In addition to previously mentioned variables such as stressfield, grout pressure, fracture apertures, grout viscosity and particle size, the relative geometry (orientation and width) of intersecting fractures is likely to be a significant factor in grout propagation and distribution. Experiments on artificial carefully controlled "fracture networks", designed similarly to the single fracture experiments, should be aimed at clarifying the underlying flow mechanics of the system.

BEST COPY AVAILABLE

Confirmatory experiments on actual rock fractures are needed, particularly to allow identification of fundamental differences, if any, between observations on idealized and on real fracture networks.

Basic difficulties and limitations inherent in laboratory simulations of field grouting require that all critical conclusions and issues identified from laboratory investigations be confirmed by field studies. The most obvious limitations associated with laboratory work are those due to the use of unrepresentative mixes and pumps, typically low-speed, low-volume. Mixing and pumping procedures significantly affect grout properties (e.g. Houlsby, 1982), and it is difficult, therefore, to correctly produce representative field grouts in the laboratory, and hence field grout flow conditions. The second type of fundamental simulation difficulties relate to in-situ rock mass behavior, particularly discontinuity behavior. For these reasons, some field evaluations would be highly desirable, and preferably should be conducted under fairly representative conditions, e.g. around excavations at great depth in jointed rock. It is premature to try to outline a field testing program in detail, in light of the need to first develop a significantly improved understanding of the issues on the basis of systematic laboratory investigations.

As outlined briefly in the introduction to Chapter Three, on grouting, considerable and well-recognized uncertainty exists about the actual performance of grouting. Much of the uncertainty is due to a lack of understanding of the detailed mechanics of grout distribution, of the sealing performance subsequent to grouting, and of the various parameters that affect it. It is probable that grouting will be required at various points of the engineered rock barrier, and virtually certain that it will be required at sealing locations. In order for NRC to be able to make an assessment of reasonable assurance with regard to the performance of these grouting barrier components, it would appear highly desirable to develop a significantly improved understanding of grouting of fractured rock.

BEST COPY AVAILABLE

CHAPTER ONE

INTRODUCTION

1.1 Objective

Current plans for the disposal of high-level nuclear waste call for its isolation in underground repositories. Fractures in the rock mass surrounding a repository and its shafts, access drifts, emplacement rooms and holes, and exploratory holes, may provide preferential flowpaths for the seepage of groundwater. In order to reduce their permeability, such cracks may have to be sealed. The likelihood that extensive or at least local grouting will be required as part of repository sealing has been noted in numerous publications addressing high level waste repository closing (e.g. Koplick et al., 1979; Gyenge, 1980a,b; Yuen and Boyd, 1982; Kelsall et al., 1982; Kelsall et al., 1983; Mott, Hay & Anderson, 1983; Kelsall et al., 1985a,b,c), as well as in studies dealing more specifically with grouting performance (e.g. Crawford and Groskopf, 1984; Lau and Crawford, 1986). The most explicit and detailed use of fracture grouting for repository sealing probably is given in the conceptual seal designs for the Nevada Nuclear Waste Storage Investigations Project (Fernandez and Freshley, 1984; Fernandez, 1985).

The fundamental objective of this "Rock Mass Sealing" research project is to assess experimentally the performance of existing products and methods for sealing rock masses. This work is aimed at determining the feasibility of sealing penetrations intersecting a repository rock mass to a level where it can reasonably be assured that they will not become preferential water flow or radionuclide migration paths. This project studies experimentally the likelihood of preventing such migrations by sufficiently reducing the hydraulic conductivity of penetrations (including the plug-rock interface and the rock directly around the plug). The work performed provides direct input to an assessment as to whether or not 10 CFR 60.134 (U.S. Nuclear Regulatory Commission, 1983, and, as amended, 1985) is likely to be satisfied by any particular proposed sealing methods. Some aspects of this study have broader implications, e.g. directly for 10 CRF.133 (d), and indirectly for 10 CFR.133 (a)(1),(2),(f) (U.S. Nuclear Regulatory Commission 1983, and as amended, 1985), (h).

General guidelines for the separation of radioactive waste from the physical environment, and in particular for the acceptable radionuclide releases following repository closure, have been finalized by EPA (U.S. Environmental Protection Agency, 1986; 40 CRF 191). Detailed implementation of the requirements is governed by 10 CFR 60 (U.S. Nuclear Regulatory Commission, 1983, 1985). The research performed as part of this ongoing contract addresses specifically some of the remaining uncertainties associated with the sealing requirements in 10 CFR 60, including §60.51,(a); §60.102,b(2),e(1),(2); §60.113; §60.133,(h), §60.142,(c), but particularly §60.134, Design of seals for shafts and boreholes.

BEST COPY AVAILABLE

1.2 Scope and Limitations

An experimental apparatus has been assembled to allow permeability testing and grouting of fractures in rock samples under a range of stresses normal to the fracture. Eleven samples have been tested. The fracture permeability has been determined as a function of the normal stress. Five cement grout types have been tested. Grout characterization included bleed testing and uniaxial compressive strength testing. Rock "fractures" included seven sawcuts in granite cubes, a natural fracture in a limestone core, and three induced (point load) tension fractures in basaltic andesite core. Hydraulic conductivity was determined at external normal stresses up to about 13 MPa (2000 psi), and low (7 kPa; 1 psi) fracture injection fluid pressure. Grout injection pressure was selected to obtain a marginally groutable fracture aperture. Sealing performance was evaluated by low pressure falling head permeameter tests, similar to pre-grouting permeability measurements, and by visual inspection of the grout distribution along the discontinuity.

1.3 Organization

This introductory chapter briefly summarizes the regulatory context of rock mass sealing requirements, quotes a number of commentaries and view points on rock mass sealing from the literature on HLW (High Level Radioactive Waste) disposal, and lists related reports issued under this contract.

The determination of the permeability of a single fracture and a discussion of laboratory studies concerned with single fracture fluid flow are given in Chapter Two. Also presented in Chapter Two is a review of field permeability test methods that have been used in grouting practice.

Chapter Three discusses properties of cement-based grouts important to their design and application. This includes the particulate nature of cement and the penetration limits it imposes. The subject of grouting pressures is covered because it is a major factor governing the grouting process itself.

Chapter Four provides a detailed description of the experimental equipment and procedures. A summary of results and the conclusions drawn are presented in Chapters Five and Six, respectively.

Comprehensive and detailed results of the various experiments are presented in Appendices A through C. Appendix D consists of a bibliography of bibliographies and major reference sources on rock mass grouting.

1.4 Rock Mass Sealing Contract No. NRC-04-78-271 - Reports Issued

This Technical Report is the latest in a series of reports issued for the subject contract. A complete list of reports issued (to be issued for South and Daemen, 1986, and Akgun and Daemen, 1986) is given below, to facilitate a general overview of work performed to date and of the overall context of ongoing work.

BEST COPY AVAILABLE

The first four reports, as well as the seventh, are literature surveys.

The fifth report is primarily a description of planning, experimental design and some preliminary tests.

The topical report by Jeffrey (1980) gives a comprehensive theoretical (analytical) discussion of transverse plug-rock interaction, based on elastic and viscoelastic calculations. This is complemented by the axial interaction discussed in Stormont and Daemen (1983), a report which is primarily experimentally oriented, but includes extensive analytical discussions.

The topical reports by Mathis and Daemen (1982) and by Fuenkajorn and Daemen (1986) present a detailed experimental assessment of drilling damage in granites and in basalts.

Experimental flow studies under polyaxial stress conditions are described in Cobb and Daemen (1982), under radially symmetric external loading in South and Daemen (1986), and on unloaded samples in Akgun and Daemen (1986). Additional data on plug performance under stressed and unstressed conditions are included in virtually all other reports.

All annual reports subsequent to (5) include a combination of experiments, results, conclusions, and plans for future work, similar to the present annual report.

Quarterly progress reports are not listed as all information contained therein also is included in the annual reports.

1. South, D.L., R.G. Jeffrey, L.W. Klejbuk, and J.J.K. Daemen, 1979, "Rock Mass Sealing - Annual Report, October 1, 1978 - September 30, 1979," prepared for the U.S. Nuclear Regulatory Commission, SAFER Division, for Contract NRC-04-78-271, by the Department of Mining and Geological Engineering, University of Arizona, Tucson.

2. Daemen, J.J.K., 1979, "Rock Mass Sealing (Research in Europe)," 48 pp., Foreign Travel Trip Report to the U.S. Nuclear Regulatory Commission, SAFER Division, for Contract NRC-04-78-271, by the Department of Mining and Geological Engineering, University of Arizona, Tucson.

3. South, D.L., 1979, "Well Cementing," 75 + vii pp., Topical Report to the U.S. Nuclear Regulatory Commission, SAFER Division, for Contract NRC-04-78-271, by the Department of Mining and Geological Engineering, University of Arizona, Tucson.

4. Sultan, H.A., "Chemical Grouting for Rock Mass Sealing - a Literature Review," 45 + iv pp., Topical Report to the U.S. Nuclear Regulatory Commission, SAFER Division, for Contract NRC-04-78-271, by the Department of Mining and Geological Engineering, University of Arizona, Tucson.

BEST COPY AVAILABLE

5. South, D.L., R.G. Jeffrey, S.L. Cobb, S.P. Mathis, and J.J.K. Daemen, 1979, "Rock Mass Sealing - Annual Report, October 1, 1979 - September 30, 1980," prepared for the U.S. Nuclear Regulatory Commission, SAFER Division, for Contract NRC-04-78-271, by the Department of Mining and Geological Engineering, University of Arizona, Tucson.

6. Jeffrey, R.G., 1980, "Shaft or Borehole Plug-Rock Mechanical Interaction," 145 + xi pp., Topical Report to the U.S. Nuclear Regulatory Commission, SAFER Division, for Contract NRC-04-78-271, by the Department of Mining and Geological Engineering, University of Arizona, Tucson.

7. South, D.L., 1980, "Borehole Sealing with Clay (Part A). Considerations in Clay Mineral Stability (Part B)," 50 + iv pp.; 25 + ii pp., Topical Report to the U.S. Nuclear Regulatory Commission, SAFER Division, for Contract NRC-04-78-271, by the Department of Mining and Geological Engineering, University of Arizona, Tucson.

8. Cobb, S.L., W.B. Greer, R.G. Jeffrey, S.P. Mathis, D.L. South, and J.J.K. Daemen, 1981, "Rock Mass Sealing - Annual Report, September 1, 1980 - May 31, 1981," prepared for the U.S. Nuclear Regulatory Commission, SAFER Division, for Contract NRC-04-78-271, by the Department of Mining and Geological Engineering, University of Arizona, Tucson.

9. South, D.L., W.B. Greer, N.I. Colburn, S.L. Cobb, B. Kousari, S.P. Mathis, R.G. Jeffrey, C.A. Wakely, and J.J.K. Daemen, 1982, "Rock Mass Sealing - Annual Report, June 1, 1981 - May 31, 1982," prepared for the U.S. Nuclear Regulatory Commission, SAFER Division, for Contract NRC-04-78-271, by the Department of Mining and Geological Engineering, University of Arizona, Tucson.

10. Mathis, S.P. and J.J.K. Daemen, 1982, "Borehole Wall Damage Induced by Drilling: An Assessment of Diamond and Percussion Drilling Effects," 171 + xii pp., Topical Report to the U.S. Nuclear Regulatory Commission, SAFER Division, for Contract NRC-04-78-271, by the Department of Mining and Geological Engineering, University of Arizona, Tucson.

11. Cobb, S.L. and J.J.K. Daemen, 1982, "Polyaxial Testing of Borehole Plug Performance," 180 + xi pp., Topical Report to the U.S. Nuclear Regulatory Commission, SAFER Division, for Contract NRC-04-78-271, by the Department of Mining and Geological Engineering, University of Arizona, Tucson.

12. Daemen, J.J.K., D.L. South, W.B. Greer, J.C. Stormont, S.A. Dischler, G.S. Adisoma, N.I. Colburn, K. Fuenkajorn, D.E. Miles, B. Kousari, and J. Bertuca, 1983, "Rock Mass Sealing - Annual Report, June 1, 1982 - May 31, 1983," NUREG/CR-3473, prepared for the U.S. Nuclear Regulatory Commission, Division of Health, Siting and Waste Management, for Contract

BEST COPY AVAILABLE

NRC-04-78-271, by the Department of Mining and Geological Engineering, University of Arizona, Tucson.

13. Stormont, J.C. and J.J.K. Daemen, 1983, "Axial Strength of Cement Borehole Plugs in Granite and Basalt, NUREG/CR-3594, Topical Report to the U.S. Nuclear Regulatory Commission, Division of Health, Siting and Waste Management, for Contract NRC-04-78-271, by the Department of Mining and Geological Engineering, University of Arizona, Tucson.

14. Daemen, J.J.K., W.B. Greer, G.S. Adisoma, K. Fuenkajorn, W.D. Sawyer, Jr., A. Yazdandoost, H. Akgun, and B. Kousari, 1985, "Rock Mass Sealing - Annual Report, June 1983 - May 1984," NUREG/CR-4174, prepared for the U.S. Nuclear Regulatory Commission, Division of Radiation Programs and Earth Sciences, Office of Nuclear Regulatory Research, Contract No. NRC-04-78-271, by the Department of Mining and Geological Engineering, University of Arizona, Tucson.

15. Fuenkajorn, K. and J.J.K. Daemen, 1986, "Experimental Assessment of Borehole Wall Drilling Damage in Basaltic Rocks," NUREG/CR-4641, Technical Report to the U.S. Nuclear Regulatory Commission, Division of Radiation Programs and Earth Sciences, Office of Nuclear Regulatory Research, Contract No. NRC-04-78-271, by the Department of Mining and Geological Engineering, University of Arizona, Tucson.

16. Daemen, J.J.K., W.B. Greer, K. Fuenkajorn, A. Yazdandoost, H. Akgun, A. Schaffer, A.F. Kimbrell, T.S. Avery, J.R. Williams, B. Kousari, and R.O. Roko, 1985, "Rock Mass Sealing - Annual Report, June 1984 - May 1985," NUREG/CR-4642, prepared for the U.S. Nuclear Regulatory Commission, Division of Radiation Programs and Earth Sciences, Office of Nuclear Regulatory Research, Contract No. NRC-04-78-271, by the Department of Mining and Geological Engineering, University of Arizona, Tucson.

17. Akgun, H., and J.J.K. Daemen, 1986, "Size Influence on the Sealing Performance of Cementitious Borehole Plugs," NUREG/CR-4738, Technical Report to the U.S. Nuclear Regulatory Commission, Division of Radiation Programs and Earth Sciences, Office of Nuclear Regulatory Research, Contract No. NRC-04-78-271, by the Department of Mining and Geological Engineering, University of Arizona, Tucson.

18. South, D.L. and J.J.K. Daemen, 1986, "Permeameter Studies of Water Flow through Cement and Clay Borehole Seals in Granite, Basalt and Tuff," NUREG/CR-4748, Technical Report to the U.S. Nuclear Regulatory Commission, Division of Radiation Programs and Earth Sciences, Office of Nuclear Regulatory Research, Contract No. NRC-04-78-271, by the Department of Mining and Geological Engineering, University of Arizona, Tucson.

BEST COPY AVAILABLE

CHAPTER TWO

FLUID FLOW THROUGH ROCK FRACTURES

Current plans call for the disposal of high-level nuclear waste in underground repositories. Fractures in the rock mass surrounding a repository and particularly its access shafts and drifts may provide paths for groundwater seepage. Such cracks may need to be sealed. Fracture grouting of the rock surrounding underground (shaft, drift, tunnel) plugs or dams, as well as grouting of the interface between plug and rock, are integral parts of plug construction.

Rock fracture grouting has most widely been practiced to reduce seepage under dams and into underground excavations. A comprehensive hydrogeologic assessment of the effectiveness of the grout job in reducing the permeability of the rock mass is rarely made. Instead, the quantity of grout injected typically is used to infer how water-tight the grouted rock is.

Primary objectives of this investigation were to assess rock fracture grouting effectiveness and the watertightness of grouted fractures, using permeability measurements and visual inspection of grouted fractures. Ordinary portland cement grout was chosen since it is commonly used in grouting and is widely accepted as a durable sealant. Rock samples containing a single fracture were subjected to a normal stress in the laboratory and pressure-grouted. Permeability measurements taken before and after grouting assess the reduction in permeability accomplished by grouting.

This chapter briefly reviews and summarizes a few important aspects of fluid flow along a single rock fracture. Grouting experiments reported on later (Chapters Four and Five) have been performed on single fractures, and include permeability measurements before and after grouting. This chapter also includes a discussion of field permeability measurements as they relate to grouting design and testing.

2.1 Fracture Flow Theory and Experiments

Grouting of fractures in rock involves the pressurized injection of grouts. Topics of particular concern with regard to the sealing effectiveness of such grouting operations include grout penetration, i.e. the distance to which the grout travels along a fracture, and the distribution of the grout along the fracture, the possibility or risk that grout pressurization might initiate or propagate fractures in the rock mass, thus potentially enhancing rather than reducing the hydraulic conductivity of the grouted rock mass, and numerous operational variables. Grout distribution depends on the grout flow path, which in turn depends on the fracture aperture (true, variable wall separation). The latter is a function of normal and shear displacements, deformations, and hence stresses, as well as of

BEST COPY AVAILABLE

injection pressure and grout characteristics such as rheology, viscosity, particle size of solids in suspension, etc.

An understanding of grout distribution will be improved by integrating recent research results in a number of areas that bear directly on grout flow mechanics. Of particular interest in this regard are studies of liquid, most commonly water, flow along fractures, studies of the injection of fluids into rock, e.g. for permeability testing or for hydraulic fracturing, as well as grouting studies themselves, the latter clearly being a specially case of the former.

Numerous studies have been performed on the flow of water along single fractures. They can conveniently and appropriately be subdivided into studies of flow along open fractures or channels, i.e. channels where no contract exists between the channel walls, and "closed" fractures, i.e. with local contact. Open channel studies include Lomize (1951), Baker (1955), Huitt (1956), Parrish (1963), Romm (1966), Louis (1969; partially summarized in Wittke and Louis, 1968), Sharp (1970), Rayneau (1972), Heise (1973), Wallner and Wittke (1974), Cruickshank (1976), Wallner (1976), and Rissler (1978). Rissler (1978) references a number of earlier German studies not usually mentioned in the English language literature. These parallel plate flow studies have resulted in the validation of fundamental flow laws, in the identification of various flow regimes (e.g. laminar, turbulent), and in empirical adjustment parameters needed to account for wall roughness.

Experiments on grout penetration into parallel plate simulations of open fractures (e.g. U.S. Army Corps of Engineers, 1956; Kennedy, 1958; Heise, 1973; Wallner and Wittke, 1974; Wallner, 1976; Houlsby, 1985) can be considered as similar open fracture flow tests, although cement flow calculations require accounting for rheological behavior. Such grout flow studies permit post-test visual observation of the flowpath, which tends to reveal complex flowpaths when substantial wall rugosity affects grout distribution, as is confirmed by observations described in Chapter Five. Similar observations, described as duning, fingering, and channeling, have been made during experimental investigations of propping agent and sand slurry distributions in hydraulic fractures (e.g. Lowe and Huitt, 1966).

More realistical for in situ rock mass simulations are the studies of flow through fractures in contact, particularly when the contact changes as a result of rock deformation, e.g. under the influence of changes in stress across the fracture. As pointed out, for example, by Sharp (1969), the actual flowpath under such realistic partial contact conditions is likely to become highly complex. Water flow studies in fractures with contact have concentrated on the influence of aperture, roughness, normal and shear stress on flow (e.g. Parrish, 1963; Sharp, 1970; Maini, 1971; Louis and Pernot, 1972; Jouanna, 1972a,b; Ohnishi, 1973; Goodman and Ohnishi, 1974; Nelson, 1975; Gale, 1975; Jones, 1975; Iwai, 1976; Louis, 1976, pp. 57-62 and Appendix V; Pratt et al., 1977; Witherspoon et al., 1977; Nelson and Handin, 1977; Summers et al., 1978; Franz et al., 1979; Witherspoon et al., 1979; Goodman and Sundaram, 1980; Trimmer et al., 1980a,b; Detournay, 1980;

BEST COPY AVAILABLE

Brar and Stesky, 1980; Morrow et al., 1980; Tsang and Witherspoon, 1981; Engelder and Scholz, 1981; Trimmer, 1982; Gale, 1982a,b; Johnson, 1983; Schrauf and Evans, 1984; Gale, 1984; Gale and Reardon, 1984; Raven and Gale, 1985; Linscott, 1985; Schrauf and Evans, 1986). The improved understanding thus obtained of likely flow mechanisms along actual rock fractures, as compared to smooth parallel plate flow, has resulted in extensive reevaluations of the conventional third power flow law, and has led to the development of significantly more comprehensive flow descriptors (e.g. Lomize, 1951; Baker, 1955; Louis, 1969; Sharp, 1970; Louis and Maini, 1970; Maini, 1971; Maini et al., 1972; Sharp and Maini, 1972; Sabarly, 1972; Iwai, 1976; Louis, 1976; Rissler, 1978; Gangi, 1978; Witherspoon et al., 1980; Walsh, 1981; Neuzil and Tracy, 1981; Tsang and Witherspoon, 1981; Engelder and Scholz, 1981; Tsang and Witherspoon, 1983; Tsang, 1984; Tsang and Witherspoon, 1985; Tsang et al., 1985; Raven and Gale, 1985). It clearly would be far beyond the scope of this report to review comprehensively this relevant literature. It deserves pointing out, however, the numerous recent developments in fracture flow studies, which could contribute to an improved understanding of fracture grouting.

Fluid flow through an individual fracture has generally been modeled by analogy to flow through parallel, planar plates representing the walls of the fracture. Considering the flow to be laminar and parallel, the hydraulic conductivity K_j for smooth, parallel plates is defined by (e.g. Zeigler, 1976, p. 10):

$$K_j = (\gamma/12\mu)e^2 \qquad (2.1)$$

where: e = parallel plate aperture, and
γ, μ = unit weight and viscosity of fluid.

By direct analogy to Darcy's law, the steady-state flow rate per change in head can be related to the parallel plate aperture by (Witherspoon et al., 1980):

$$Q/\Delta h = C\, e^3 \qquad (2.2)$$

where: Q = flow rate, and
Δh = change in hydraulic head.

The constant C represents the flow geometry and fluid properties. For the case of radial flow:

$$C = \frac{2\pi}{\ln(R/r)} \quad \frac{\gamma}{12\mu} \qquad (2.3)$$

BEST COPY AVAILABLE

and for the case of straight flow:

$$C = \frac{W}{L}\frac{\gamma}{12\mu} \tag{2.4}$$

where R,r = outer and inner radius of a radial flowpath, and
W,L = width and length of a straight flowpath.

In order to relate the hydraulic conductivity of a single fracture to a set of parallel, planar joints, it is often assumed that the flow through each fracture is isotropic in the plane of the fracture. Considering the permeability of the rock matrix to be negligible, the equivalent hydraulic conductivity, K_s, parallel to the joint set, assuming laminar flow is given by (Louis and Maini, 1970):

$$K_s = (e/b)K_j \tag{2.5}$$

where K_j = hydraulic conductivity of a single fracture,
e = mean parallel plate aperture, and
b = mean joint spacing.

Zeigler (1976, pp. 76-79) illustrates how directional permeabilities can be obtained from the superposition of equivalent hydraulic conductivities of two or three orthogonal joint sets.

2.2 Laboratory Studies of Fluid Flow through a Single Fracture

The cubic law and the related formula defining the hydraulic conductivity of a single fracture are based on the assumptions that fluid flow is laminar and parallel, that the walls of the fracture are smooth, planar and parallel, and that the fracture is open. In reality, fracture walls can exhibit significant roughness. When considered in conjunction with the Reynolds number, fluid flow may or may not be laminar and parallel. In addition, fractures are typically closed by stress creating contact areas that cause a reduction in area available for fluid flow. The validity of the cubic law has been questioned under such a condition. The following laboratory studies deal with these problems as well as with the fundamental problem of relating the hydraulic properties of laboratory fractures to those found in the field.

Louis (1968) investigated the effects of roughness and turbulence on fluid flow through open fractures. He based his work on pipe flow experiments and model fractures made of parallel slabs of concrete of varying roughness. To characterize the roughness of a fracture he defined a surface roughness index (Louis, 1968, p. 54):

$$S = Y/e \tag{2.6}$$

where Y = mean height of the asperities
e = fracture aperture.

BEST COPY AVAILABLE

Louis defines different flow regimes as a function of the surface roughness index of the fracture and of the Reynolds number of the flow (Figure 2.1). Empirical equations determine the flow rate for each of the regimes. The equations corresponding to the laminar flow regimes obey the cubic law with a correction factor based on the surface roughness index incorporated to account for nonparallel flow. The turbulent flow regime equations obey the Missbach flow laws (Zeigler, 1976, p. 12). These laws modify Darcy's law to account for the nonlinearity of turbulent flow.

Heise (1973) performed "radial flow" experiments on 2 m x 2 m concrete plates with separations ranging from 100 to 1,000 μm, at waterheads of up to 40 m. He monitored pressure distributions along the "fracture", observed turbulent flow at many conditions corresponding to dam foundation testing and grouting, and cautions that rock deformation is likely to affect the results. The author notes that roughness has not been measured nor investigated. In a further series of experiments a deformable fracture is simulated by inserting various combinations of rubber cylinders in between the concrete slabs and a loading frame. This allows demonstration of the range of flow laws that can be encountererd (Figure 2.1), and leads the author to issue a strong warning about the need for a comprehensive analysis of such results, especially if they are to be used for evaluating groutability.

Jones (1975) performed air permeability tests on portland cement, plaster of Paris, marble and dolomite cylinders with simulated or natural fractures, and demonstrated the strong dependency of fracture permeability on normal stresses. The characteristic rapid closure at low stress and virtually asymptotic behavior at increasing stress is immediately obvious in his results.

Pratt et al. (1977) observed pronounced deviations from parallel plate flow predictions for a series of flow tests on a joint in a 2 m x 2 m x 2 m cube under polyaxial stresses. They postulate that bridging occurs along the joint, allowing flow even after joint "closure".

Other geometric properties, in addition to aperture and rugosity, that affect flow through fractures include wedge-shaped or nonparallel walls and fracture waviness. An excellent literature review as well as results from numerical and analytical investigations of these parameters is given by Iwai (1976).

A major factor when considering the permeability of fractures closed by stress is the effect of contact area on fluid flow. Fracture surface contact areas cause a reduction in fluid flow since some flowpaths are blocked and others become extremely tortuous. The normal stress acting across the fracture will determine the actual reduction in the flowrate as the degree of contact area is dependent upon it.

Iwai (1976, p. 77) determined the contact area of fractured marble and granite specimens subjected to different normal stresses. His method consisted of inserting thin plastic film in the fractures and observing the subsequently formed puckered areas by unaided eye and by

BEST COPY AVAILABLE

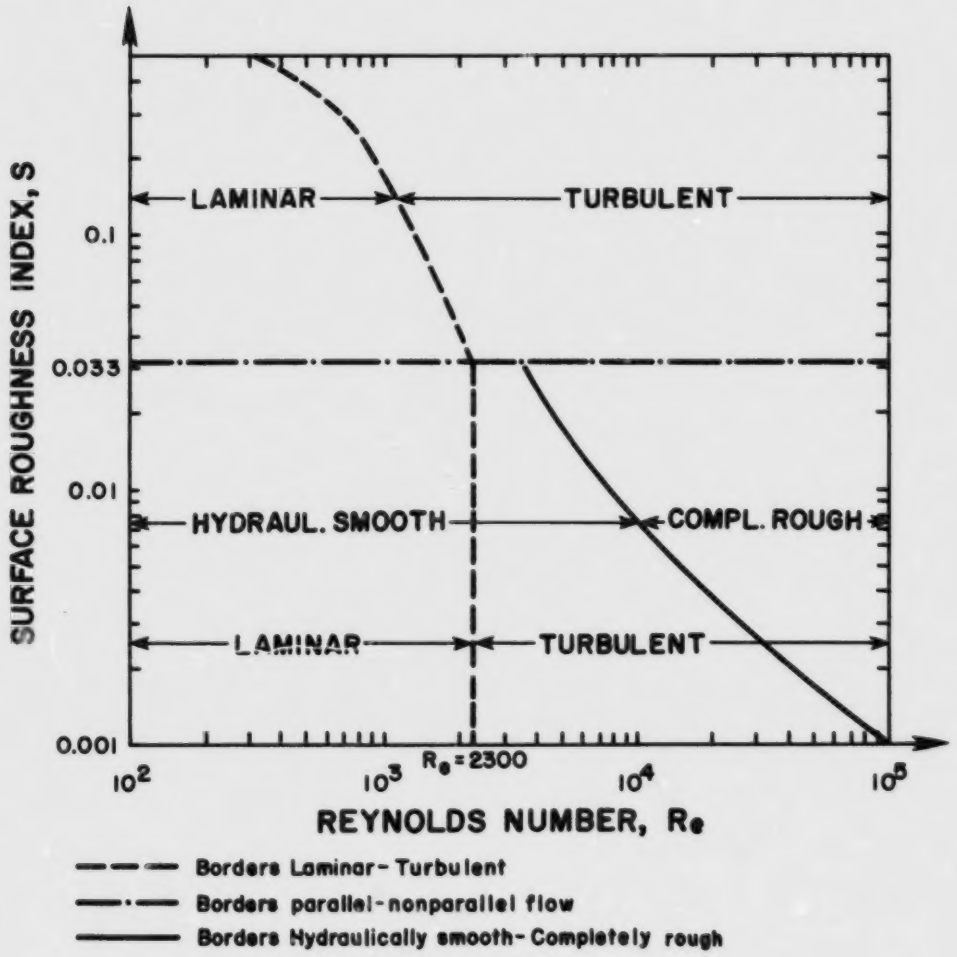

Figure 2.1 Range of validity of flow laws proposed by Louis (1968, p. 66).

(Reproduced with permission from C. Louis, 1968, "Etude des Ecoulements d'Eau dans les Roches Fissurees et de leurs Influences sur la Stabilite des Massifs Rocheux," Electricite de France, Bulletin des Etudes et Recherches - Serie A - No. 3, pp. 5-132.)

BEST COPY AVAILABLE

microscope. By considering the degree of contact area as the ratio of the contact area to the total fracture area expressed as a percentage, he obtained the results presented in Table 2.1.

Table 2.1 Degree of Contact Area for Fractures in Granite and Marble (from Iwai, 1976)

	Normal Stress MPa (psi)		
	0.26 (38)	1.3 (189)	20 (2900)
Granite	< 0.1%	1%	10 - 20%
Marble	< 0.1%	1%	25 - 35%

Since the contact area of a fracture causes a reduction in flow, the question arises as to whether the cubic law is still valid under closed conditions. Iwai (1976) conducted flow experiments on specimens of granite, marble, and basalt at normal stresses from 0 to 20 MPa (2900 psi). Fractures were made by inducing a tension crack in the specimens by a modified Brazilian test. The cubic law was valid for apertures greater than 20 μm. For smaller apertures a deviation from the cubic law occurred in the marble sample, a deviation attributed to a high degree of contact area.

Cruickshank (1976) found reasonable agreement for a free surface parallel plate flow study between cubic law and experiment, but recommended modifications to some friction factors proposed by Louis (1968).

Rissler (1978) investigated radial flow along an open parallel plate model with controlled aperture and rugosity. Rissler studied the relation between head and flowrate for a range of heads and as a function of aperture (and rugosity). He found reasonable agreement between experimental and semi-empirical (i.e. including friction coefficients) theoretical results for various laminar and turbulent flow regimes. Extensive parametric analyses of various flow laws are included, as well as discussions of the applicability and limitations of the results with regard to in situ testing of rock mass permeability.

Summers et al. (1978) conducted a flow test on a saw cut in a granite cylinder, at 300 C and under 500 bars confinement. Flow was variable, and decreased abruptly and drastically after three days, primarily due to mineral alteration. Franz et al. (1979) describe flow tests on split granite cylinders with controlled (ground) surface roughness fractures under pressures up to 2 kbars. They consider the conventional flat plate model as inadequate for a description of their results.

BEST COPY AVAILABLE

Trimmer et al. (1980a,b) (also, Trimmer, 1982) conducted pulse flow tests on gabbro and granite cores with a throughgoing fracture at confining pressures up to 60 MPa, pore pressures up to 30 MPa, and stress differences up to 88% of the intact rock strength. They observed the typical permeability decrease under increasing stress normal to the fracture, but also a decrease with increasing normal stress parallel to the fracture. The gabbro fracture shows a third power dependence of fracture permeability on fracture width. The authors conclude that electrical conductance and seismic pulse amplitude changes exhibit the best potential for monitoring fracture permeability changes.

Witherspoon et al. (1980) reanalyzed Iwai's data introducing a fracture surface characteristic factor f, a fitting parameter obtained from the experimental data. They concluded that the cubic law was valid for apertures as small as 4 μm, the smallest aperture obtained for an induced tension crack subjected to 2900 psi (20 MPa) normal stress. Deviations from the cubic law causing a reduction in flow were accounted for by incorporating the factor f into equation 2.2:

$$Q/\Delta h = (C/f)e^3 \qquad (2.7)$$

The factor f varied from 1.04 to 1.65.

Gale (1982a) conducted flow experiments on natural as well as induced tension fractures in specimens of gneissic granite at normal stresses from 0 to 30 MPa (4350 psi). The testing procedures followed those of Iwai (1976) and Gale (1975). A breakdown of the cubic law occurred when the induced cracks were subjected to normal stresses greater than 20 MPa (2900 psi). For the natural fractures, this breakdown occurred at lower stresses when apertures were approximately 10 μm.

Goodman and Sundaram (1980) conducted radial flow experiments on fractures in limestone cylinders. Considerable permanent aperture reduction occurred at normal stresses of 2 MPa (300 psi).

Detournay (1980) conducted straight flow experiments on an artificial fracture in granite. For normal stresses at up to 7.2 MPa, flow injection pressures up to 0.7 MPa, pressure gradients of up to 3 N/cm^3, and apertures in the 0.2 to 0.3 mm range, Detournay confirmed the validity of the cubic law for closed joints, but with a modification accounting for aperture at zero normal stress, presumably directly related to joint roughness.

Engelder and Scholz (1981) performed flow tests on very smooth ground saw cut samples at pressures of up to 200 MPa. They confirm the conventional cubic law at low stresses, as well as the results by Kranz et al. (1979) that confining pressure has a greater effect than pore pressure. They conclude that joint aperture only is inadequate to calculate joint permeability, and that the effective cross section available for flow needs to be accounted for.

BEST COPY AVAILABLE

Johnson (1983) describes flow experiments on a simulated fracture with asperities in the form of a monolayer of small glass spheres. He studies elastic deformation, brittle fracture, and plastic deformation of the asperities, and derives a theoretical mechanical model for fracture permeability as a function of normal stress.

Sundaram and Fink (1983) use an electrical analog to simulate water flow along a rock fracture. They investigate the effect of contact area and contact area distribution on flow rate. Of particular interest within a grouting context is their analysis of divergent flow along a fracture partially plugged near an injection hole, showing that flowrates can be underestimated severely under such conditions. As discussed in Chapter 5, plugging of primary flowpaths directly adjacent to the injection hole has been a frequent observation in the experiments reported on here.

Gale and Reardon (1984) show the typical stress-permeability relation for a fracture in granite, including decreasing cyclic hysteresis. This relation was no longer observed after the fracture had been cement grouted.

Schrauf and Evans (1984, 1986) conducted radial and straight gas flow tests on a natural fracture in a 30 x 30 x 30 cm granodiorite block. They studied the influence of applied fluid pressure gradient, of average fracture aperture and of fracture roughness on flow, as well as, independently, on fracture deformation. They found linear and smooth transitional flow, the latter well described by a flow equation in which losses are accounted for by the square of the velocity. A fourth power inverse relation was obtained between flow rate and fracture aperture.

Sato et al. (1984) conducted flow tests on four artificial and on three natural fractures in granite, for normal stresses at up to 0.5 MPa. They performed detailed surface roughness profile measurements, of which the Fourier spectrum analysis is performed.

Reba and Hadley (1985) performed two long term (200 hours and 700 hours) steady state and transient fracture flow tests in welded tuff. They observed substantial flow (permeability) reductions with time, which they explain as a fracture healing process due to asperity deformation and meshing.

Gale et al. (1985) review the main literature on single fracture flow (and have been used as an essential and helpful guide for the review presented here), and also present new data on flow tests on a large (1.5 m diameter) fracture. Their analyses identify a number of important remaining uncertainties in closed fracture flow modeling. Of particular interest within a grouting context is their observation that in many closed fracture flow studies, at normal stresses up to about 10 MPa, the flowrate to aperture appears to approach a fourth power law, a relationship repeatedly emphasized and illustrated with examples, by Sabarly (e.g. 1968, 1972; also Londe and Sabarly, 1966) for estimating dam foundation permeabilities by means of the Lugeon (injection) test (Section 2.3.1).

BEST COPY AVAILABLE

Linscott (1985) and Makurat (1985) are among the few direct studies of the influence of the influence of shear on joint permeability. Makurat, in a first experiment, observes a substantial flow increase under very small shear displacement, and complex, if any, relations between cycling, dilatancy and flow. A parallel plate cubic law based on measured aperture does not adequately describe observed flow. Witherspoon et al. (1981) observed rapid permeability increase, explained by shear dilatancy, when the large (1 m diameter) Stripa granite sample approached failure during an axial compression test.

The numerous deviations observed by experimenters between parallel plate calculations and observed flow-pressure relations have resulted in intense efforts to develop improved models of fracture flow. Gangi (1978) proposed a "bed of nails" model, in which a Hertzian (i.e. purely elastic) contact calculation describes asperity deformation, and a simple power law variation the asperity length distribution. Witherspoon et al. (1980) argue that the deviations from the ideal parallel plate can be accounted for by an apparent reduction in flow, expressed through the factor f in the above equation (2.7). Tsang and Witherspoon (1981) develop an equivalent cubic law by calculating the deformation of the voids along a fracture, and a resulting weighted average aperture, as a function of normal stress across the fracture. The generalization of the Witherspoon et al. (1980) variable aperture model developed by Neuzil and Tracy (1981) assumes variable apertures normal to the flow direction, i.e. represents the flowpath as a set of parallel plates, with different apertures. They suggest that a lognormal function best fits the aperture frequency distribution, based on the earlier work of Snow (1970) and Sharp (1970). The model is justified to some extent by the flowpaths observed in Maini (1971). Tsang and Witherspoon (1983) generate aperture or fracture void distributions from measured joint roughness profiles. They model the closure as a function of the normal stress by means of the Tsang and Witherspoon (1981) void deformation derivation, and hence derive a flow law as a function of void distribution along the fracture.

Sato et al. (1984) performed detailed numerical (finite difference) calculations of flow along variable aperture variable roughness flowpaths. They point out the potential importance of stagnant domains, and conclude that, in general, relative roughness, wave length and phase angle need to be included in fracture flow modeling, as well as the Reynolds number. On the basis of measured roughness profiles, they propose a permeability formula formally similar to those developed by Lomize (1951) and Louis (1968), but with constants derived from fracture profile measurements. The proposed equation provides a better fit to their experimental data than the conventional one.

Schrauf and Evans (1984, 1986) developed a pipe flow analogy to model fracture flow, and find adequate agreement with their experimental gas fracture flow experiments. The model explains the observed fourth power relation between flow rate and fracture aperture.

Tsang (1984) and Tsang and Witherspoon (1985) performed electrical analog numerical simulations of flow along a fracture plane. The

BEST COPY AVAILABLE

resistance to flow along the plane varies and is determined on the basis of measurements and of assumed void distributions. The authors demonstrate that for large contact areas the flow becomes highly tortuous, and can decrease by orders of magnitude compared to idealized parallel plate predictions.

Elsworth and Goodman (1986) develop expressions for the weighted average cubed fracture aperture based on transverse and longitudinal offsets between idealized (sinusoidal or sawtooth) fracture surfaces. The results show qualitative agreement with typically observed normal stress-flow fracture relations. Numerical studies of tortuous flow are used to illustrate general trend agreement for such conditions.

Grouting requires fluid injection under pressure, as does the typical injection testing for groutability (Section 2.3.1 below). A realistic analysis of such a procedure in all probability requires a truly mechanically hydrologically coupled analysis (e.g. Bawden et al., 1980; Tsang et al., 1985; both publications list numerous references).

Size effect is an important problem when attempting to relate hydraulic properties of laboratory to field fractures. Witherspoon et al. (1979) describe the influence of sample size on fracture permeability as depending on the degree of contact across the fracture. With increasing sample size, the degree of contact area reaches some average value that is representative of the fracture as a whole. They suggest that laboratory samples, commonly less than 15 cm (6 in) in diameter, significantly underestimate fracture permeability.

Tsang and Witherspoon (1983) studied the mechanical deformation of fractures and their implications for fracture flow, including conclusions as to the required test sample dimensions.

However, the results of Gale and Raven (1980) (see also Raven and Gale, 1985) suggest a decrease in the minimum fracture permeability at the maximum applied normal stress with increasing sample size for four of five different size samples tested. This trend is confirmed, although weakly, by data from measurements on an additional five samples (Gale, 1984; Gale et al., 1985). Intuitively, if one considers the aperture frequency distribution to be approximately log normal (Neuzil and Tracy, 1981), it would appear that if sample size is decreased, fewer of the largest, least-frequent flow channels would be included, resulting in a decrease in fracture permeability. Given the above conflicting results and the significance of the problem, it would seem that more research into the effects of sample size on fracture permeability is warranted (Witherspoon, 1981).

It is apparent from the earlier discussion that the application of a normal stress across a fracture lowers its permeability. This is due to the aperture reduction and contact area increase.

Iwai (1976) demonstrated hysteresis and a permanent reduction in permeability when a fracture is subjected to cyclic loading. These effects were attributed to permanent deformation of fracture

BEST COPY AVAILABLE

asperities in contact. Granite samples exhibited greater permanent deformation than basalt samples. These effects diminished during subsequent loading cycles, suggesting that after five or more cycles a reproducible curve without permanent set would be obtained.

Two results common to most stress-permeability research are (Garrity, 1983, p. 191):

(a) The greatest rate of change in fracture permeability occurs at the lower normal stresses.

(b) Even under high normal stresses fractures exhibit a small, residual flow and can not be considered hydraulically closed.

These two characteristics of fracture permeability have significant implications on the hydraulic conductivity of a rock mass at depth subjected to stresses induced by excavation and thermal changes.

2.3 Field Permeability Tests Used in Grouting

2.3.1 Lugeon Test

The water pressure test traditionally used for grouting work is the Lugeon test. It is popular because it is relatively economical and quick to perform. The test is performed in 46 to 76 mm (1.8 to 3 in) diameter boreholes over a test section length of 1 to 2 m (3.3 to 6.6 ft) for a period of 5 to 10 min. The test results indicate the quantity of water taken in by the borehole and are expressed as Lugeon units. A value of one Lugeon unit (Zeigler, 1976, p. 46) is defined as a water take of 1 liter/min/m of borehole tested at an injection pressure of 1 MPa (145 psi). This corresponds to a permeability of roughly 1×10^{-5} cm/sec. Rissler (1978) presents an extremely comprehensive analysis of the water injection test, and in particular of the various energy losses in the system components. Rissler includes numerous charts for various flow regimes, depending on joint orientation, aperture, roughness, and injection pressure, as well as extended procedures for test analysis. Carter (1982) argues forcefully for the need to assure that monitoring during water pressure testing and during grouting is designed to allow monitoring flow into the rock, and not flow dominated by the injection system. Kutzner (1985) graphically summarizes several relations that have been proposed between Lugeon values and permeabilities.

Although the Lugeon unit is defined at a specified pressure, it is often desirable to conduct water tests at different pressures. Figure 2.2 illustrates the effect of testing at pressures that are too high. Past a particular pressure, turbulence causes a reduction in the directly proportional pressure-flow rate relationship for laminar flow. At still higher pressures, fracture widening causes the opposite effect. Other conditions that can affect the flow through fractures by testing at pressures that are too high are the washing out of joint infilling materials and the filling of voids. A method for testing at different pressures and the interpretation of the results to determine the occurrence of the above effects is given by

BEST COPY AVAILABLE

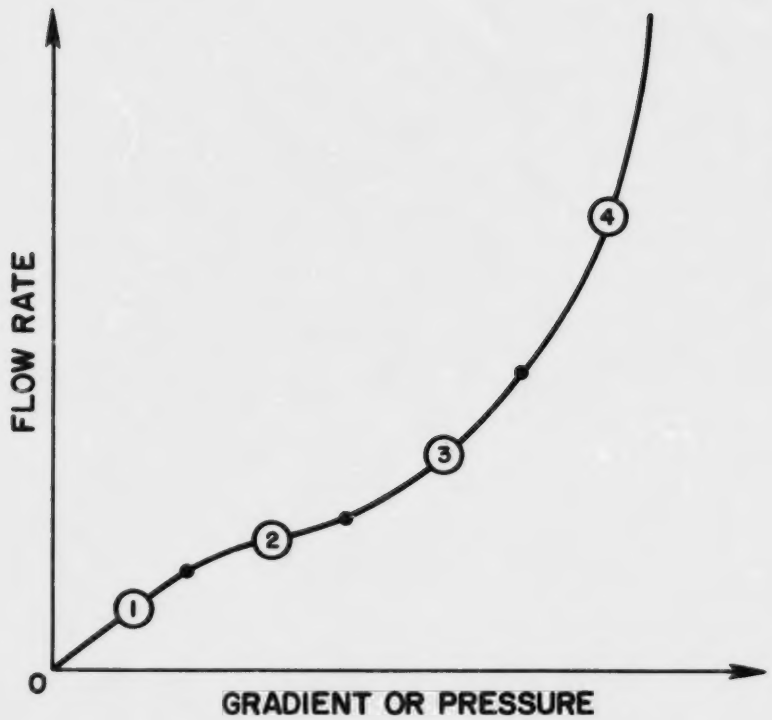

1. Laminar flow
2. Turbulence effect
3. Turbulence offset by fissure expansion
4. Predominance of fissure expansion effects

Figure 2.2 Typical results of field water test (after Louis and Maini, 1970).

(Reproduced with permission from The 2nd Congress of the International Society for Rock Mechanics, Vol. 1, Louis, C. and Y.M. Maini, 1970, "Determination of In Situ Hydraulic Parameters in Jointed Rock," International Society for Rock Mechanics, Belgrade, Yugoslavia.)

BEST COPY AVAILABLE

Houlsby (1976). He also gives a formula for adjusting water tests at different pressures:

$$\text{Lugeon value} = \text{water taken in test (l/min/m)} \times \frac{145 \text{ psi (1 MPa)}}{\text{test pressure psi (MPa)}} \qquad (2.8)$$

The formula is correct only if the flow is laminar.

The Lugeon values are used to determine the necessity for grouting as well as groutability. A major drawback of the Lugeon test for use in determining groutability is that it does not provide a simple measurement of fracture aperture. However, generalizations can be made. Houlsby (1977) gives examples of typical joint thicknesses for various Lugeon values (Table 2.2). The information is based on data from dam foundations and appears mainly applicable at shallow depths. The Water Resources Commission (1981, p. E1) also gives suggestions on choosing a starting grout mix based on Lugeon values or estimates of joint thicknesses derived from them. Rissler (1978) uses numerical (finite element) analyses of water injection tests, confirmed to some extent by experiments on parallel plate models, but stresses the need for confirmatory experiments (Rissler, 1978, p. 140). Kutzner (1985) emphasizes the need for better criteria to relate the results from water injection tests to groutability, and proposes more extensive grouting tests and flow calculations than are usually performed (for dam foundation grouting). Houlsby (1977, 1985) argues that the number of factors influencing the results is so large that a single hole relation between permeability and groutability should not be expected, and maybe not even a large area (multiple hole) average relation. Sabarly (1968) postulates that one of the reasons for the complete absence of correlation between Lugeon values and grout takes is that grouting typically is performed at substantially higher pressures than water testing, hence on fractures of larger aperture. Also complicating any such relation is the fact that a single Lugeon value can correspond to a wide range of combinations of number of fractures and fracture apertures. This latter argument is forcefully repeated by Lombardi (1985), who restricts the use of Lugeon testing to comparing the rock mass sealing obtained through grouting by comparing Lugeon test results before and after grouting. Data by Sims and Rainey (1985) provide good examples of cases where the correlation between measured permeability and grout take is marginal, at best. Carter (1982), conversely, presents a clear correlation between hydraulic conductivity and grout takes, and develops a strong argument that many of the cases of poor correlation might have been influenced very significantly by questionable measurement procedures, in which the potentially dominant effects of piping, valving, etc., might not have been accounted for. Jawanski (1970) presents results confirming his conclusion of a relatively good correlation between water injection and grout take in only slightly tectonically disturbed rock masses, and poor correlation in intensely disturbed rock. He emphasizes the strong influence of grouting and test procedures on results.

BEST COPY AVAILABLE

Table 2.2 Typical Lugeon Values and Joint Thicknesses

(Reprinted with permission from Journal of Geotechnical Division, Vol. 103, no. GT9, Houlsby, A.C, "Engineering of Grout Curtains to Standards," 1977, p. 956, American Society of Civil Engineers, New York.)

Lugeon Value	Strong, massive rock, continuous jointing	Weak heavily jointed rock
0	Completely tight	Completely tight
1	Occasionally open to thickness of about 0.050 (1)	Occasionally open to hair crack size, 0.010 (0.3)
3-5	Occasionally open to 0.100 (2.5)	Occasionally open to 0.050 (1)
20	Frequently open to 0.05 (1)	
50	Frequently open to 0.100 (2.5)	
100	Frequently open to 0.250 (6)	

NOTE: Examples are very generalized and subject to many exceptions. Joint openings are in inches (millimeters).

BEST COPY AVAILABLE

2.3.2 Other Field Permeability Test Methods

Snow (1968) described a method whereby the fracture porosity and average aperture can be determined from field permeability measurements. The flow is assumed to be laminar and through parallel-walled, interconnected fractures only. Furthermore, he assumes the presence of three orthogonal joint sets with identical spacing and aperture. Hence, the joint system is cubic and rock mass permeability is isotropic.

The fracture porosity determined by this method does not appear to be a reliable indicator of the volume of cement grout that can be expected to be taken. This is due to the viscous and particulate nature of cement grout as opposed to water. The author feels that the method is better suited to the volume predictions for a chemical grout of low viscosity.

The average fracture aperture determined by this method may correlate well with single fracture permeability measurements taken in the field. Scott (1969) discusses the determination of individual fracture apertures in an occasionally fissured limestone formation at a depth of about 610 m (2000 ft) for the purpose of developing a criterion governing when to use cement or chemical grout. He found that the average of his individual measurements agreed with an equivalent calculation for average aperture using Snow's method to within 20 percent.

Well tests have become increasingly important in the prediction of water inflows prior to the construction of deep shafts or tunnels. One such test, the drill stem test, has been used by the petroleum industry for a number of years at depths exceeding 1000 m (3000 ft). The drill stem test is much faster in operation than a conventional aquifer pumping test and can be performed in a single borehole. It also determines the flow properties of a rock mass over a larger distance than a water pressure test.

In drill stem testing, the water-bearing zone of interest is isolated with packers. Water is then allowed to flow up through the drill stem causing a partial depressurization of the aquifer. This is followed by a shut-in period during which the pressure recovery over time is recorded by a pressure gage in the test interval. Data obtained during the test can then be used to determine the permeability and the hydrostatic pressure of the aquifer. A more detailed discussion of the drill stem test method is given by Earlougher (1977, pp. 90-104). Chalmers, Daw, and Scott (1979) discuss the interpretation of test results and also present a modified test that utilizes a submersible pump to make it suitable for very strong aquifers.

Pregrouting is typically performed ahead of an advancing tunnel or shaft if it appears that water inflow will present a hazard to the operation. Initially, four to six probe holes drilled from the tunnel face or shaft sump are water tested. The measured inflows are expressed as flowrates or as flowrates per length of borehole as is done with Lugeon values. If the inflow from one or more of the holes

BEST COPY AVAILABLE

exceeds a predetermined criterion, grouting is performed. A ring of holes typically 30 m (100 ft) long are drilled so as to intersect the ground surrounding the area to be excavated. The resulting grout cover may then be water tested as before. If the residual inflows are deemed excessive, further grouting is performed. Case studies on the pregrouting of deep excavations are given by Holl and Harte (1981).

2.3.3. Assessment of Grouting

Water testing to assess the permeability of a grouted rock mass is rarely performed upon completion of a job, because water tests are considered too time consuming and expensive. It is more common to assess the watertightness of a grouted rock mass based on the quantity of grout that was injected. A discussion of this procedure as well as two case studies where permeability testing was performed after grouting are given below.

When grouting is performed, the quantity of grout taken by each borehole is recorded. After a grouting sequence is completed, an assessment is made as to tightness of the rock based on the grout absorption obtained. Typical values that indicate varying degrees of grout absorption are given by Deere (1976, p. 79). A particular value which constitutes an acceptable grout take is chosen depending on the degree of watertightness desired. If grout takes exceed this values, a decision is made to grout more holes at a smaller spacing or to add another row or ring of holes. If grout takes are equal to or less than the target value, the job is considered complete. A major drawback with this approach is that although a vague relationship between grout take and water take exists over large areas, usually no close correlation between them occurs in discrete zones (Houlsby, 1969). Furthermore, grout take is influenced by such factors as the water-cement ratio of the grout and the pumping pressures used.

An example illustrating the use of water pressure tests to assess the permeability of a grout blanket for a rock-fill dam is given by Thiers et al. (1976). The Little Blue Run Dam is 128 m (420 ft) high and is located in southwestern Pennsylvania. The dam foundation consists of a variable sequence of sedimentary rocks, the upper 6 to 12 m (20 to 40 ft) of which is highly fractured. The permeability of this fractured zone was determined to be on the order of 10^{-3} to 10^{-4} cm/sec. Blanket grouting was performed on the portion of the zone that would underlie the core of the dam. A typical grout hole pattern for the blanket consisted of seven rows of holes on 3 m (10 ft) centers (Thiers et al., 1976, p. 302). After grouting, packer tests were carried out from exploratory holes along the middle row. The permeability of the grouted zone was reduced to below 10^{-5} cm/sec. Since 1×10^{-5} or 1 Lugeon is generally regarded as the limit of groutability, these results appear suspect. Furthermore, most grout curtains engineered to high standards approaching 1 Lugeon value generally have grout holes spaced on 1.5 m (5 ft) centers. Since it was noted that grout had entered some of the exploratory holes, necessitating their redrilling (Thiers et al., 1976, p. 303), it appears that packer test results may be biased by conditions close to the borehole.

BEST COPY AVAILABLE

Black et al. (1982) describe the pregrouting of deep shafts sunk at two sites in the Selby Coalfield in Yorkshire, England. Prior to shaft sinking, a detailed hydrogeological assessment that included drill stem testing was performed. Estimates of potential water inflows to the shafts were made using the results from the drill stem tests together with the dimensions of the shafts and a knowledge of the reservoir characteristics and boundary conditions. Also for this project, an apparatus was developed that enabled a pressure recovery test similar to the drill stem test to be performed in vertical probe holes sunk from the shaft sump.

The initial investigation revealed two major water-bearing zones that would require grouting as the primary form of ground treatment. One zone was at the base of a massive limestone, called the Lower Magnesian limestone, whose permeability was due to fractures and vugs. The other zone was in a weakly cemented sandstone underlying the Lower Magnesian limestone and overlying the coal measures. The permeability of this sandstone, called the Basal Sands, was mainly due to its matrix.

The pregrouting of the limestone was effective in reducing water inflows. In one shaft, a pressure recovery test indicated a potential inflow of 750 liters/sec. After a primary sequence of cement grouting, water testing revealed that inflows were still unacceptably high. Further grouting was performed using cement and a sodium silicate based chemical grout. Residual inflows after treatment were 0.73 liters/sec resulting in a potential shaft inflow reduction of about 1000. Water testing in two other shafts revealed much smaller potential inflows due to finer fracturing and fewer vugs. After cement and chemical grouting, potential shaft inflows were reduced by factors of about 35 and 50.

For the sandstone, chemical grout was used exclusively since permeation of the rock matrix was required. In one shaft, a potential shaft inflow reduction factor of 5 was obtained. This corresponds to a permeability reduction of about 50 for the 2 m (6.6 ft) thick grout cover. For the two other shafts, inflows were reduced by factors of 3 and 4. Since the residual inflows were still unacceptably high, pressure relief wells were used to reduce them further.

BEST COPY AVAILABLE

CHAPTER THREE

ROCK FRACTURE GROUTING

3.1 Introduction

Current plans for the disposal of high-level nuclear waste call for its isolation in underground repositories. Fractures in the rock mass surrounding a repository and along the penetrations through it may provide preferential flowpaths for the seepage of groundwater. In order to reduce their permeability, such cracks may have to be sealed. The likelihood that extensive or at least local grouting will be required as part of repository sealing has been noted in numerous publications addressing high level waste repository closing (e.g. Koplick et al., 1979; Gyenge, 1980a,b; Yuen and Boyd, 1982; Kelsall et al., 1982; Kelsall et al., 1983; Mott, Hay & Anderson, 1983; Kelsall et al., 1985a,b,c), as well as in studies dealing more specifically with grouting performance (e.g. Crawford and Groskopf, 1984; Lau and Crawford, 1986). The most explicit and detailed use of fracture grouting for repository sealing probably is given in the conceptual seal designs for the Nevada Nuclear Waste Storage Investigations Project (Fernandez and Freshley, 1984; Fernandez, 1985). Reservations based on possible negative consequences of fracture sealing have been expressed by Fyfe et al. (1984).

Rule 10 CFR 60 (U.S. Nuclear Regulatory Commission, 1983, 1985) requires, in addition to the seals for shafts and boreholes (§60.134), that "the design of the underground facility shall provide for control of water or gas intrusion" (§60.133,d) and that "the design of the underground facility shall incorporate excavation methods that will limit the potential for creating a preferential pathway for groundwater or radioactive waste migration to the accessible environment" (§60.133,f, U.S. Nuclear Regulatory Commission, 1983), or "... that will limit the potential for creating a preferential pathway for groundwater to contact the waste packages or radionuclide migration to the accessible environment" (unsaturated zone amendment, §60.133,f, U.S. Nuclear Regulatory Commission, 1985).

Of particular concern within the context of repository sealing are fractures within the damaged zone directly adjacent to excavations, especially shafts and access drifts, at locations where primary seals or plugs are to be installed.* A fractured zone in the rock

---

*It is recognized that the most severe conditions of the type discussed here are most likely to be encountered around the HLW packages themselves, especially if a swelling packing were to be used, or if steam or gas were generated. This contract does not address that rock barrier, and it is unclear whether any performance will be expected of that barrier, or whether grouting in that area would be considered.

BEST COPY AVAILABLE

surrounding main seals can readily provide a dominant bypass flowpath around the seals, thereby negating the effectiveness of the plug. The concern about bypass flowpaths is the main reason why extensive grouting of the rock surrounding plugs (as well as the interface between the plug and the rock) is virtually always required in underground mining and construction (e.g. Garrett and Campbell Pitt, 1961; Wittke, 1973; Loofbourow, 1973; National Coal Board, 1982; Moller et al., 1983; Chamber of Mines of South Africa, 1983; Auld, 1983). Considerable uncertainty remains about the optimum grouting conditions, for example with regard to the preferable injection pressures. This controversy has persisted for a long time, not only in deep underground grouting, but possibly even more pronounced in dam foundation grouting. Deere (1982) lists numerous references on this topic, particularly with regard to high-pressure European grouting practice vs. American low-pressure grouting practice, although he also argues that the differences might be less pronounced than commonly perceived. Deere and Lombardi (1985) are among recent reviewers of the closely related uncertainties about the preference for the use of thick or thin grout mixes. Lau and Crawford (1986, p. 117) state that the considerable controversies on so many grouting issues arise from differences in background and experience, and that their different positions are substantiated by successful case histories. Ewert argues repeatedly (e.g. 1979, 1982a,b, 1985) that claims of successful grouting frequently are questionable, and rarely based on sufficient post-grout testing to adequately validate the claims.

The fundamental ambiguity frequently encountered in grouting requirements is stated clearly and forcefully in the Independent Panel Review of the Teton Dam Failure - probably the most visible and dramatic recent grouting failure - in the last sentence preceding the Summary of Chapter Twelve, Cause of Failure: "It is perhaps paradoxical that if, on the one hand, the grout curtain were not effective, failure would result directly from the underseepage, whereas, on the other hand, if the grout curtain were fully effective, failure would tend to develop as a result of hydraulic fracturing" (Chadwick et al., 1976). Specific technical conclusions with regard to grouting can be quoted from the cover letter (Chadwick et al., 1976, p. iii): "... openings existed through inadequately sealed rock joints ...", and from the Panel's conclusions (p. viii): "The records show that great effort was devoted to constructing a grout curtain of high quality, and the Panel considers that the resulting curtain was not inferior to many that have been considered acceptable on other projects. Nevertheless, the Panel's on-site tests and other field investigations showed that the rock immediately under the grout cap ... was not adequately sealed, and that additional unsealed openings may have existed at depth ...". Recognizing the considerable differences between dam foundations and repository sealing, especially with regard to expected flow rates, it nevertheless is apparent that a fundamentally similar uncertainty exists: sealing the rock, hence allowing a pressure build-up, or allowing flow, with potential piping and channeling?

BEST COPY AVAILABLE

Many of the difficulties and uncertainties associated with rock grouting are especially well outlined in the introduction to a recently published major book on the subject (Ewert, 1985), e.g. "...our methods of appraising rock permeability and grouting procedures often result in very uneconomical grouting programs in which a satisfactory sealing of the rock is not attained." Similarly, after an extensive discussion of the detailed study of eight dam foundation grouting projects, Ewert (1985, p. 137) concludes "...there exists a rock-type-specific optimum extent of grouting work, and when further grouting is done the remaining permeability will in fact not decrease, but may be enlarged again because the stresses around the borehole can loosen the rock along the discontinuities and induce a higher permeability again." The latter observation obviously is particularly relevant with regard to repository sealing, where, at a number of important locations, e.g. the waste package itself, some types of backfill (e.g. swelling clays) and some types of seals (e.g. swelling cements or clays), internal pressures will be induced in the rock mass, in particular within openings (emplacement holes, rooms, access drifts) within the rock mass. Thermal effects (e.g. steam formation) might further amplify the internal pressure, and enhance the permeability of the rock surrounding the openings (e.g. Apps et al., 1982, Section 3.3.1). (Possible detrimental consequences of internal pressures have been illustrated experimentally in Akgun and Daemen, 1986.) This combination of factors is certain to create an environment extremely hostile to effective rock mass sealing by means of grouting. It therefore must be considered highly desirable to gain a considerably improved understanding of the consequences of grouting, in order to allow an independent assessment of what the consequences of grout injection into the rock component of the engineered barrier system might be.

Grouting rock around repository seals, e.g. to reduce bypass flow through the damaged zone around an excavation, involves pressurizing a grout, typically a fairly viscous fluid, into a fractured rock mass. Because the rock is close to an excavation, and an excavation at considerable depth, it is probable that the rock into which the grout is injected is in a highly anisotropic state of stress. Typically, one normal stress component, the radial stress, is likely to be relatively low, while another one, the tangential stress, might be relatively large, unless stress relief due to slip along discontinuities or due to rock fracturing has reduced it, or unless the virgin pre-construction stressfield is highly anisotropic. The stress component parallel to the excavation is most likely to be in between the two mentioned previously. Predicting the effects of injecting grout into a fracture system within a rock stressed in this configuration is far from trivial, because it involves a complicated interplay between grout injection, a three-dimensional fracture geometry and a three-dimensional stressfield. The objective of grouting, in this particular case, being to reduce the hydraulic conductivity of the rock, requires a careful weighing of factors that might increase the hydraulic conductivity as well as factors that reduce the conductivity.

BEST COPY AVAILABLE

Of particular concern in this regard is the possibility that grout injection might displace rock blocks into the excavation, thus increasing the effective hydraulic aperture along the affected fractures. Similarly, partial filling of a fracture might increase the aperture beyond the tip of grout penetration, thus increasing, rather than reducing, the conductivity, especially if the opened discontinuity were connected to other fractures. Finally, grout injection at excessive pressures could readily induce new fractures, particularly so around openings excavated in a rock mass in which the virgin stressfield already is markedly anisotropic.

The experimental work reported on here addresses primarily the issues of grout distribution along a fracture perpendicular to an applied stress, and the influence of grout injection pressure (relative to the applied pressure) on sealing effectiveness of the grouting.

Grouting has most frequently been performed to reduce seepage under dams and into underground excavations. In most cases, no detailed hydrogeologic assessment is made of the effectiveness of the grout job in reducing the permeability of the rock mass. Instead, the quantity of grout injected is used to infer how watertight the grouted rock is.

The primary objective of this investigation is to assess the watertightness of grouted fractures in rock, using permeability measurements. Ordinary Portland cement grout has been chosen as a grouting material since it is commonly used in grouting and is widely accepted as being a durable sealant. Rock samples containing a single fracture have been subjected to a normal stress and pressure-grouted. Permeability measurements taken before and after grouting assess the reduction in permeability due to grouting. All experiments performed to date have been performed in the laboratory.

One phase of this laboratory research involves the characterization of cement-based grouts. Two sedimentation stable cement-bentonite mixes and three neat cement mixes have been designed. Uniaxial testing has been performed to determine the effect of bentonite on the grout compressive strength. Bleed testing has been performed to verify that the stable mixes were properly designed and prepared.

A subsidiary phase of this research involves the determination of the relationship between normal stress and permeability for each fracture to be grouted. The fractures are loaded, unloaded, and reloaded incrementally to obtain measurements showing the dependence of permeability on normal stress and fracture deformation. This is illustrated with hydraulic conductivity versus normal stress graphs, as well as with a least squares determination of the empirical parameters in various equations that have been proposed to determine the relation between fracture hydraulic conductivity and normal stress across the fracture.

For this study, grouting pertains to the injection of cement into rock fractures for the purpose of reducing their permeability. The use of chemical grouts is not considered since they are assumed not to offer a durable, long-term solution to the problem of fracture sealing. For

BEST COPY AVAILABLE

the following introductory discussion, emphasis is placed on ordinary portland cement (ASTM Type I) (ASTM C150-85a) and bentonite as grouting materials since they were used for this laboratory investigation. These materials have been used widely for rock grouting, i.e. are considered to be well demonstrated technologically, and they are being studied in other phases of this rock mass sealing research.

3.2 Grout Mix Selection

Of prime importance in grouting is the selection of a grout mix that allows for efficient pumping and easy penetration of the slurry into the fractured rock. The mix chosen should also produce a cement that is sufficiently strong, durable, and impermeable upon curing. Among the principal parameters determining these properties is the water-cement ratio of the grout, which, for this study, is defined as the weight of water divided by the weight of cement.

When the water content of a grout is increased, its viscosity is reduced, thereby allowing it to flow easier (Figure 3.1). Increasing the water content also reduces the compressive strength of the grout and enhances the formation of excess bleed water. In addition, the use of an excessive amount of water in a grout mix results in a nondurable cement that is susceptible to leaching and erosion by groundwater. Houlsby (1985b) suggests that exceeding a 3.3:1 water to cement ratio has to raise doubts about grout durability. It is therefore imperative that the minimum amount of water needed for the grout's emplacement be used.

During the mixing of a grout, the cement particles are in suspension with the water. Unless the grout mix is very thick, the cement grains then settle out, a process called sedimentation. The clear liquid that forms at the top of the grout mix as a result of sedimentation is the bleed water. The final volume of bleed water occurring after settlement divided by the total volume of the mix is termed the bleed capacity (Farmer, 1970, p. 22).

Based on its bleed capacity, a grout mix may be characterized as being stable or unstable. From European practice, a mix is considered unstable if its bleed capacity is greater than 5 percent (Deere, 1982). This corresponds to a water-cement ratio of about 0.67 for ordinary Portland cement. Since mixes with water-cement ratios ranging from 1.0 to 4.0 are commonly used in grouting fractured rock [ranges from 1.0 to 8.0 are used, for example, in the deep South African mines (Du Bois, 1978), and the ASCE Task Committee on Cement Grouting (American Society of Civil Engineers, 1962) lists ratios of up to 20, although 0.8 to 5 as the most widely used ones], it can be concluded that most cement grouts are unstable.

The bleed capacity depends somewhat on the particle size distribution of the cement. A reduction in particle size reduces bleeding. However, reducing the particle size is effective only in controlling bleed in relatively thick mixes. To eliminate bleed in the mixes commonly used in fracture grouting, an anti-bleed additive is needed.

BEST COPY AVAILABLE

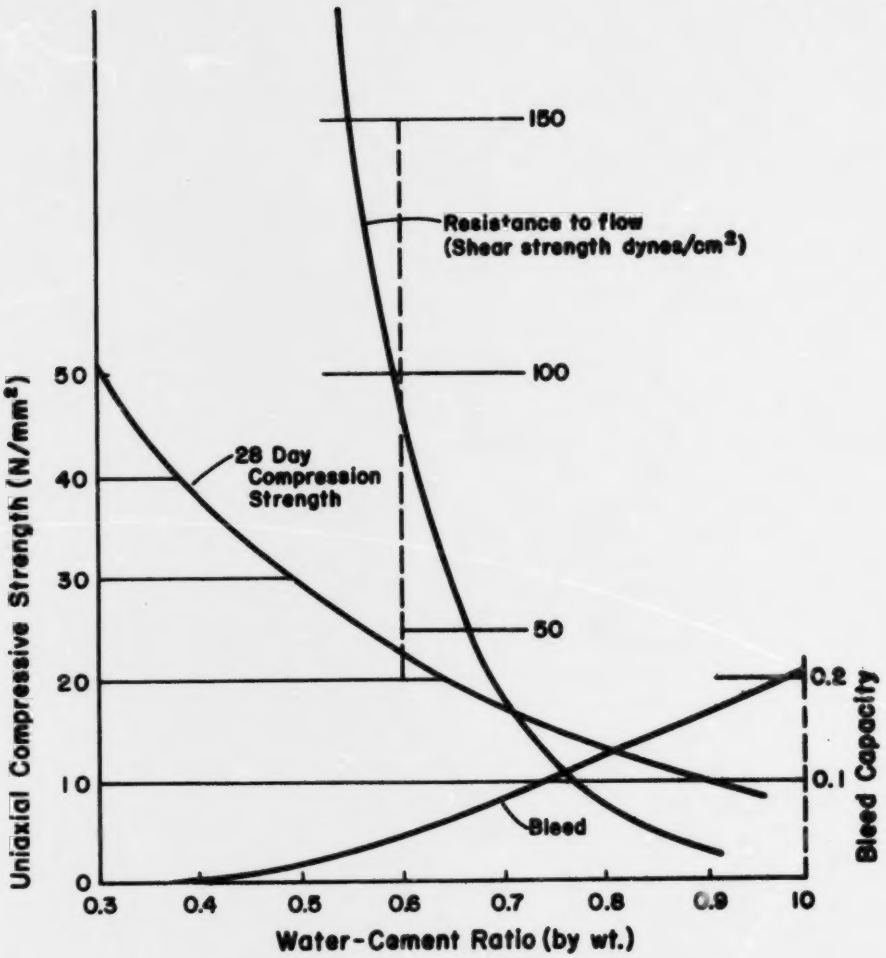

Figure 3.1 Effect of water-cement ratio on grout properties. (After Farmer, 1970, p. 5)

BEST COPY AVAILABLE

One such additive is bentonite. Its use in controlling bleed will be discussed in Section 3.3.

Because the uniaxial compressive strength of a grout depends on its water-cement ratio, it is useful in determining variations in grout quality, a topic discussed in Section 3.4. It may also be used to determine the effect of additives and fillers on a grout mix.

The uniaxial compressive strength of a grout does not necessarily indicate the increase in the strength of a rock mass due to grouting. Any such increase would be due to the bonding of the grout onto the walls of the fracture, making a direct shear test more appropriate. The U.S. Army Corps of Engineers (1956; Kennedy, 1958) performed such tests on fractures grouted in a horizontal position. Based on the test results and visual observations, they concluded that even a very small amount of bleed water prevents good bonding between the grout and the upper fracture surface. Bonding only appeared good when water-cement ratios lower than 0.4 were used.

The uniaxial compressive strength of a grout is indicative of its ability to resist erosion by groundwater, and water pressure has been used, under extreme conditions, as a criterion for minimum strength, if not an indisputable one (Du Bois, 1978). Also important are the aperture and surface characteristics of the grouted fracture, as well as the water pressure and state of stress. Ballivy and Niemants (1982) describe a laboratory test for determining the erosion resistance of a grouted fracture. A cylindrical sample with a fracture perpendicular to its axis is grouted and placed in a modified radial permeameter in which water pressure and axial load can be varied. The stress and flow conditions necessary to cause the wash-out of the grout can thus be determined. Goodman and Sundaram (1980) use a similar apparatus and procedure to study soil piping through rock fractures, Gale and Reardon (1984) to study chemical grout alteration.

In order for a grout to be durable, it must be able to resist leaching by groundwater. The solubility of the grout is an important property. A simple laboratory procedure for determining the solubility of a grout is described by Ruiz and Leone (1970), who give results for two cement type mixes, both with and without clay and pozzolan. Petrovsky (1982) presents details on field investigations of leaching of cement grout curtains at three dams, with curtain ages varying from 4 to 12 years. He concludes that the amount of lime was negligible at all three sites, but cautions that "regional" ground water chemistry monitoring of the type described for these investigations could underestimate localized higher leaching rates.

The cement component most susceptible to leaching is lime. It is formed during cement hydration and contributes nothing to the strength of a grout (Bowen, 1981, p. 25). The solubility of a cement is affected by its water-cement ratio and its curing age. If grout leaching is of concern, a pozzolan may be added to the grout mix. Pozzolans are water-insoluble and chemically active materials that react with the free lime in a cement in the presence of water to form

BEST COPY AVAILABLE

a stable cementitious compound. Examples of naturally occurring pozzolans are pumicite, volcanic glass, opal, and ground calcined clay minerals. Flyash and ground blast furnace slag are artificial pozzolans.

3.3 Cement-Bentonite Grout Mixes

As mentioned in Section 3.1, most mixes used for grouting fractured rock are unstable, in order to give the grout sufficient mobility to penetrate fine fractures. The U.S. Army Corps of Engineers (1956; Kennedy, 1958) found during their laboratory research that the thickest grout that could be pumped through a 0.01 in (0.25 mm) crack had a water-cement ratio of 1.33. Such a grout is neither stable nor durable.

In grouting practice, those who commonly use thin, unstable mixes contend that the excess bleed water is driven off by the pumping pressure and by gravity. However, it is doubtful that the pumping pressure would have any effect in squeezing out water from the grout except in the immediate vicinity of the borehole. Gravity would facilitate drainage of bleed water in steeply inclined cracks but not in near horizontal holes. Even so, numerous bleed pockets would still exist. Hence many feel that the use of sedimentation stable grouts is essential. The U.S. Army Corp of Engineers (Albritton, 1982), among many others, commonly uses bentonite as an anti-bleed additive. Deere (1982) describes cement-bentonite grouting for dam foundations, while Du Bois (1963; 1978) and Holle and Harte (1981) discuss its use in deep, underground excavations. Houlsby (e.g. 1985a) considers the use of bentonite unnecessary, provided first class grout mixes and proper injection techniques are used. Du Bois (1978) cites evidence based on the density measured on grout recovered in cores that the final water content is relatively constant for grouts with a wide range of pumped water:cement ratios, and considers this observation as confirming the driving off of considerable bleed water with pumping pressure and gravity.

When added to a water-cement slurry, bentonite acts as a suspending agent. The bentonite is converted to its calcium-exchanged form as a result of reaction with free lime that is liberated during cement hydration (Jones, 1963). Flocculation of the calcium bentonite then takes place, the gelatinous flocs thus produced prevent sedimentation of the cement particles.

As seen in Figure 3.2, the addition of a small percentage of bentonite greatly reduces bleeding in cement grouts. The addition of bentonite also causes an increase in a grout's viscosity. The viscosity measurements shown in Figure 3.3 were obtained using a Marsh funnel, which gives viscosity in terms of grout flow time. This test is described in Section 3.4. From consideration of both figures, it can be seen that by using only a small amount of bentonite, a grout comparable in viscosity to a stable, neat cement can be formulated. Du Bois (1963) and Borden and Groome (1984) have shown that bentonite can also improve the pumpability of a grout by acting as an internal lubricant.

BEST COPY AVAILABLE

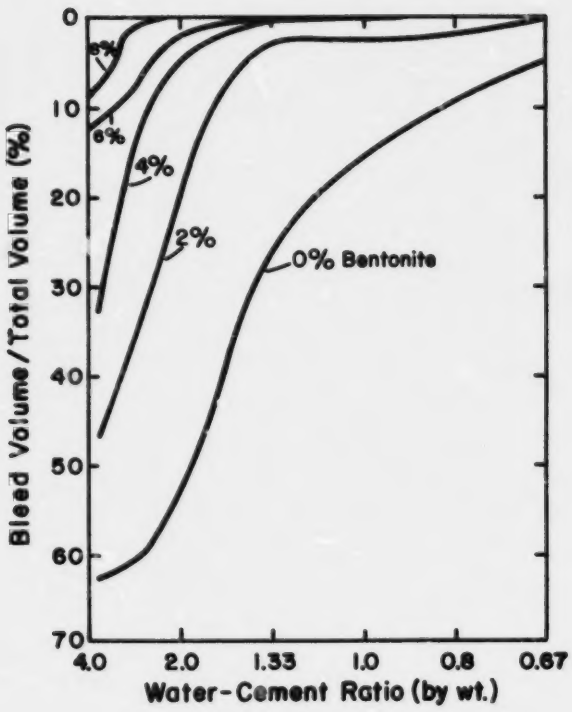

Figure 3.2 Relationship between bleeding and water-cement ratio. (After Burgin, as referenced by Deere, 1982)

Reproduced with permission from Grouting in Geotechnical Engineering, Proceedings of the Conference on Feb. 10-12, Deere, D.U., "Cement-Bentonite Grouting for Dams," 1982, p. 286, American Society of Civil Engineers, New York.

BEST COPY AVAILABLE

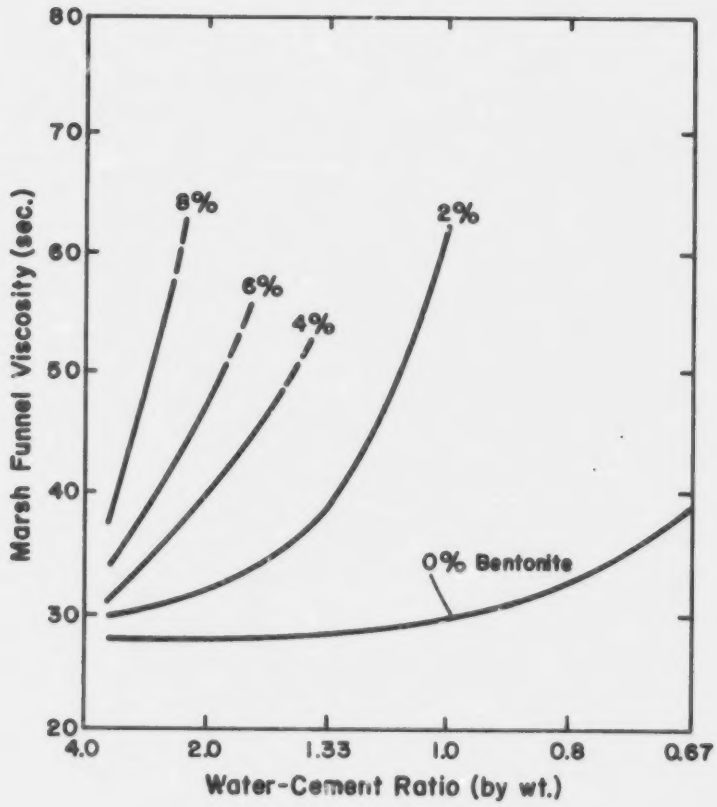

Figure 3.3 Effects of water-cement ratio on Marsh funnel viscosity. (After Burgin, as referenced by Deere, 1982)

Reproduced with permission from Grouting in Geotechnical Engineering, Proceedings of the Conference on Feb. 10-12, Deere, D.U., "Cement-Bentonite Grouting for Dams," 1982, p. 286, American Society of Civil Engineers, New York.

BEST COPY AVAILABLE

An advantage of using bentonite as an anti-bleed additive is that it will not significantly affect the setting and hardening time of a cement grout. A major disadvantage reported by Deere (1982) is that bentonite reduces the uniaxial compressive strength of a hardened grout mix. This is attributed to the fact that the final water-cement ratio of an unstable mix after bleeding will be lower than that of a stable mix. However, this effect is considered negligible for the thicker of the mixes shown in Figures 3.2 and 3.3. Nonveiller and Habekovic (1961) argue that almost any grout strength is sufficient, if sealing only is the objective of the grouting. Du Bois (1978) observed uniaxial compressive strengths essentially independent of bentonite contents up to 2%. Wallner and Wittke (1974) and Wallner (1976, p. 54) state that a small (3%) bentonite content has an insignificant effect on the strength of (thick, stable) grout. Heise (1973, Section 3.7.1) observed a 10% decrease in tensile strength with 5% bentonite, 29% with 10% bentonite, and 66% with 15% bentonite over a water:cement ratio range from 0.5 to 5.

3.4 Grout Quality

The uniaxial compressive strength of a grout depends on its water-cement ratio and thus is useful in evaluating the influence of any variation in the proportions of cement and water used in a mix from those specified in the grout design. Other variations, such as those arising from the quality of the cement and its storage and mixing, can also be determined. For this study, testing was performed to determine the effects of pumping as well as the effect of bentonite on compressive strength.

The relative variation of a set of test results is assessed using the coefficient of variation, the standard deviation as a percentage of the mean. For a compressive strength representing the mean of three tests performed in the same laboratory, ASTM designation C109-80, note 10 (ASTM, C109-80) states that, "the single-laboratory coefficient of variation has been found to be 3.8 percent." This test method is for a standard cement mortar containing sand. Nonetheless, this kind of precision may be obtainable for grouts with minimal bleed water if good laboratory procedures and equipment and high quality materials are used.

As shown in Figure 3.3, the viscosity of a grout depends on its water-cement ratio and its bentonite content. A simple device for determining the apparent viscosity of a grout slurry consists of a standardized funnel. The time it takes for a standard volume of grout to pass through the funnel is measured. The funnel is calibrated by determining the flow time of an equal volume of water. The two most commonly used funnels are the Marsh Funnel (American Petroleum Institute, 1985, standard RP13B) and the Portland Cement Association flow cone (ASTM C939-81). Lombardi (1985) presents a detailed analysis of cone flow, stressing the need to take into account cone wall rugosities, and proposes the use of a simple plate cohesion meter to obtain a more complete definition of grout rheology than can be obtained with funnels only.

BEST COPY AVAILABLE

The flow cone test can be performed rapidly in the field. Thus, it can be used to check the quality of a freshly mixed batch of grout. Although it only measures the flow time of a grout, according to some authors it can be calibrated against plastic viscosity and yield point determinations obtained from a viscometer (Deere, 1982; Farmer, 1970, p. 17). Lombardi (1985) demonstrates that at least one additional measurement type is required to make such a correlation. Heise (1973, Section 3.5.3) found excellent correlation between Marsh and Fann viscosities for water-cement ratios over 3 for cement only suspensions, as well as for water-cement ratios over 2 in the presence of 5% bentonite. For water-cement ratios less than 1, no direct correlation was found.

3.5 Filter Blockage of Cement Based Grouts

The particulate nature of a cement places an absolute limit on the size opening that can be grouted. When such grouts are injected into a fracture, the larger particles can be filtered out of suspension by flowpath constrictions. Once this happens to even a small number of particles, blockage of the flowpath occurs, resulting in the premature refusal of cement by the fracture.

Shown in Figure 3.4 are the grain size distributions of three different types of cement. Also shown is their specific surface area, an alternative way to express the grain size of a cement. Of greater significance is the maximum particle size of the cement, since the largest particles are chiefly responsible for filter blockage. For ordinary portland cement (ASTM C150-85a), the largest size usually 100 is μ or more.

An important investigation concerning the groutability of fine fractures was performed by the U.S. Army Corps of Engineers (1956; Kennedy, 1958). The purpose of the study was to determine the lowest water-cement ratios for different cement-based grouts that could be used to penetrate fine fractures. Fracture specimens 0.25, 0.50, and 0.75 mm (0.01, 0.02, and 0.03 in) wide were constructed from concrete slabs and held open with shims to obtain the desired thickness. Grouting pressures of 0.17, 0.34, and 0.69 MPa (25, 50, and 100 psi) were used to pump neat cement grouts and cement grouts containing different additives. The 0.5 and 0.75 mm (0.02 and 0.03 in) cracks were all groutable using thick mixes. For neat cement, the lowest water-cement ratio that could be used to penetrate a 0.25 mm (0.01 in) crack was 1.33. Increasing the pumping pressure from 344 to 689 kPa (50 to 100 psi) did not allow a reduction in the water-cement ratio. Grouts containing flyash could not be pumped through a 0.25 mm crack.

The results for the 0.25 mm crack were attributed to filter blocking of the fractures by the grout particles. Sieve analysis showed the maximum particle size of the cement to be 0.15 mm (0.006 in). By considering the ratio of the fracture width to the maximum particle size as a blockage criterion, it was concluded that the limit of groutability occurs when this ratio is 1.7. The flyash could not be pumped since it had a maximum particle size greater than 0.25 mm (0.01 in).

BEST COPY AVAILABLE

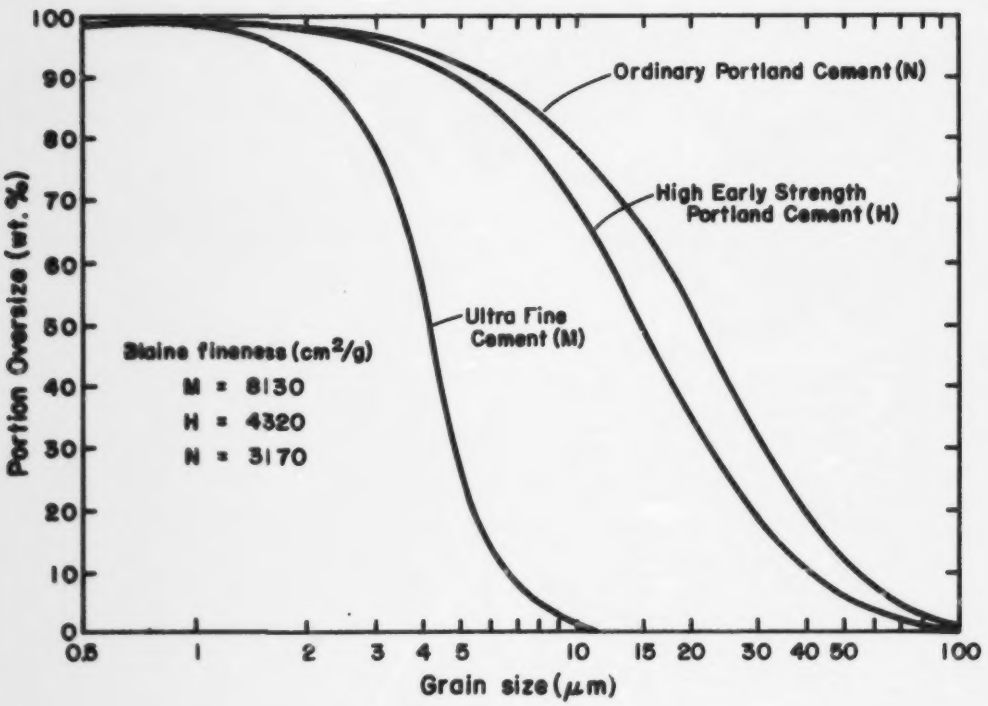

Figure 3.4 Grain size distributions for three types of cement. (After Shimoda and Ohmori, 1982)

Reproduced with permission from Grouting in Geotechnical Engineering, Proceedings of the Conference on Feb. 10-12, Shimoda, M. and H. Ohmori, "Ultra Fine Grouting Material," 1982, p. 286, American Society of Civil Engineers, New York.

BEST COPY AVAILABLE

Since the fractures used in this research were open, the above conclusion pertains to slot-like openings of great lateral extent. The Corps of Engineers also states that a groutability ratio of 3.0 or more would be safer. This result was obtained from the mineral processing field where the largest ratio of filter opening to maximum particle size necessary to cause filter-cake formation is generally regarded as 3.0.

Sabarly (1968) considers the fraction of oversize particles, i.e. cement particles with a size equal to or longer than the fracture aperture, and considers a 0.2% oversize fraction as unacceptable. He considers a groutability ratio of 2 fully acceptable. A minimum fracture width of two or three times the particle size is considered necessary for proppant injection in hydraulic fracturing (e.g. Daneshy, 1978).

Heise (1973, Section 4.2) found that no standard cement grouts could be injected in fractures with apertures of 0.1 mm, that all grouts [i.e. wide range of water, cement, bentonite (and other additives)] could be injected easily in 0.3 mm aperture models, and that 0.25 mm fractures required high pressure, removal of all particles over 100 μm, considerable bentonite (or plasticizer) addition, or some combination of these measures. Ordinary portland cement showed pronounced fingering.

Wittke et al. (1978, Section 4.1) obtained excellent penetration of 0.1 mm aperture models with very thick grouts in which various fractions (0 to 33%) of the cement had been replaced by blast furnace flyash, to which 3% bentonite had been added, and which had been sheared intensely. Cores drilled at a field site subsequent to grouting revealed several cement grout layers of about 0.1 mm, confirming the feasibility of grouting very fine fractures.

A laboratory study on groutability ratios was conducted by Crawford and Groskopf (1984). Glass ballotini, serving as particulate grout, was passed through glass capillaries and open rock fractures by means of dry vibration and hydraulic flow-through tests. Results are in general agreement with those of the Corps of Engineers in that filter blockage occurred in the capillaries at groutability ratios less than 3 and in the fractures at ratios less than 2.

Lau and Crawford (1986, p. 119) conclude from their parallel plate experiments that the groutability ratio should be greater than 3, and that the use of a maximum particle size alone may not be sufficient to define groutability. They state that the minimum groutability ratio also will be a function of joint aperture, cement type, water:cement ratio, hydraulic gradient, and the presence and dosage of superplasticizer.

Bowen (1982, p. 42) and Consulting Engineer (1969) state that the minimum crack width that can be grouted with ordinary portland cement is 0.1 mm (0.004 in), which is about its maximum particle size. Wallner (1976, p. 57) references several German studies that confirm 0.1 mm as the minimum groutable fracture width for ordinary cement

BEST COPY AVAILABLE

suspensions, and Wittke (1969) gives the same value for stable fluidized cement-bentonite pastes. Wallner and Wittke (1974) obtained satisfactory penetration with an extremely thick (37% water content) plasticized cement paste, at very low injection pressures, in 0.1 to 0.2 mm wide fracture models. However, from the preceding discussion it would appear that such fractures may not be groutable unless pumping pressures sufficiently high to cause fracture widening are used. This topic will be discussed in Section 3.6.

From the preceding discussion it is evident that ordinary portland cement will not penetrate very fine fractures. Such fractures may be the dominant kind found at depth. Snow (1968), using the method described in Section 2.3.2, found average fracture apertures at 61 m (200 ft) depth to be about 50 μm. Scott (1969), using single fracture measurements, determined that the average fracture aperture for a limestone at 2000 ft (610 m) was 33 μm. It should be pointed out that these are hydraulicly determined apertures unlike the actual crack widths just presented. The equivalent aperture represents a distribution of opening sizes (Section 2.2) and is, at any rate, smaller than a measured crack width because of the assumptions regarding flow through smooth, parallel plates. Nonetheless, apertures as small as these are probably not groutable unless very high grouting pressures are used. Yet, as will be illustrated in Section 3.6, these fine fractures may allow significant rock mass permeabilities, potentially significant at least within the context of HLW repository sealing performance.

It thus becomes apparent that an alternative grouting material may be needed to seal rock fractures at repository depths. One alternative is high early strength Portland cement (ASTM Type III) (ASTM C150-85a). Typical grain size characteristics are included in Figure 3.4. Improved penetrability may be obtained by using Type III cement since it is finer than ordinary portland cement. However, as indicated by Farmer (1970, p. 7), it is more susceptible to shrinkage and cracking. Ruiz and Leone (1970) tested the fraction of an ordinary portland cement obtained from a dust collector at the cement mill. This cement has a Blaine fineness of about 5000 cm^2/gm. Little is known about its durability. Ultrafine cement would offer much improved penetrability since its maximum particle size is about 10 μm (Figure 3.4). However, this type of cement is considered to be extremely sensitive to air hydration and carbonation making it difficult to store for periods longer than 7 days (Farmer, 1970). Likewise, it is not considered to be durable. Wittke et al. (1978) reject its use because of excessively fast and difficult to control setting time. A description of its properties and its use is given by Shimoda and Ohmori (1982) and by Clarke (1984). Moller et al. (1983) and Clarke (1984) present a case study of its application in a fractured rock around an underground (tunnel) plug. Chemical grouts, since they are fluids that can be made to have a low initial viscosity, offer the best penetrability, but are not considered to be durable.

BEST COPY AVAILABLE

3.6 Grouting Pressures

Grouting is performed at pressures that are high enough to provide for an ample flow of grout over a relatively large pentration radius. This can lead to expansion of the fracture, and is used to improve penetration of cement grout. The question as to when the use of excessively high pressures causes irreparable damage to the rock mass is of concern.

Vaughan (1963) illustrates the relationship between mean fracture aperture and permeability for a set of parallel, planar joints at various spacings. The results were derived with equation 2.5. Although this is probably not an accurate indication of the permeability of a rock mass, it does provide, at least for continuously jointed rock, lower bound permeability values as the addition of other joint sets would increase permeability. At a permeability of 10^{-4} cm/sec (10 Lugeons), it appears that the apertures indicated are not groutable except for possibly the largest spacing of 1.5 m (5 ft). At lower values, approaching 10^{-5} cm/sec (1 Lugeon), considered the lower limit of groutability, it is clear that none of the apertures can be considered groutable. Since the target values strived for in most grouting projects are within this range, it must be concluded that some degree of fracture widening does occur in practice.

It is common to use a rule of thumb when specifying maximum allowable grout pressures. These range from 6.9 to 2.76 KPa (1 to 4 psi) per ft of depth. The lower value is widely used in American practice and is arrived at by consideration of the weight of the overburden. Since most engineers are primarily concerned with the heaving of the ground surface, this rule of thumb is typically abandoned for a higher one when grouting is performed in sound rock at depth since uplift of the surface is then unlikely to occur. The upper value is widely used by European engineers who have a penchant for displacement grouting. The ASCE Task Committee on Cement Grouting (American Society of Civil Engineers, 1962) presents a chart with a rather wide range of injection pressures, and leaves the issue largely unresolved.

Cambefort (1977) discusses the use of high grouting pressures in displacement grouting. He states that pressures must be high enough to cause fracture widening. This allows the cement to fully penetrate the fracture. When the pressure is discontinued, the rock springs back and compresses the cement. Thus, a perfectly sealed fracture is formed. Cambefort also discusses "claquage" grouting. A "claquage" is simply a hydraulic fracture which can be permeated with grout as it is propagated. It is postulated that such fractures will not propagate far since they will be terminated by the presence of other fractures. These "claquages" are believed to form a highly effective water barrier since they will intersect one another if initiated from different points in a number of boreholes.

Sabarly (1968) agrees that the differences between American low pressure and European high pressure practice might have developed to a significant extent in response to differences in grouting procedures,

BEST COPY AVAILABLE

in particular American emphasis on large volume pumping, with a grout recycle circuit. This point of view is endorsed by Deere (1982), who also points out that the differences might be far smaller in actual practice than as perceived from the generally cited "rules".

Vaughan (1963) discussed the water pressure testing of a shale after curtain grouting. The initial permeability of the shale was at about the limit of groutability for ordinary portland cement. Both high and low pumping pressures were used. The area where grouting was performed with low pressures had about the same permeability as before grouting and there was little evidence of any grout having been injected. The area grouted with high pressures showed some increase in permeability, and there was evidence that the rock had been fractured. Although these results were obtained from very limited information, it appeared that grouting with fracturing pressures had done more harm than good.

Attempts have been made to develop a method for determining a grout pressure criterion based on hydraulic fracturing theory. The first investigation into the feasibility of using such an approach was conducted by Morgenstern and Vaughan (1963). Their analysis did not consider the disturbance of the in-situ stressfield by the borehole.

Wong and Farmer (1973) discuss mechanisms governing hydraulic fracture initiation and propagation. They consider the effect of the ground porosity on fluid pressure and attempt to quantify the fractions of fluid force used to expand the borehole and induce seepage flow. Hydrofracture propagation is analyzed using an energy balance approach. Their method is applicable to the case of a vertical borehole about which both horizontal principal stresses are equal.

Some of their significant conclusions were:

(a) In weak, fractured rocks and soils, hydrofracture initiation will occur at a pressure close to the overburden pressure.

(b) In competent rocks, depending on their tensile strength, the initiation pressure will be greater.

(c) Pressures much greater than the initiation pressure are needed to propagate a hydrofracture a short distance from the borehole. This is due to the fact that only a small portion of the grout pump energy is available to extend the fracture.

3.7 Fracture Grout Penetration Model Studies and Analyses

Model studies and theoretical analyses of grout penetration along fractures have clarified grout penetration mechanisms, and have identified many of the remaining difficulties associated with predicting penetration. The models and theories remain exceedingly simplified compared to the in-situ grouting of fractured rock, as emphasized and detailed, for example, by Ewert (1979). It probably is not unfair to compare the present state of the art of fracture grout penetration modeling and predicting to that of parallel plate water flow studies of about a decade ago (Section 2.2).

BEST COPY AVAILABLE

The previously referenced Kennedy (1958) reports on an extensive series of parallel plate flow studies performed by the U.S. Army Corps of Engineers (1956). Neat cement, cement with flyash, with an intrusion aid, with calcium lignosulfonate, with flyash and calcium lignosulfonate, with slag, with pumicite and with calcined shale have been tested for a continuously varying water:cement ratio from relatively thin to very thick. Crack size that can be penetrated has been determined as a function of injection pressure and grout consistency. Extensive grout characterization (consistency, bleeding, setting time, solubility) has been performed in conjunction with the flow tests. Important conclusions of this classic and trailblazing investigation have been repeatedly quoted throughout this report. A few additional ones are mentioned briefly here. Rough surfaces substantially increased the minimum water-cement ratio needed to allow flow. Maximum grain size of the solids provided a good indication of minimum crack width that could be grouted. Pressure drops along the (straight line) flowpath were markedly nonlinear, even for most of the relatively thin mixes, for the thin (0.025 mm) cracks, but tended to approach a straight line for wider (0.05 and 0.075 mm) cracks. Visual inspection of grout distribution showed a clear correlation between water content and uniformity of grout distribution, with all thin mixes showing stringy patterns with highly localized grouting only, i.e. with numerous bleed channels. Little general correlation was found between viscosity and pumpability. Only very limited squeezing out of excess water was observed. It appears that the flow data base provided might be sufficient to warrant further analysis in terms of non-Newtonian flow modeling of the results.

Houlsby (1985) reports on penetration tests between concrete slabs performed by the N.S.W. Australia, Water Conservation and Irrigation Commission in 1962. The simulated cracks were tapered from 1.5 mm to 3 mm, and radial grout flow was induced. Considerable attention was paid to mixing and pumping. Numerous bleed paths persisted in most tests, and crack filling typically was very incomplete, although significantly better with thick mixes.

Wittke (1968) develops a Bingham fluid model for penetration of a stable thick cement-bentonite grout from a borehole into a single parallel plate fracture with impermeable walls. Wittke identifies the numerous simplifying assumptions made in order to derive a close form solution, notably steady state conditions, including constant grout properties, and derives an elliptical propagation front as a function of fracture inclination, grout shear strength and viscosity, fluid pressure in the fracture, and injection pressure. Parallel plate tests for a quite thick (water content of 37%) cement bentonite grout with 3% bentonite on horizontal and inclined fractures show qualitative agreement with the proposed predictor equation, and excellent quantitative agreement if the shear strength is adjusted (i.e. modified from viscometer measurements) by a factor of nearly four. Wallner (1976, p. 60) explains the deviation on the basis of inadequate (i.e. different) grout preparation for the two shear strength measurements, emphasizing the critical importance of mixing and pumping control.

BEST COPY AVAILABLE

Ruiz and Leone (1970) performed extensive viscosimetric characterization tests on two portland cements with substantially different size ranges mixed with various contents of artificial pozzolan, clay and commercial Intrusion Aid. They summarize the results in terms of the Bingham fluid yield stress and plastic viscosity. These parameters were essentially constant for water to cement ratios exceeding 0.9, and increased rapidly for lower ratios. The yield stress was reduced substantially by 0.5% of the Intrusion Aid. Theoretical predictions of grout depth penetration are performed by integration of a radial Bingham fluid flow equation. Sedimentation, and its considerable influence on grout strength, was investigated by parallel plate flow studies.

Wallner (1976) (summarized in Wallner and Wittke, 1974) identifies limitations of a few grout penetration equations developed prior to his work, including Newtonian, Bingham, empirical, and pseudo-plastic material models. For thick grouts he considers the Bingham fluid most appropriate, and develops equations for two- and three-dimensional propagation, including transient (time-dependent) effects. Included is a finite element model for flow into rock with multiple open fractures. The theoretical models have been used to analyze a variety of parallel plate flows, including various boundary conditions (e.g. constant (injection) pressure, constant volume, gradual pressure build-up), fracture apertures and orientations, as well as variable (converging) apertures and intersecting (branching) fractures. Parallel plate flow tests have been conducted to evaluate the theoretical models by injecting cement paste, after tightly controlled preparation, mixing, and shearing in between rigid smooth and rough lucite plates equipped with pressure sensors. Shear limit and viscosity measurements were performed over a range of velocities comparable to the injection rates. The decreasing branch of the viscometer results shows substantial deviations from a Bingham model (Wallner, 1976, Figures 33,35; Wallner and Wittke, 1974, Figure 1), suggesting the likely need for a pseudo-plastic model under at least some flow ranges. The measurements confirm general penetration trends predicted by the theoretical model, as well as nonlinear pressure distributions for converging fracture widths. Instrumentation was not sufficient to allow detailed comparisons. No sedimentation and very little bleeding was observed. Post-test calculations in which parameters were adjusted based on observations made during the experiments allowed close bracketing of the experimental results.

Heise (1973) (which includes an extremely comprehensive literature survey) performed extensive viscosity testing in support of his parallel plate flow tests. He concludes that cement-only suspensions can be considered as Newtonian fluids for water cement ratios larger than 1, as Bingham fluids for smaller water contents, but with pseudoplastic behavior at lower shear rates, and particularly so when bentonite is added. Moreover, bentonite addition causes reproducibility problems, mixing and instrument sensitivity complications, and, in general, considerable uncertainty. Heise further presents observational discussions on some 142 parallel plate grout injection experiments. Monitored pressure distributions on thin mixes suggest Newton fluid type pressure drops. Thin mixes virtually always left a

BEST COPY AVAILABLE

gap near the top of the (horizontal) fracture model, and numerous water channels. Thick stable mixes provided complete uniform crack filling. Penetration depths and pressures deviate significantly from the simplified Bingham fluid calculation according to Wittke (1968), a deviation explained by Heise as probably due to predominantly turbulent flow. No clear correlation was obtained between water and grout volumes injected. Cylinder sedimentation tests were found unreliable in comparison with sedimentation behavior in fracture model flow. Marsh funnel viscosity and particularly flow limit estimates proved highly unreliable, and even rotating viscometers proved not entirely successful in simulating the time and flow dependent changes taking place in the grout required to adequately describe the true flow limits.

Shimooka et al. (1983) briefly mention apparently highly successful grouting of thin fractures in granite stressed to an average repository depth level by means of superfine cement grouts. The success is mentioned as one of the initial results of the Japanese repository investigation program, but neither details nor references are given.

Lombardi (1985) summarizes Newton, Bingham and plastic (extrusion) material models and corresponding smooth and rough parallel plate flow equations. He present a numerical scheme for integrating the equations, thus obtaining pressure distributions, pressure flow relations, penetration and total grout take expressions. By adding a frictional term to the Bingham flow model he points out the increased flow resistance due to the addition of sand to grouts.

Lau and Crawford (1986a), summarized in Lau and Crawford (1986b), performed detailed flow behavior studies for two cement types at various water-cement ratios and with two superplasticizers. The authors present ranges of validity for Newton, Bingham and visco-plastic behavior models, and ranges for sedimentation stability. They derive one-dimensional steady state flow equations for the three material models investigated. Parallel plate model flow studies were performed on joint apertures of 0.425 mm and 0.725 mm, at injection pressures of up to 410 kPa (60 psi). Apparent blockage occurred in some experiments at surprisingly large groutability ratios (Table 7). Flow rates in all parallel plate tests were significantly below the theoretically calculated values, discrepancies explained by the authors on the basis of the fact that the material properties had been determined at shear rates several orders of magnitude below those in the flow tests.

Several studies or proppant distribution along hydraulic fractures bear mentioning, because they have interesting implications for grout penetration and distribution. A comprehensive review of the topic is beyond the scope of this report. The few publications cited here all contain numerous additional references.

Lowe and Huitt (1966) studied sand distribution in fracturing fluids with Fann viscosities and yield points in ranges roughly overlapping with those of thin (Newtonian) and thick (Bingham fluid) cement

BEST COPY AVAILABLE

grouts. Their experiments cover a small particle size to fracture width range (< 0.2), and essentially are equivalent to sedimentation studies in very liquid mixes. Finger formation and duning, i.e. highly nonuniform sand deposition, was observed for particle size to fracture width ratios of 0.1 to 0.8, corresponding to groutability ratios where one would expect easy up to no grout penetration.

Daneshy (1978) uses Newtonian and pseudo-Newtonian (equivalent secant viscosity) models to study sand transport, with emphasis on sedimentation and fluid bleed-off into the formation. He outlines a numerical scheme to estimate sand distribution along a fracture.

An extremely comprehensive and sophisticated numerical treatment is given by Settari and Price (1984). One aspect is the modeling of fluid propagation and particle sedimentation in the form of an isothermal rheological power law relating shear rate to shear stress, specifying the constants as a function of temperature, and entering time-dependent changes as tabular functions, initiated with respect to the mixing time. The approach suggests obvious possibilities for fundamental grout propagation studies.

BEST COPY AVAILABLE

CHAPTER FOUR

EXPERIMENTAL APPARATUS AND PROCEDURES

4.1 Apparatus

The design of this experimental apparatus had as a major objective to allow maintaining a constant normal stress across the fracture while measuring permeability and during grouting. Also important was the capability to vary the normal stress so that cyclic stress-permeability measurements could be obtained. A pump capable of delivering small quantities of cement at high pressures was needed so that tight laboratory-size fractures could be grouted.

Normal loads are applied to the rock fracture using a load frame and hydraulic jacking system, shown in Figures 4.1 and 4.2. The load frame was designed (Cobb and Daemen, 1982) for a 100 ton (90.7 metric ton) capacity. The hydraulic jacking system consists of an Enerpac EH-80 hand pump, a shut-off valve, pressure gauge, and either a 50 ton (45.4 metric ton) Magnus or 100 ton (90.7 metric ton) Enerpac JSL-1002 lifting cylinder.

Permeability testing is accomplished with a falling head permeameter using either a 50 or a 5 ml buret (Figures 4.1 and 4.2). A falling head test was chosen because a low pressure is desirable to ensure a laminar flow. A radial flow model is used as it facilitates experimental control (Iwai, 1976, pp. 93-94).

The grout pump is a simple positive displacement piston pump driven by nitrogen gas (Figures 4.1 and 4.3). It has a capacity of 200 cc (12.2 cu in) and can deliver pressures in excess of 13.8 MPa (2000 psi).

To facilitate the making and breaking of connections during the grout test, cutaway platens are used to transmit load (Figure 4.4). Although this creates an asymmetric loading condition, the upper half of the rock sample is made sufficiently thick to ensure that the load is uniformly distributed on the fracture plane. The lower platen transmits load directly to the rock and is designed so that the grout tube can be attached and removed by turning it 90 degrees (Figure 4.5).

4.2 Cement Preparation and Uniaxial Compressive Strength Testing

Initially, two grout mixes were selected. The first mix, hereafter called grout mix 1, has a 0.64 water-cement ratio by weight. This is the maximum water-cement ratio that allows for a stable mix. A second, thinner, mix was chosen to penetrate finer cracks. Grout mix 2 has a water-cement ratio of 1.33 plus 2% bentonite by weight of water to keep it stable.

BEST COPY AVAILABLE

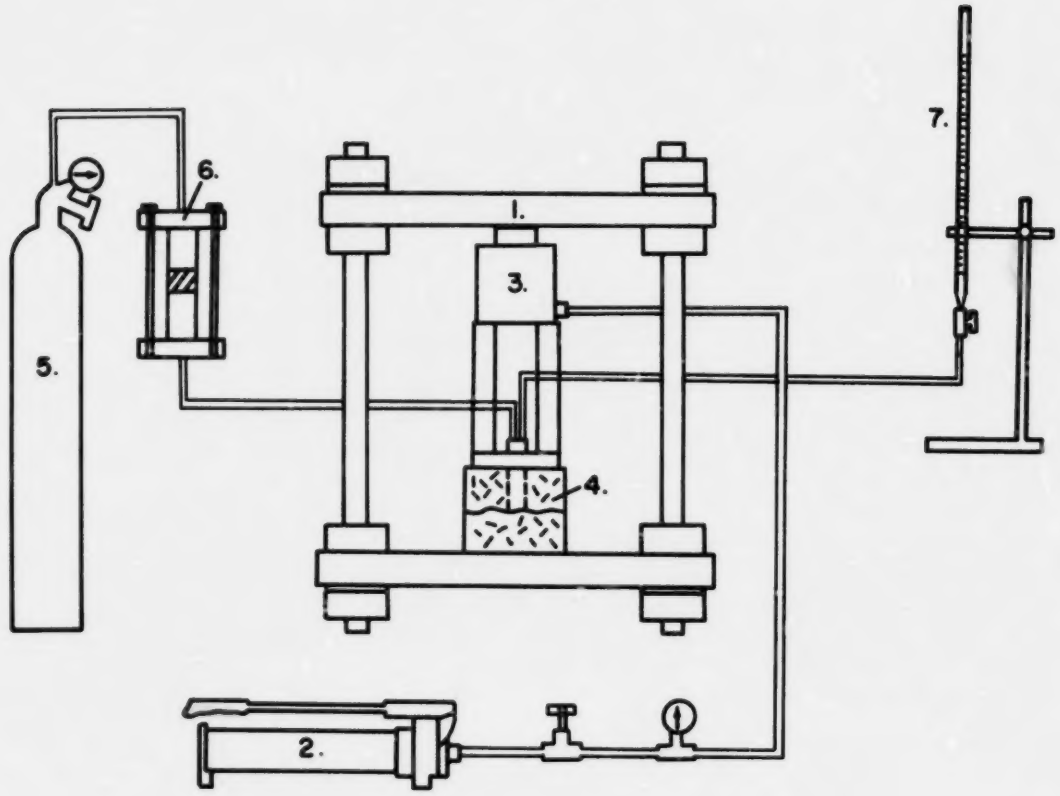

1. - Load frame
2. - Hydraulic hand pump
3. - Hydraulic lifting cylinder
4. - Rock sample
5. - Nitrogen gas tank
6. - Grout pump
7. - Falling head permeameter

Figure 4.1 Schematic drawing of equipment used for fracture permeability testing and grouting.

BEST COPY AVAILABLE

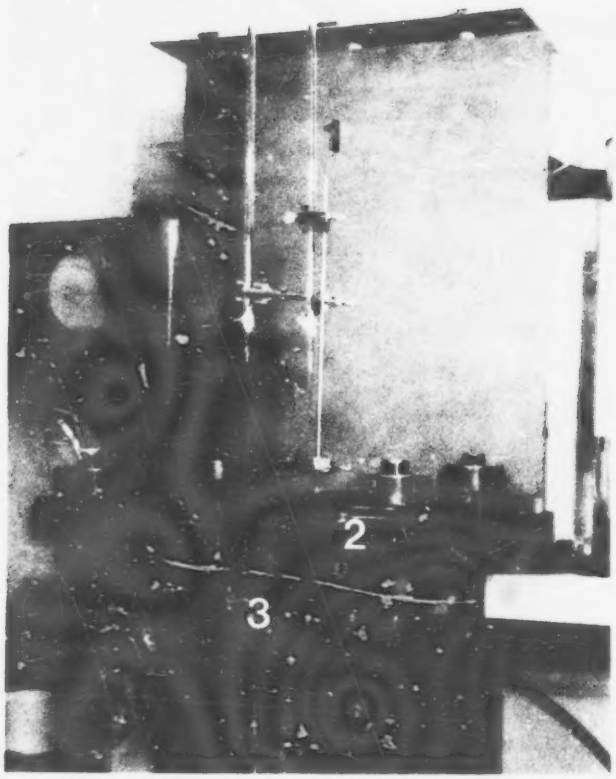

Figure 4.2 Laboratory set-up for permeability testing of rock fracture.

1 - Falling head permeameter
2 - Load frame
3 - Hydraulic lifting cylinder

BEST COPY AVAILABLE

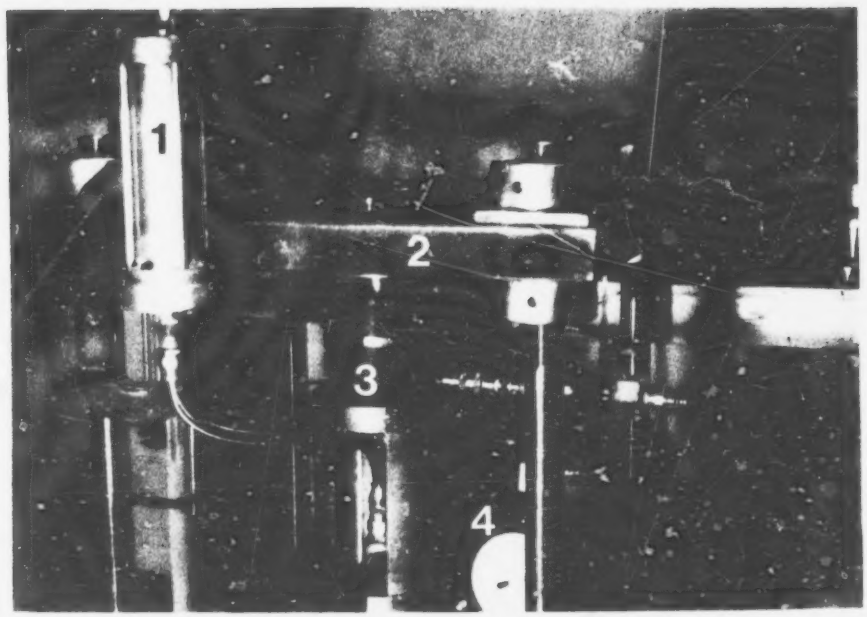

Figure 4.3 Laboratory set-up for rock fracture grouting.

1 - Grout pump
2 - Load frame
3 - Hydraulic cylinder
4 - Pressure gage

BEST COPY AVAILABLE

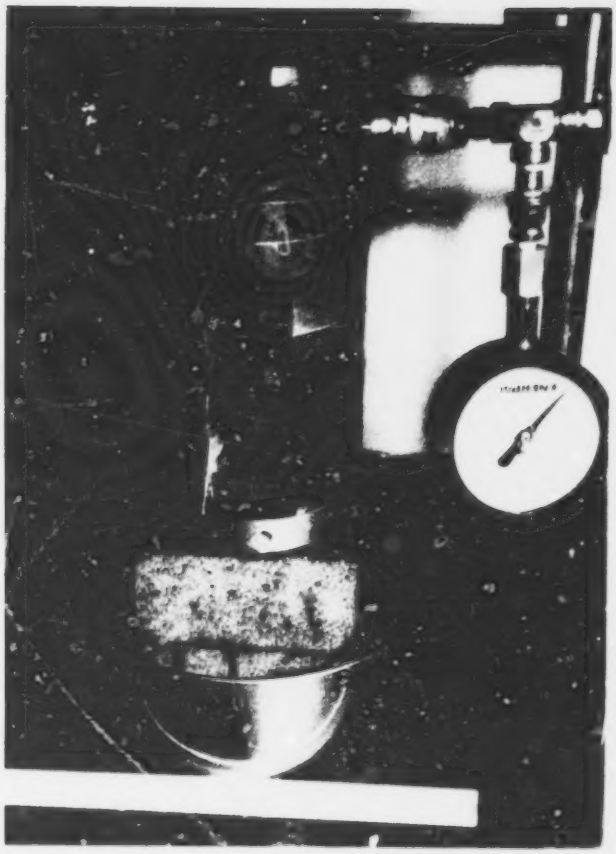

Figure 4.4 Cutaway platens used to transmit load. Connection for falling head permeameter also visible.

BEST COPY AVAILABLE

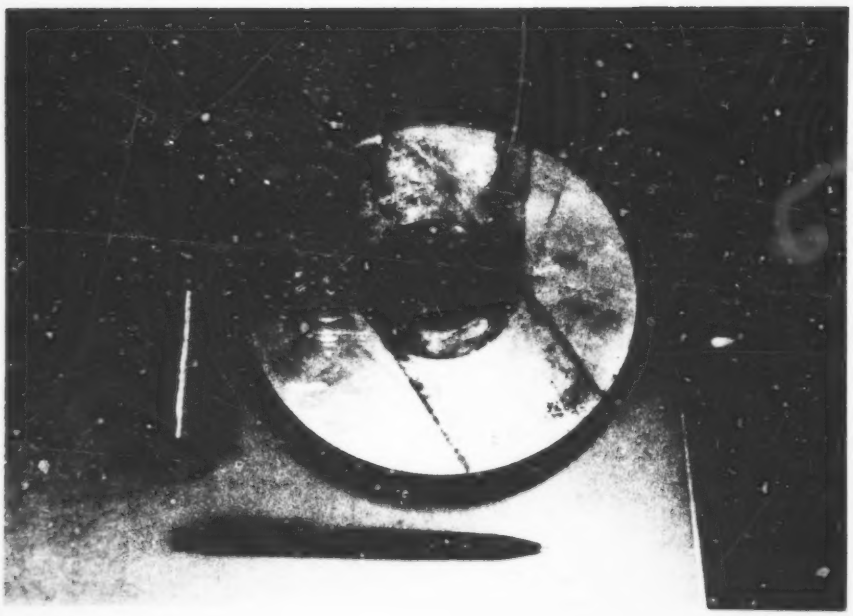

Figure 4.5 Lower platen and grout tube.

BEST COPY AVAILABLE

Because of difficulties encountered when attempting to grout the first four samples, it was decided to select an even thinner grout mix. Grout mix 3 has a water-cement ratio of 2.0 plus 2.5% bentonite by weight of water to keep it stable. Two unstable mixes with the same water-cement ratio as the cement-bentonite mixes were made. Grout mix 4 has a water-cement ratio of 1.33 and grout mix 5 a water-cement ratio of 2.0, corresponding to stable grout mixes 2 and 3, respectively. The compositions of all five mixes, with components shown relative to the weight of the cement, are given in Appendix A, Table A.1.

Grout mixes used for uniaxial testing and grouting were prepared according to API standards no. RP-10B (American Petroleum Institute, 1977) with two modifications. In preparing grout mixes 2 and 3, the bentonite was added to 15% of the water to be used and allowed to hydrate for two hours prior to blending with the cement (Deere, 1982). The blender was then run at high speed for a longer period of time so that thorough mixing could be achieved.

To characterize the uniaxial compressive strength of the grout mixes, specimens were cured in 2.86 cm (1 1/8 in) internal diameter acrylic tubes. Testing was performed after 8 and 28 day curing. Samples with failure loads less than 2.22 kN (500 pounds) were tested on a screw type testing machine using a loading rate of approximately 1.3 mm (0.05 in) per minute in accordance with ASTM standard C39-84 (ASTM C39-84). Samples with failure loads greater than 500 pounds were tested on a hydraulicly operated machine using a loading rate of 2.1 to 4.1 MPa (300 to 600 psi) per minute. A detailed description of the sample preparation and testing procedure is given in Daemen et al. (1983, Ch. 9, pp. 257-262).

4.3 Bleed Testing

Bleed capacities of the stable mixes were determined and a comparison made with their unstable counterparts. The method used involved filling 1000-ml graduated cylinders with grout and noting the volume of bleed water that formed at the top of the column (Deere, 1982). A more rigorous method for determining the bleeding of cement pastes is given by ASTM standard C243-85 (ASTM, 1985b).

The test was performed by placing a 1-liter grout sample in a 1000-ml graduated cylinder and observing the bleed water volume and the total volume. Measurements were continued at selected time intervals in order to determine the rate of bleeding. Each test was run from 2 to 4 hours and was terminated when the volume of bleed water remained constant. The total bleed capacity was obtained by dividing the final bleed water volume into the total volume. Two tests were performed on grout mixes 4 and 5, the only mixes showing significant bleeding.

4.4 Rock Sample Preparation

The first three and the last four samples were 15 cm (6 in) cubes of Charcoal granite obtained from the Charcoal Black Quarry, St. Cloud,

BEST COPY AVAILABLE

Minnesota. The specimens were cut in half. Sawcuts served as artificial fracture surfaces. A different type of saw was used for each of the first three samples. Fractures for samples 8, 9, 10, and 11 were made with the same saw used for sample 1, since the fractures it produced were sufficiently wide to be groutable.

The fourth sample was a 15 cm (6 in) diameter core of marblized limestone from the Escabrosa Formation obtained from the Oracle Ridge Mine, north of Tucson, Arizona. This rock sample, hereafter called Oracle Ridge marble, contained a natural horizontal fracture suitable for testing. The ends of the sample were cut so the top and bottom halves were approximately 7.5 cm (3 in) high.

The fifth, sixth and seventh samples were 22.5 cm (9 in) diameter cores of Grande Basaltic andesite obtained from Sentinel Peak Quarry, Tucson, Arizona (Daemen et al., 1983, Section 4.2, pp. 97-109). A single, diametrical fracture was created in each sample by point loading (e.g. Hoek and Brown, 1980, p. 52). The samples were cut to a length to diameter ratio of 1.5. The sample was then loaded at mid-height across its diameter between two steel points and loaded to failure (Figure 4.6). The sample halves were cut to 7.5 cm (3 in) in height.

A 2.5 cm (1 in) diameter hole was drilled through the top half of each sample to allow for the placement of the grout tube. Two modifications were subsequently made to this procedure. The first modification was made to preclude the formation of a cement plug at the base of the borehole, a plug which for sample 1 prevented measurement of the permeability of the grouted fracture. Subsequent samples had a 1.25 cm (0.5 in) deep hole drilled in their lower half to allow thorough cleaning of the borehole wall at the fracture level. The second modification was made to prevent the formation of a cement ring in the fracture around the circumference of the borehole as observed in sample 2. This was due to the drill breaking a small area of rock as it exited the top half of the sample. Subsequently, the top half of each sample had its borehole drilled from the fracture surface to the outer surface that serves as the top of the sample during testing. The 1.3 cm (0.5 in) deep hole in the lower half of the sample was then drilled using the upper half as a template.

4.5 Determination of Hydraulic Conductivity

A falling head permeameter was used to determine the hydraulic conductivity of the fracture. The unloaded fracture was initially submerged in water for one day in an attempt to saturate it. The hydraulic conductivity along the fracture was then measured while the sample was incrementally loaded, unloaded, and reloaded so the dependence of permeability on normal stress and fracture deformation could be obtained. A sufficient number of tests were run at each stress level to ensure that the rate of head drop was constant. After questionable results were obtained for rock sample 1, it was decided to carry out permeability tests after maintaining the applied stress level for at least one day in order to allow for full saturation and any time-dependent deformation of the fracture to occur. For low

COPY AVAILABLE

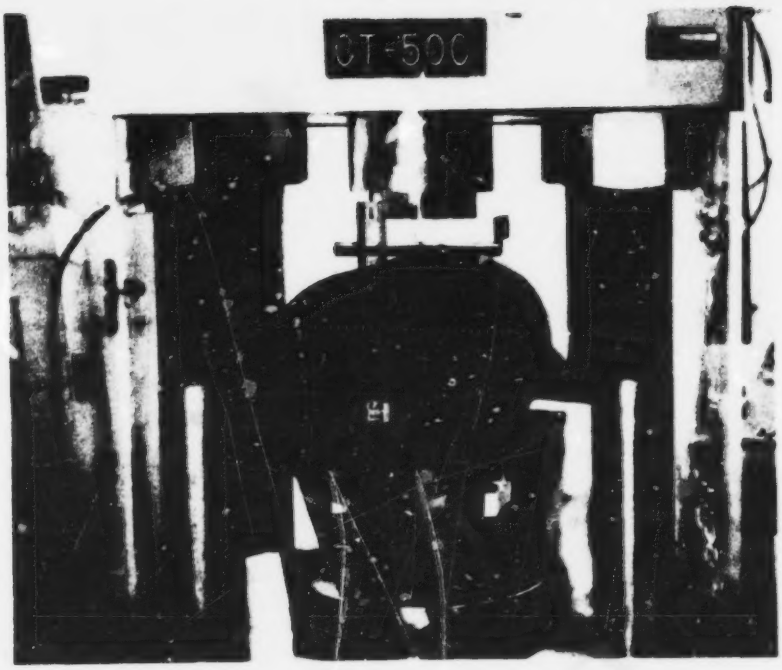

Figure 4.6 A 229 mm (9 inch) diameter core sample of Grande basaltic andesite ready for point loading. The sample is loaded diametrically to failure.

BEST COPY AVAILABLE

flows requiring a long test period, a buret identical to the permeameter was used to measure evaporation.

The hydraulic conductivity for laminar and parallel fluid flow through smooth, parallel plates is defined by Equation 2.1.

For radial flow normal to a borehole, the equivalent parallel plate aperture as determined from a falling head test is given by (modified from Maini, 1971):

$$e = \left[\frac{\ln(H_1/H_2) r_b^2 \ln(R/r) 6\mu}{(t_2 - t_1)\gamma} \right]^{1/3} \qquad (4.1)$$

For straight flow, the equivalent parallel plate aperture becomes (modified from Witherspoon et al., 1979):

$$e = \left[\frac{\ln(H_1/H_2) \pi r_b^2 L 12\mu}{(t_2 - t_1) W \gamma} \right]^{1/3} \qquad (4.2)$$

where:

γ, μ = unit weight and viscosity of fluid,

H_1, H_2 = excess pressure head at beginning and end of test,

t_1, t_2 = time at beginning and end of test,

r_b = buret radius,

R, r = outer and inner radius of a radial flowpath, and

W, L = width and length of the fracture.

The above equations assume idealized laminar flow conditions. Turbulent and nonparallel flow are not considered.

The hydraulic conductivity and the parallel plate aperture were calculated for each test and presented in tables. A plot of hydraulic conductivity versus normal stress illustrates their dependence.

4.6 Fracture Grouting

Upon completion of the permeability testing each fracture is grouted. A 6.9 MPa (1000 psi) normal stress across the rock fracture was applied for the first two samples. It was originally intended to grout at high normal stresses such as those likely to be encountered at repository depths. However, the fracture apertures obtained in the laboratory under such stresses were too tight to be grouted. The

BEST COPY AVAILABLE

normal stress across subsequent samples was reduced so grouting could be performed on a wider fracture aperture.

Once the aperture to be grouted was determined, a grout mix was chosen for use. After examining the results obtained using a 2.76 MPa (400 psi) grout injection pressure on sample 1, injection pressures were raised close to the applied normal stress, since it was believed that increasing the pressure would result in optimal grout takes. During grouting, the pressure was slowly increased to the desired maximum amount in order to avoid surges in the flow of grout. This pressure was then maintained for 5 to 10 minutes. When grouting was completed the grout tube was removed and the borehole thoroughly cleaned. After two or more days curing time, permeability measurements were initiated.

BEST COPY AVAILABLE

CHAPTER FIVE

EXPERIMENTAL RESULTS

5.1 Uniaxial Compressive Strength Testing of Cement Grouts

Uniaxial compressive strength results for the five grout mixes are given in Appendix A, Tables A.2 through A.6. Figures A.1 through A.5 are photographs of the failed specimens. Results for the stable grout mixes 1, 2 and 3 are very consistent as evidenced by the coefficients of variation for unit weights and uniaxial strengths. These results reflect laboratory conditions which can not be expected in the field. According to Farmer (1970, p. 15), good uniaxial compressive strength results for cement grout made on site should have a coefficient of variation no greater than 15 percent. The unstable grout mixes 4 and 5 show a wider variation. Most of this scatter was due to one particular sample in each test set.

The average uniaxial compressive strengths for the grout mixes are given in Table 5.1. The unstable mixes are consistently weaker than their stable counterparts (mix 4 compared to 2,5 compared to 3). The lower final water-cement ratio of the unstable mixes, after bleeding, does not result in a higher strength cement. This is probably due to variability in the compositions of the hardened cement cylinders.

Cement specimens subjected to pumping during grouting were collected from the pump and grout hose and cured for 28 days. Five specimens of grout mix 2 and two specimens of grout mix 3 were tested. Three of the grout mix 2 specimens were obtained from the grouting performed on sample 2 and the other two specimens were obtained from sample 4. The two grout mix 3 specimens were obtained from the grouting performed on sample 6. The grout batches used on rock samples 2, 4 and 6 were subjected to injection pressures of 6.21 MPa (900 psi), 1.24 MPa (180 psi) and 2.07 MPa (300 psi), respectively. The compressive strength test results are given in Tables A.7 and A.8. Photographs of the failed specimens are presented as Figures A.6 and A.7. A comparison with the results in Tables A.3 and A.4 reveals a significant decrease in strength for the pumped cement. Also shown is a slight decrease in the unit weights of the pumped batches. For grout mix 2, Table A.7 shows that the grout subjected to the higher injection pressure is the weaker of the two pumped batches. Although there is no certain explanation for this, it seems that some sedimentation of the cement occurs due to the applied pumping pressure.

5.2 Bleed Testing

Bleed test data for the five mixes are given in Appendix B, Tables B.1-B.5, and photographs of the graduated cylinders at the end of testing are shown in Figures B.1 through B.5. A summary of the total bleed capacities (Table 5.1) reveals that the amount of bleeding is somewhat less than that reported by others (Farmer, 1970; Deere,

BEST COPY AVAILABLE

Table 5.1 Uniaxial Compressive Strengths and Total Bleed Capacities of Grout Mixes

Grout Mix*	8-Day Strength MPa (psi)	28-Day Strength MPa (psi)	Total Bleed Capacity (%)
1	17.49 (2540)	27.77 (4030)	0.3
2	3.32 (481)	5.29 (767)	0.6
3	0.98 (142)	1.54 (224)	0.5
4	2.09 (303)	4.84 (702)	22.5
5	0.70 (101)	1.12 (162)	36.0

*Grout mix compositions are given in Appendix A, Table A.1.

BEST COPY AVAILABLE

1982). This may be due in part to the Dowell dispersant and expansive agent blended in the cement. The results may also have been affected by the grain size distribution of the cement. The grain size distribution of the cement is unknown. The results indicate that the compositions of the three stable mixes could be optimized. In particular, the water-cement ratio of grout mix 1 could be increased and the bentonite contents of grout mixes 2 and 3 decreased with stable, lower viscosity mixes being obtained.

An attempt was made to determine the rate of bleed by taking several readings over time (Tables B.1-B.5). Plots of bleed rate vs. time were constructed for each of the tests performed on unstable mixes (Figure B.6). The plots show that after a constant initial bleed rate, an increase in the bleed rate occurred prior to the end of bleeding. This increase was the opposite of what was expected and may be due to the cement additives. It may also be due to the use of a narrow graduated cylinder in which the rate of settlement is less at the wall than in the center. If such is the case, the ASTM method mentioned in Section 4.3 would be a preferable procedure for determining the bleed rate.

5.3 Fracture flow and Grouting Tests

The sections below give a comprehensive description of the fracture flow and grouting experiments performed on each sample, as well as a description of the grouting performance.

5.3.1 Sample 1

The equivalent parallel plate aperture and the hydraulic conductivity results from the permeability testing of a single fracture in Charcoal granite sample 1 are given in Appendix C, Table C.1. Although the results do show changes in permeability with respect to the applied normal stress, these changes were not nearly as great as anticipated. Possible explanations are that the rock fracture was not fully saturated or that time-dependent deformation of the fracture contact areas took place. As mentioned in Section 4.5, the testing procedure was modified such that a waiting period of 1 day at each stress level is allowed to remedy these problems.

Upon completion of the permeability testing, sample 1 was grouted under a normal stress of 6.9 MPa (1000 psi) and at a grout injection pressure of 2.76 MPa (400 psi). Based on the last permeability measurement at 6.9 MPa, it was decided to grout with mix 1.

The grouted sample is shown as Figure 5.1. The rock fracture accepted grout over limited portions of its area. This fracture had an equivalent aperture of 69 μm (Table 5.2). Based on the limitations of cement particles to penetrate small openings, it can be surmised that the actual widths of the grouted areas are several times larger than the parallel plate aperture (Section 3.5), an average value.

Permeability measurements were attempted to assess the effectiveness of the cement grout seal (Table 5.2). An 0.32 cm (0.125 in) thick

BEST COPY AVAILABLE

Table 5.2 Permeability Test Results Before and After Grouting for Sample 1, Charcoal Granite

Test	Time (sec)	Initial Height (cm)	Final Height (cm)	Aperture (cm)	Hydraulic Conductivity (cm/sec)
Before Grouting:	31.3	127.48	95.08	69.1×10^{-4}	0.354
5 Days after Grouting:	86,400	128.45	128.13	1.01×10^{-4}	7.55×10^{-5}
Retest 6 weeks after Grouting:	46.4	127.48	95.08	60.8×10^{-4}	0.274

Normal stress: 6.89 MPa (1000 psi)
Grout injection pressure: 2.76 MPa (400 psi)
Buret radius: 0.54 cm
Ratio of sample radius to drillhole radius: 6.0
Initial height and Final height refer to water level in falling head permeameter buret.

Figure 5.1 Sample 1 (Charcoal granite) after grouting. The left block shows the 2.5 cm diameter grout hole normal to the "fracture" surface. A sawcut simulates a fracture, and the sawcut asperity pattern governs grout penetration or grout flowpaths.

BEST COPY AVAILABLE

plug had formed at the base of the borehole and prevented measurement of flow through the fracture. As discussed in Section 4.4, the sample preparation procedure was modified to prevent such cement plug formation.

The fracture permeability was retested after the sample had been stored for 6 weeks under room conditions. A 23% decrease in the hydraulic conductivity of the fracture had occurred. Since the sample was removed from the apparatus and re-emplaced, its alignment before and after might not be identical. It is not known whether this had a significant effect on the results. Nonetheless, based on such a meager decrease in hydraulic conductivity, it was decided to raise future grout injection pressures close to the applied normal stress.

5.3.2 Sample 2

The results from the permeability testing are given in Appendix C, Table C.2, and a graph of the hydraulic conductivity as a function of normal stress is presented as Figure C.1. The results clearly show the decrease in permeability with increasing normal stress and the irreversible permeability decreases, presumably due to fracture deformation.

Upon completion of the permeability testing, an attempt was made to grout the fracture under a normal stress of 6.9 MPa (1000 psi) at an injection pressure of 6.21 MPa (900 psi). Based on the last permeability measurement at 6.9 MPa, it was decided to grout with mix 2.

The only grout accepted by the sample was in the area immediately around the borehole wall (Figure 5.2) that was broken when, during sample preparation, the drill exited the top half of the sample. This small cement ring affected the permeability measurements after grouting (Table 5.3). The results show a slight decrease in permeability over time which was attributed to the curing of the cement. Since the purpose of these measurements is to determine fracture groutability and permeability, the sample preparation procedure was modified (Section 4.4) to prevent recurrence of this problem.

5.3.3 Sample 3

The results of the permeability testing are given in Appendix C, Table C.3. and Figure C.2. As for sample 2, the graph clearly shows the decrease in permeability with increasing normal stress and the irreversible decreases in permeability due to fracture deformation.

Upon completion of the permeability testing, the normal stress on the fracture was reduced to 1.38 MPa (200 psi) so grouting could be performed on a wider aperture. The equivalent aperture and hydraulic conductivity prior to grouting are given in Table 5.4. It was decided to try grout mix 2 and use a grout injection pressure of 1.24 MPa (180 psi).

BEST COPY AVAILABLE

Table 5.3 Permeability Test Results Before and After Grouting for Sample 2, Charcoal Granite

Test	Time (sec)	Initial Height (cm)	Final Height (cm)	Aperture (cm)	Hydraulic Conductivity (cm/sec)
Before Grouting:	14,340	119.75	119.20	2.25×10^{-4}	3.76×10^{-4}
After Grouting:					
2 days	86,700	131.26	130.50	1.34×10^{-4}	1.32×10^{-4}
3 days	80,400	130.50	129.86	1.30×10^{-4}	1.25×10^{-4}
4 days	96,600	129.86	129.21	1.23×10^{-4}	1.12×10^{-4}
5 days	72,600	129.21	129.78	1.18×10^{-4}	1.03×10^{-4}

Normal stress: 6.89 MPa (1000 psi)
Grout injection pressure: 6.20 MPa (900 psi)
Buret radius: 0.54 cm
Ratio of sample radius to drillhole radius: 6.0

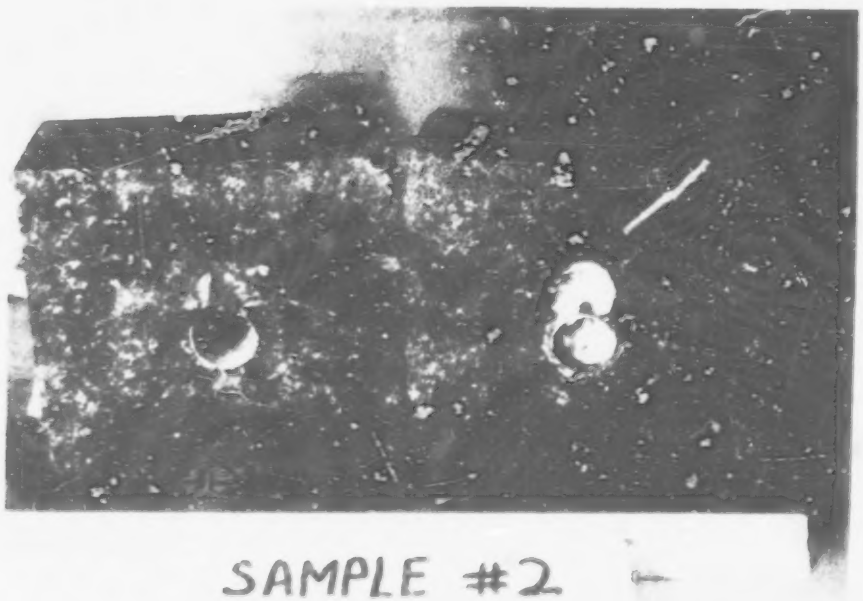

Figure 5.2 Sample 2 (Charcoal granite) after grouting. Only a ring of grout around the borehole was emplaced (white circle on the right block).

Table 5.4 Permeability Test Results Before and After Grouting for Sample 3, Charcoal Granite

Test	Time (sec)	Initial Height (cm)	Final Height (cm)	Aperture (cm)	Hydraulic Conductivity (cm/sec)
Before Grouting:	954	144.86	139.61	11.2×10^{-4}	9.34×10^{-3}
2 Days after Grouting:	25.9	137.61	106.11	--*	--*

Normal stress: 1.38 MPa (200 psi)
Grout injection pressure: 1.24 MPa (180 psi)
Buret radius: 0.55 cm
Ratio of sample radius to drillhole radius: 6.0

*Sample fractured during grouting (Section 5.3.3).

AVAILABLE

Upon reaching the maximum injection pressure, a vertical crack developed through the upper half of the sample and the grout squirted out through it (Figure 5.3). Figure 5.4 shows that except for the lower edge denoted by the arrows and one small area near the upper corner, the fracture extended throughout most of the block. Figure 5.4 also shows that this new crack is well filled with grout. However, subsequent testing revealed that water flowed through the crack at the rate of 30 ml in 26 seconds (Table 5.4). No grout was accepted by the original fracture.

5.3.4 Sample 4

Permeability test results and a graph of hydraulic conductivity versus normal stress for a natural fracture in Oracle Ridge Marble are given in Appendix C, Table C.4, and Figure C.3, respectively. The testing did not yield meaningful results. This may be due in part to difficulties in fully saturating the fracture. For the results indicating smaller apertures, this may also be due to a deviation from the cubic law because, as observed by Iwai (1976, p. 78), of a high degree of fracture contact area for marble (Table 2.1).

Grouting was performed at a normal stress of 1.38 MPa (200 psi) and a grout injection pressure of 1.24 MPa (180 psi) with Grout mix 2. Permeability measurements before and after grouting (Table 5.5) indicate a substantial permeability reduction due to grouting. A small additional decrease in hydraulic conductivity occurred over time, attributed to the curing of the injected cement. Upon removal of the sample from the apparatus, it was apparent that only a small spot of cement had actually been emplaced (Figure 5.5). This small spot restricted the predominant flow path out of the hole. Its effect on restricting flow along the fracture in any other direction probably would have been insignificant.

5.3.5 Sample 5

An attempt was made to obtain cyclic normal stress-permeability measurements (Appendix C, Table C.5). However, upon loading to 6.9 MPa (1000 psi) normal stress, two vertical tension cracks were induced in the sample, resulting in a large increase in the rate of head drop. This may have been due in part to the numerous vesicles in this basaltic andesite.

Grout mix 1 was injected at a pressure of 3.45 MPa (500 psi). The crack in the upper half of the sample is well filled with grout (Figure 5.6), while no grout flowed through the crack in the lower half. Permeability measurements before and after grouting (Table 5.6) reveal a marked decrease in the rate of head drop. No attempt was made to calculate the hydraulic aperture or the single fracture permeability since the flow geometry for the cracked samples was unknown. Measurements with a micrometer show that the grouted fracture is approximately 0.25 mm (0.01 in) to 0.50 mm (0.02 in) wide.

COPY AVAILABLE

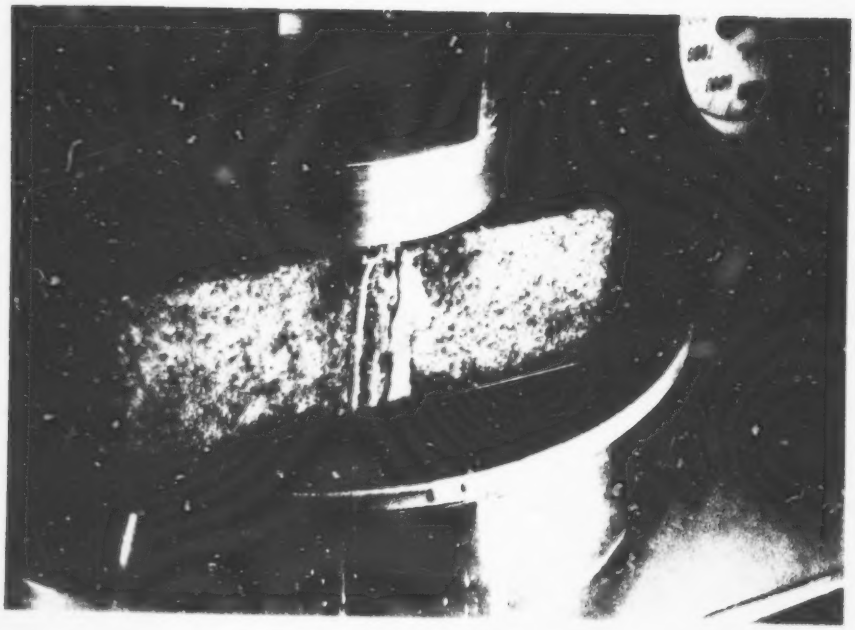

Figure 5.3 Loss of grout through an induced tension crack, sample 3, Charcoal granite.

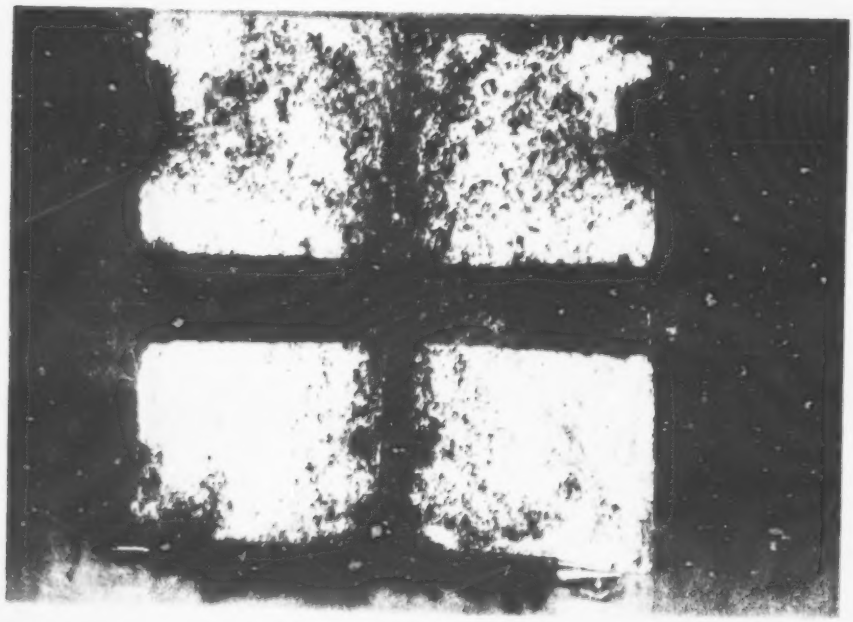

Figure 5.4 Close up of extended tension crack. Arrows denote lower edge of sample normal to fracture surface.

Table 5.5 Permeability Test Results Before and After Grouting for Sample 4, Oracle Ridge Marble

Test	Time (sec)	Initial Height (cm)	Final Height (cm)	Aperture (cm)	Hydraulic Conductivity (cm/sec)
Before Grouting:	92	140.01	129.21	31.3×10^{-4}	7.28×10^{-2}
After Grouting:					
2 days	5220	145.09	144.65	2.75×10^{-4}	5.59×10^{-4}
3 days	10020	145.30	144.55	2.64×10^{-4}	5.17×10^{-4}
5 days	9060	146.06	145.30	2.74×10^{-4}	5.55×10^{-4}
7 days	8700	145.63	144.98	2.64×10^{-4}	5.15×10^{-4}
10 days	8520	147.03	146.49	2.49×10^{-4}	4.59×10^{-4}
14 days	9600	145.63	145.09	2.40×10^{-4}	4.26×10^{-4}

Normal stress: 1.38 MPa (200 psi)
Grout injection pressure: 1.24 MPa (180 psi)
Buret radius: .54 cm
Ratio of Sample Radius to drillhole radius: 6.0

Figure 5.5 Sample 4 (Oracle Ridge marble) after grouting. Small dark area is the only grout emplaced. Light areas denote fracture deformation.

BEST COPY AVAILABLE

Table 5.6 Permeability Test Results Before and After Grouting for Sample 5, Grande Basaltic Andesite

Test	Time (sec)	Initial Height (cm)	Final Height (cm)	Aperture (cm)	Hydraulic Conductivity (cm/sec)
Before Grouting:	31.9	140.01	107.61	--*	--*
2 Days after Grouting:	159	140.01	137.85	--*	--*

Normal stress: 6.89 MPa (1000 psi)
Grout injection pressure: 3.44 MPa (500 psi)
Buret radius: 0.54 cm
Ratio of sample radius to drillhole radius: 9.00

*Flow geometry unknown (Section 5.3.5).

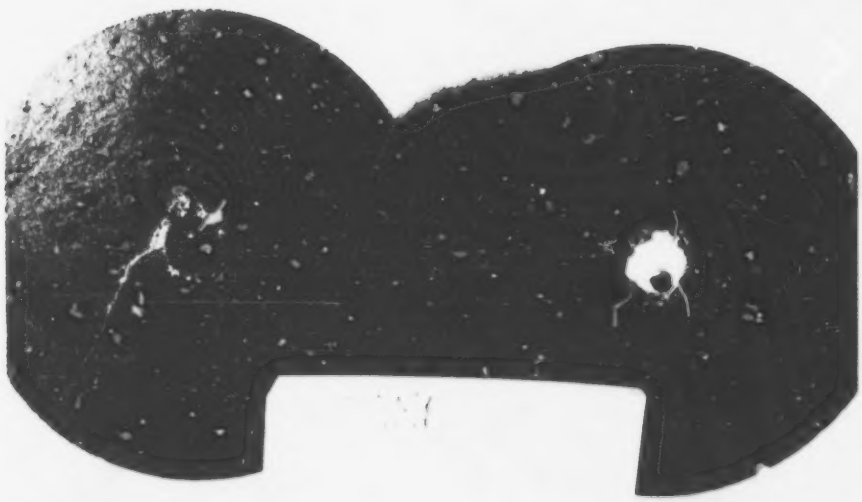

Figure 5.6 Sample 5 (Grande basaltic andesite) after grouting.

AVAILABLE

5.3.6 Sample 6

Permeability test results and a graph of hydraulic conductivity versus normal stress for a natural fracture in Grande basaltic andesite are given in Appendix C, Table C.6 and Figure C.4. The graph shows the decrease in permeability with increasing normal stress and the irreversible decreases in permeability due to fracture deformation. A comparison between the reloading curves of the granite (Figures C.1, C.2) and of the basaltic andesite sample (Figure C.4) reveals that a somewhat greater portion of the basaltic andesite's fracture deformation was elastic as evidenced by the higher position of the reloading curve relative to the unloading curve.

Upon completion of the permeability testing, the normal stress on the fracture was reduced until only a slight, unmeasurable holding pressure was applied to the fracture. This was done to obtain the widest possible aperture for grouting. Grout mix 3 was chosen since permeability measurements revealed that the aperture of the unloaded fracture was still very small (Table 5.7). A grout injection pressure of 2.07 MPa (300 psi) was used.

As can be seen by Figure 5.7, the fracture is well filled with grout. This was unexpected for a 16μm crack. Apparently, the rubber pad between the loading platen and the top of the sample was readily deformable under the slight holding pressure allowing for the lifting of the crack by the pumping pressure. Permeability test results given in Table 5.7 show no reduction in the hydraulic conductivity of the grouted fracture. Possible explanations are that the flow paths responsible for fluid flow through the fracture remained unfilled, that the lifting of the crack resulted in a different alignment of the fracture surfaces upon reseating, or that the flow is determined by the compressibility of the test system.

Figure 5.7 reveals severe grout shrinkage in the large voids around the periphery of the sample. These openings were well filled with grout when the sample was removed from the loading frame. The shrinkage developed within one day exposure to room conditions. The swelling/shrinkage of the bentonite may have been responsible for this behavior.

5.3.7 Sample 7

Sample 7 was severely damaged by fracture generation point loading, making it too leaky to obtain permeability measurements. When grouting was first attempted using grout mix 1, the cement readily ran through the sample under a head of 13.8 kPa (2 psi). The permeability of the sample was still too large to be measured and a second attempt at grouting was made. A cement with a 0.43 water-cement ratio was used. This is the maximum permissible mix used for grouting anchor tendons (Water Resources Commission, 1978). This second attempt did seal the fracture, as evidenced by Table 5.8. Photographs of the grouted sample are presented as Figures 5.8 and 5.9. Even these thick mixes show some shrinkage cracking in the larger voids after only two days exposure to room conditions.

BEST COPY AVAILABLE

Table 5.7 Permeability Test Results Before and After Grouting for Sample 6, Grande Basaltic Andesite

Test	Time (sec)	Initial Height (cm)	Final Height (cm)	Aperture (cm)	Hydraulic Conductivity (cm/sec)
Before Grouting:	145	140.01	137.85	15.6×10^{-4}	1.8×10^{-2}
2 Days after Grouting:	135	140.01	137.85	16.0×10^{-4}	1.9×10^{-2}

Normal stress: 0+ MPa (Seating pressure)
Grout injection pressure: 2.07 MPa (300 psi)
Buret radius: 0.54 cm
Ratio of sample radius to drillhole radius: 9.0

Figure 5.7 Sample 6 (Grande basaltic andesite) after grouting. Note severe shrinkage of grout mix 3 in large voids. Photograph taken after 1 day exposure of grouted surface to room conditions.

BEST COPY AVAILABLE

Table 5.8 Permeability Test Results Before and After Grouting for Sample 7, Grande Basaltic Andesite

Test	Time (sec)	Initial Height (cm)	Final Height (cm)	Aperture (cm)	Hydraulic Conductivity (cm/sec)
Before Grouting*:	--	--	--	--	--
2 Days after Grouting*:	--	--	--	--	--
4 Days After Grouting	456	141.09	140.01	8.4×10^{-4}	5.3×10^{-3}

Normal stress: 3.44 MPa (500 psi)
Grout injection pressure: 13.8 kPa (2 psi)
Buret radius: 0.54 cm
Ratio of sample radius to drillhole radius: 9.0

*Permeabilities too high to be measured.

BEST COPY AVAILABLE

Figure 5.8 Sample 7 (Grande basaltic andesite) after second grouting.

Figure 5.9 Close-up of sample 7 showing shrinkage cracks in large voids. Photograph taken after 2 days exposure of grouted surface to room conditions.

BEST COPY AVAILABLE

5.3.8 Sample 8

The last four samples, 8 through 11, were 15 cm (6 in) cubes of Charcoal granite containing a sawcut. They were made with the same saw used for sample 1, because the "fractures" it produced were groutable. These samples were prepared similarly so that information regarding the minimum equivalent aperture that can be grouted and a comparison of the performance of different mixes used on the same crack width could be obtained.

Since grout was accepted by the 69 μm fracture of sample 1, it was decided to attempt to grout at a narrower aperture. A 51 μm aperture was obtained for grouting at a normal stress of 6.9 MPa (1000 psi) with grout mix 2 at a grout injection pressure of 6.21 MPa (900 psi).

Permeability test results (Table 5.9) show a marked decrease in hydraulic conductivity. However, visual observation revealed that only a negligible amount of cement had been emplaced (Figure 5.10). It is not certain why the permeability measurements show such an improvement due to grouting. Nonetheless, based on the quantity of cement injected, this sample does not appear to be successfully grouted.

5.3.9 Sample 9

For sample 9, it was decided to attempt to grout a fracture with the same aperture as sample 8, but with a thinner mix. A 46 μm aperture was obtained using a normal stress of 1.72 MPa (250 psi). Grout mix 5, the thinnest mix used in this research, was injected at a pressure of 2.41 MPa (350 psi).

Permeability test results before and after grouting are given in Table 5.10. A marked decrease in single fracture hydraulic conductivity was obtained. Only a negligible amount of cement had been accepted by the fracture (Figure 5.11). The quantity of cement injected into sample 9 was even smaller than that injected into sample 8. Similarly, this grout attempt appears to be unsuccessful.

5.3.10 Sample 10

Since the attempts to grout samples 8 and 9 were unsuccessful, it was decided to grout samples 10 and 11 at an aperture similar to that of sample 1. A different mix would be used for each sample. For sample 10, a 68 μm aperture was obtained using a normal stress of 13.8 MPa (2000 psi). This stress was maintained throughout the test. It was decided to try mix 4 at an injection pressure of 5.52 MPa (800 psi).

Permeability test results before and after grouting and a photograph of the grouted sample are presented as Table 5.11 and Figure 5.12, respectively. A seven-fold decrease in the rate of head drop was obtained. A significant amount of grout was injected into the fracture as shown by the photograph. Since this "fracture" is actually a sawcut, the flowpaths created are highly anisotropic and it

BEST COPY AVAILABLE

Table 5.9 Permeability Test Results Before and After Grouting for Sample 8, Charcoal Granite

Test	Time (sec)	Initial Height (cm)	Final Height (cm)	Aperture (cm)	Hydraulic Conductivity (cm/sec)
Before Grouting:	70.3	140.01	107.61	51.1×10^{-4}	1.94×10^{-1}
3 Days after Grouting:	3300	147.89	147.35	3.4×10^{-4}	8.59×10^{-2}

Normal stress: 6.89 MPa (1000 psi)
Grout injection pressure: 6.2 MPa (900 psi)
Buret radius: 0.54 cm
Ratio of sample radius to drillhole radius: 6.0

Figure 5.10 Sample 8 (Charcoal granite) after grouting.

BEST COPY AVAILABLE

Table 5.10 Permeability Test Results Before and After Grouting for Sample 9, Charcoal Granite

Test	Time (sec)	Initial Height (cm)	Final Height (cm)	Aperture (cm)	Hydraulic Conductivity (cm/sec)
Before Grouting:	93.8	140.01	107.61	46.4×10^{-4}	1.60×10^{-1}
3 Days after Grouting:	4080	147.89	144.98	2.7×10^{-4}	5.44×10^{-4}

Normal stress: 1.72 MPa (250 psi)
Grout injection pressure: 2.41 MPa (350 psi)
Buret radius: 0.54 cm
Ratio of sample radius to drillhole radius: 6.0

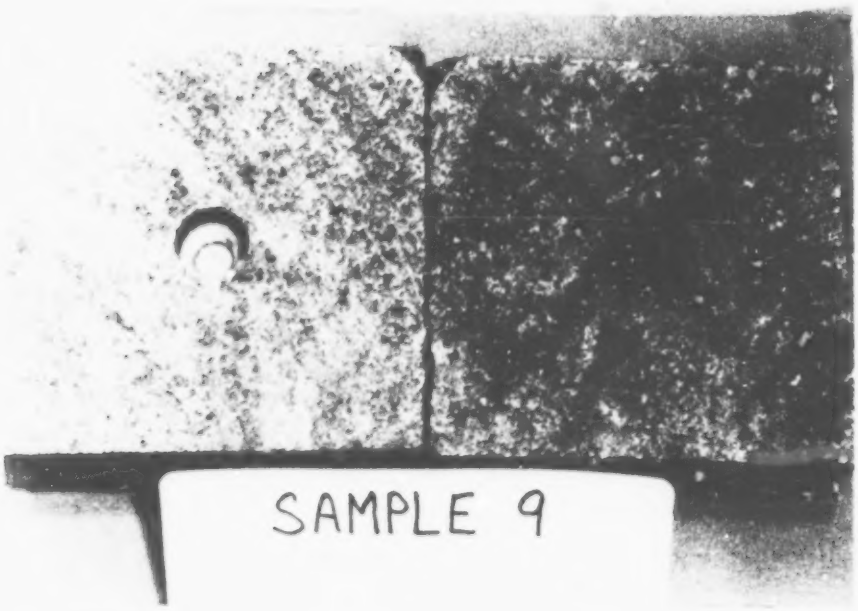

Figure 5.11 Sample 9 (Charcoal granite) after grouting.

BEST COPY AVAILABLE

Table 5.11 Permeability Test Results Before and After Grouting for Sample 10, Charcoal Granite

Test	Time (sec)	Initial Height (cm)	Final Height (cm)	Aperture (cm)	Hydraulic Conductivity (cm/sec)
Before Grouting:	29.3	140.01	107.61	68.4×10^{-4}	3.47×10^{-1}
3 Days after Grouting:	207	140.01	107.61	35.6×10^{-4}	9.40×10^{-2}

Normal stress: 1.38 MPa (2000 psi)
Grout injection pressure: 5.51 MPa (800 psi)
Buret radius: 0.54 cm
Ratio of sample radius to drillhole radius: 6.0

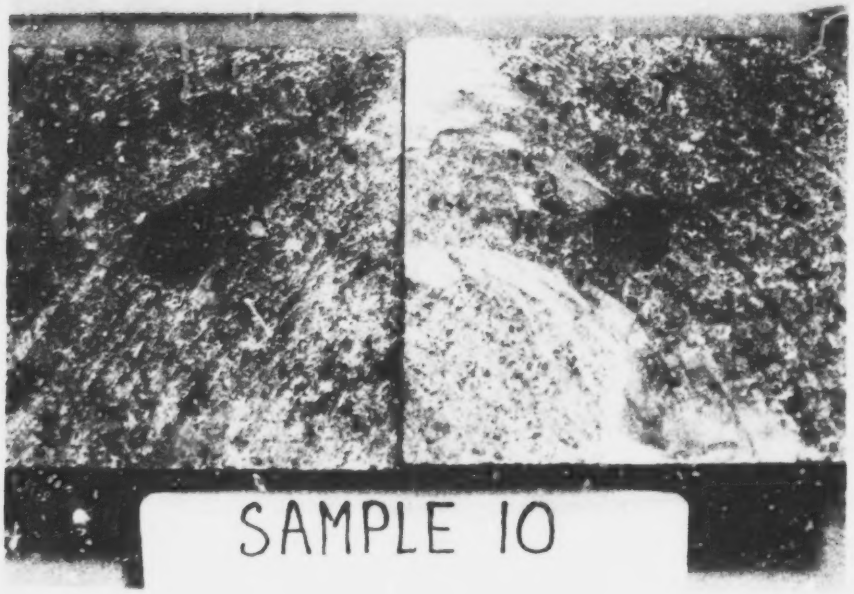

Figure 5.12 Sample 10 (Charcoal granite) after grouting.

BEST COPY AVAILABLE

can not be considered possible for grout to completely fill the "crack". This is evident for all five samples cut with this particular saw. The flow can not be considered truly radial either. The fracture could be approximated by two linear flowpaths, each 7.5 cm (3 in) long and 5 cm (2 in) wide. If these were replaced by one flowpath 7.5 cm (3 in) long and 10 cm (4 in) wide, the aperture prior to grouting could be calculated using equation 5.3. The equivalent aperture thus obtained is e = 94 μm. The equivalent aperture calculated using this assumption represents a better estimate, and is 37 percent larger than the 68 μm aperture determined by assuming a radial flow model.

5.3.11 Sample 11

For sample 11, an aperture of 66 μm was obtained under a normal stress of 1.38 MPa (200 psi). Grout mix 3, the thinner of the two cement-bentonite mixes, was chosen so that its performance could be compared against the two neat cement mixes used to grout samples 1 and 10. A grout injection pressure of 2.07 MPa (300 psi) was used.

Permeability test results before and after grouting and a photograph of the grouted sample are presented as Table 5.12 and Figure 5.13. A marked decrease in fracture hydraulic conductivity was obtained, significantly greater than for sample 10. Although these measurements have been shown to be uncertain grout acceptance predictors, it appears possible that a cement-bentonite mix behaves as a better sealant than a neat cement mix when kept in a saturated state. An examination of the fracture reveals that a somewhat greater quantity of grout was injected into sample 11 than into either samples 1 or 10. However, since these fractures are not identical, no firm conclusions regarding the relative penetrability of the three mixes can be made.

Disregarding the results of sample 6, whose fracture was subjected to a large displacement, sample 11 is the tightest fracture that has been successfully grouted. If one considers the flow to be linear, similar to the analysis of sample 10, the equivalent aperture prior to grouting is e = 92 μm This is 38 percent larger than the 66 μm aperture obtained assuming radial flow. The minimum parallel plate aperture that has been grouted in the course of these experiments, using ordinary portland cement, thus appears to be about 92 μm.

5.4 Influence of Normal Stress on Fracture Flow

Because normal stress across a fracture changes the fracture aperture, it changes the hydraulic conductivity of the fracture. The flow experiments performed in preparation of grouting, i.e. to estimate groutability of a fracture, provide an opportunity for evaluating various relations that have been proposed between normal stress and hydraulic conductivity.

Complete results of the fracture flow experiments are given in Appendix C.* Included are the best fit parameters for the following relations between normal stress across the fracture and fracture hydraulic conductivity:

BEST COPY AVAILABLE

Table 5.12 Permeability Test Results Before and After Grouting for Sample 11, Charcoal Granite

Test	Time (sec)	Initial Height (cm)	Final Height (cm)	Aperture (cm)	Hydraulic Conductivity (cm/sec)
Before Grouting:	32.0	140.01	107.61	66.4×10^{-4}	3.27×10^{-1}
3 Days after Grouting:	9720	140.01	137.63	4.0×10^{-4}	1.17×10^{-3}

Normal stress: 1.38 MPa (200 psi)
Grout injection pressure: 2.07 MPa (300 psi)
Buret radius: 0.54 cm
Ratio of sample radius to drillhole radius: 6.0

Figure 5.13 Sample 11 (Charcoal granite) after grouting.

BEST COPY AVAILABLE

$$K_f = K_o(e^{-cP}) \qquad (5.1) \qquad \text{(Louis, 1976, p. 57)}$$

where K_f = fracture hydraulic conductivity

P = normal stress across fracture

K_o = fracture conductivity at zero normal stress

c = slope of $\log(K_f/K_o)$ vs. stress P

$$K_f = K_a + (K_{o1} - K_a)e^{-c_1 P} \qquad (5.2)$$

where K_a = limit (asymptotic) conductivity at $P = \infty$

K_{o1} = fracture conductivity at zero normal stress

c_1 = slope of $\log[(K_f - K_a)/(K_{o1} - K_1)]$ vs. normal stress P

$$K_f = K_1(P^{-\alpha}) \qquad (5.3) \qquad \text{(Gale, 1977, 1982; Kranz et al., 1979; Raven and Gale, 1985)}$$

where K_1 = hydraulic conductivity at unit normal stress P

α = slope of $\log (K_f/K_1)$ vs. $\log P$

$$K_f = K_m(P/P_m)^{-\alpha_1} \qquad (5.4)$$

where K_m = hydraulic conductivity at minimum normal stress P_m

P_m = minimum normal stress, e.g. corresponding to sample dead weight or to seating load

$P \geq P_m$

$$K_f = (K_{m1} - K_{a1})(P/P_m)^{-\alpha_2} + K_{a1} \qquad (5.5) \qquad \text{(after Nelson, 1975)}$$

where K_{m1} = conductivity at minimum normal stress P_m

K_{a1} = lower limit of conductivity, asymptotic at $P = \infty$

$P \geq P_m$

$$K_f = K_{o1}[1 - (P/P_1)^m]^3 \qquad (5.6) \qquad \text{(Gangi, 1978)}$$

---

*The cooperation of Messrs. Kittitep Fuenkajorn, Shoung Ouyang and Terry Miley, who performed the least squares curve fitting and produced the graphs is gratefully acknowledged.

BEST COPY AVAILABLE

where P_1 = effective asperity modulus

m is determined by asperity distribution, $0 < m < 1$

P_1, K_{o1} and m have been treated as curve fitting parameters in some analyses, while in others K_{o1} has been imposed identical to the zero stress conductivity (e.g. Table C.6.2) (Appendix C).

$P \leq P_1$

$$K_f = K_m \left[\frac{\log(P/P_{max})}{\log(P_m/P_{max})}\right]^3 \qquad (5.7) \qquad \text{(Jones, 1975)}$$

$P \leq P_{max}$

where K_m is the permeability measured at the reference normal stress P_m.

P_{max} is the "healing" normal stress, at which the fracture probability reduces to zero.

$$K_f = K_m \left[1 - (4H/e_m)^{1/2} \ln(P/P_m)\right]^3 \frac{1 - A(P - P_m)}{1 + A(P - P_m)} \qquad (5.8)$$

(Walsh, 1981)

where H is the root mean square value of the asperity height distribution

e_m is the fracture aperture at the reference normal stress P_m

A is the rate of change of the contact area, as a function of the normal stress P.

Walsh (1981) simplifies equation (5.8) to:

$$K_f = K_m \left[1 - (4H/e_m)^{1/2} \ln(P/P_m)\right]^3 \qquad (5.9) \qquad \text{(Walsh, 1981)}$$

In the numerical application of the above (Appendix C), P is treated as the total normal stress across the fracture. It is recognized that treatment of P as an effective normal stress, and, especially, as a weighted normal stress to evaluate the difference in influence between the total and the pore pressures, would be preferable (e.g. Kranz et al., 1979; Engelder and Scholz, 1981; Settari and Price, 1984). The paucity of data, the narrow range of injection pressures used, and the very small magnitude of the injection pressures compared to the

BEST COPY AVAILABLE

applied stress does not appear to warrant such a refinement in the numerical analysis of the here available data.

All aperture and conductivity calculations have been performed assuming laminar smooth parallel wall flow. Using the aperture and maximum velocities thus obtained, the maximum Reynolds number for the results presented in Appendix C falls well below the critical value, and, for all but the zero stress flows, several orders of magnitude below the critical value. No fracture wall roughness measurements have been made.

Detailed results of least square fits of several of the equations to experimental fracture flow data are presented in Appendix C. A major problem encountered in this effort is the uncertainty about the zero pressure, i.e. the seating pressure applied during the initial unstressed measurement, as well as at the end of each cycle. An attempt at bracketing the influence of the zero pressure has been made, as illustrated in Table C.6.2, by estimating minimum, most likely, and maximum seating pressures. The results clearly indicate the need for an accurate determination of the "zero" pressure.

For most measurements the number of data points is not sufficient to allow an identification of the "best" curve fit. The power laws (e.g. equations 5.3, 5.4) tend to give better fits than the exponential (5.1). The Gangi (1978) "bed of nails" model can be fitted satisfactorily to most results, although the fit is far from unique (Table C.6.3, Figures C.6.7 through C.6.11). Fundamentally questionable would seem the assumption by Gangi (1978) of a single asperity distribution, and of elastic deformation, for fractures in which the unloading and loading curves during any one cycle are substantially different. As pointed out by Gangi (1978), this is most readily explained by asperity breakage. The latter is likely to be a progressive development during load increase, hence the implication of nonelastic deformation and changing asperity distribution. This also implies that the last factor in equation (5.8) probably is not constant, as discussed by Walsh (1981).

BEST COPY AVAILABLE

CHAPTER SIX

CONCLUSIONS AND FURTHER RESEARCH RECOMMENDATIONS

6.1 Conclusions

6.1.1 Grout Characterization Testing

The narrow variations in the uniaxial compressive strengths and unit weights for the stable cement grouts mixed and tested show the high degree of precision in material preparation that can be accomplished under laboratory conditions. Laboratory testing also indicates a decrease in strength for cement grout that has been pumped. Samples of grout mixed in the field and pumped through field grouting equipment should be collected and tested so they may be compared with laboratory specimens if one is going to determine "realistic" grout strengths. Even then, of course, considerable uncertainty remains as to what the strength might be of the emplaced grout, i.e. grout pumped through a fracture, in a relatively thin highly irregular sheet, subject to sedimentation, hydration and dehydration, rock mass deformation, etc. The complexities clearly suggest the desirability of treating any type of grout strength as an index property primarily, rather than as a functional design strength parameter.

The stable cement-bentonite mixes have a higher uniaxial compressive strength than their unstable counterparts. This contradicts the more accepted belief that bentonite weakens a grout mix. Unstable mixes cured in cylinders appeared to be more variable in composition than stable mixes. This led to lower compressive strengths even though their final water-cement ratios after bleeding were lower. Unit weight and compressive strength results for unstable mixes also were more erratic. In the field, the sedimentation process is complicated by such factors as the dip, aperture and roughness of the grouted and intersecting fractures, the flow conditions, the magnitude and duration of the applied pumping, and the sustained pressure. Therefore, for an unstable mix, the final composition and properties of the hardened cement emplaced in fractures would be unpredictable. Stable mixes would have more predictable properties because of their uniform composition before and after emplacement. Thus, their use in grouting seems preferable.

The determination of bleed capacities using graduated cylinders was useful in verifying that the mixes designed to be stable did, in fact, not exceed an acceptable percentage of bleed water. For the unstable mixes, the determination of the rate of bleed proved unsuccessful. Although this aspect of the sedimentation process is not overly important, information regarding the bleed rate of an unstable mix would have been useful in obtaining a feel for the time needed to drive off excess bleed water. Based on information in the literature, it appears that a period in excess of one hour is needed for most of the bleed water to rise out of suspension.

BEST COPY AVAILABLE

6.1.2 Fracture Permeability Testing

The permeability testing confirms the dependence of fracture permeability on applied normal stress, as well as the fact that the greatest permeability change occurs at low stresses. An irreversible decrease in permeability occurs after the first loading/unloading cycle due to the permanent deformation of asperities resulting in a better mated fracture surface. This irreversible change makes it unlikely that any purely elastic model could realistically describe the changes in hydraulic conductivity as a function of normal stress.

These stress-permeability results show that a zone around a repository subject to stress relaxation might increase in permeability because of fracture widening. If these zones of increased permeability result in significant inflows into the repository, fracture grouting will be needed. Because stress relaxation is a time-dependent phenomenon, the question concerning when to grout becomes important.

The implications for grouting around underground excavations, e.g. at seal locations, are far from obvious or resolved, because of the complexity of stress redistribution across fractures near such excavations. If the rock remains elastic, the tangential stress may increase or decrease, depending upon the in-situ stressfield, while the radial stress is most likely to decrease. The resulting changes in stress across any pre-existing fracture depend on the orientation of the fracture. They will involve changes in shear stresses as well as in normal stresses, in general. The picture becomes less clear if inelastic behavior occurs (e.g. rock fracture or joint slip), and this occurrence, moreover, implies a much deeper propagation of stress redistributions, and hence of the zone within which substantial permeability changes might occur. An extensive analysis would be required in order to estimate the range of conditions that might be expected to be encountered. Suffice it to say that such an analysis will be essential to determine likely bypass flow conditions through rock adjacent to seals.

The falling head permeameter performed well for most of the permeability testing. Problems were encountered in saturating some samples. Some stress-permeability tests of sample 4 are suspected of being unsaturated. Samples 5 and 6, containing tension cracks, were difficult to saturate while initially unloaded. A large number of flow tests were required before a steady head drop rate was obtained. A large capacity constant head permeameter or a recirculating capability would have been preferable to the falling head apparatus.

6.1.3 Grouting Implications

The permeability measurements taken after the grouting of samples 4, 8 and 9 indicate that such measurements can be misleading. Ineffective grouting of the samples resulted in major reductions in apparent permeability. A radial flow can be heavily influenced by conditions close to the borehole, as demonstrated by electrical analogy by Sundaram and Finks (1983). It is recommended that an independent flow path be used to assess the effectiveness of a grout seal.

BEST COPY AVAILABLE

Whether displacement grouting is beneficial or detrimental to the sealing of rock fractures can not be answered. This is in part because the stiffness of the test apparatus is unknown compared to that of a rock mass. With the exception of sample 6, which was tested in an unloaded state, it is assumed that fracture displacements were negligible. The test results for sample 6 did show that the fracture hydraulic conductivity was unchanged by grouting despite the fact that the fracture was well filled with grout. This evidence is inconclusive, however, since it is based on only one sample and it is not known how much actual fracture displacement occurred.

The gain in strength of the grouted fractures was generally negligible. With the exception of sample 7, grout would only bond to the lower half of the fracture surface. For sample 7, two grout applications using thick mixes were emplaced, resulting in the need for a screwdriver to pry the sample apart two days after grouting. For samples 3 and 5, grout was seen to bond both vertical fracture surfaces. In general, the need to use watery mixes in order to grout the tight cracks commonly found at depth will preclude any appreciable gain in rock mass strength.

The problem of grout mix durability should be of concern when "large" openings are grouted, as pointed out by the severe shrinkage of cement-bentonite grout in the large voids of sample 6. It seems that the addition of bentonite in a cement grout can lead to a nondurable mix if it does not remain saturated. Shrinkage cracking was not noticed in any of the tighter fractures grouted with these mixes. Thick mixes of neat cement in a large void of sample 7 exhibited minor shrinkage cracking. It appears that these cracks would not have had an appreciable effect on the permeability of the fracture.

The equivalent aperture of a fracture may provide a criterion governing the use of cement for fracture grouting. It can aid in the selection of a starting grout mix. The practicality of its use will depend on the feasibility of obtaining fracture information for the intervals of rock that are to be water tested. For narrow fractures in particular it probably needs to be complemented by an aperture variation, channel continuity, and tortuosity estimate.

The failure to inject any grout into the finer cracks, in addition to reported claims regarding the limitations of cement based grouts, confirms the inadequacy of ordinary portland cement to penetrate fine fractures. Such fractures may result in significant rock mass permeabilities.

Visual observations during grouting (i.e. fracture outflows) as well as inspection of the grout distributions typically show a highly non-uniform flowpath, i.e. strongly preferential channeling or fingering. Flowpaths clearly are dominated by fracture aperture variations, and grout penetration in narrow fractures can easily be dominated by early blockage of a few channels.

AVAILABLE

6.2 Research Recommendations

The grouting experiments presented here can be considered, at best, as only a preliminary investigation of a few of the many aspects that will influence the sealing performance that can be accomplished by grouting the rock directly adjacent to various repository openings, and in particular at permanent seal locations. Emphasis has been placed on narrow fractures grouted under relatively high pressure with rather thick conventional mixes.

The most apparent needs from the results obtained thus far appear to be for experiments on larger size "fractures", i.e. fractures with longer flowpaths. This unfortunately is difficult to perform at stress levels even approximating repository conditions, due to the large load requirements. However, even experiments over short flowpaths can be highly revealing, as illustrated here. Alternatively, it deserves investigating to what extent effective stress can be used as a grouting criterion, thus possibly obviating the need for total stress similarity.

Recommended further experimentation along the lines introduced here would include experiments on natural joints and experiments on artificial joints. Natural joint experiments, almost certainly supplemented with artificial joints, e.g. induced tensile fractures, should focus on a detailed study of the joint morphology (e.g. Roko, 1987; Roko et al., 1986) and grout distribution. Virtually all experiments performed here confirm the frequent observation in fracture flow studies of a highly nonuniform flow, i.e. pronounced fingering. Fracture grout studies can provide considerable insight into fracture flow mechanics, because they allow direct observation and mapping of the preferred flowpaths. Therefore, a detailed comparison of fracture morphology and flowpath would allow a much more realistic assessment of fracture flow, in addition to the immediate objective of obtaining an improved understanding of grout flow and grouting sealing performance. To some extent, grouting can be considered as a simplified procedure for determining void geometry and contact area (Pyrak et al., 1985). An essential prerequisite for achieving the maximum possible benefits from such a study would be considerably improved instrumentation during fracture grouting, as well as pressure distribution monitoring. Particularly desirable would be displacement monitoring at multiple positions along and across the fracture, as well as visual and/or acoustic emission monitoring of the grouting progress, e.g. grout propagation. A precise control and measurement of grout rheology is needed, over the range of flow conditions (e.g. turbulent and laminar, various velocities and shear stresses) likely to be encountered. The experiments need to be performed under a range of external and injection pressures, as well as for a range of fracture orientations with respect to the stressfield.

The experiments on "artificial" fractures identified earlier would consist of grouting experiments in gaps between parallel plates with carefully designed and controlled apertures and rugosities. In this testing configuration, it is possible to vary the surface morphology,

BEST COPY AVAILABLE

and thus establish a much better controlled investigation of the relation between flowpaths, injection parameters (e.g. pressure, rate, pump shear), grout characteristics (e.g. viscosity, yield stress, particle size, composition), sealing effectiveness, and fracture characteristics. Such investigations also would be particularly appropriate to study the effectiveness of a wide range of grout mixes. Even though chemical, especially organic, grouts might be deemed undesirable for repository grouting because of uncertainty about their durability, they have the considerable advantage over cementitious grouts of allowing tightly controlled yet widely ranging viscosities. Therefore, they might be an ideal "fluid" to introduce an additional controlled parameter in the experimental matrix. Such experiments would seem essential in order to obtain an improved understanding of fracture grout flow mechanics, even though their immediate representativeness of repository conditions and materials is not satisfied.

As in all aspects of HLW repository performance, longevity or durability of any barrier component will be a major concern. Several tests suggest themselves naturally to address this issue: extended time flow testing of grouted fractures; experiments to identify flow conditions resulting in grout damage, e.g. piping or channeling through grout; accelerated aging experiments by means of thermal and load cycling (e.g. both normal and shear); drying experiments; chemistry of flowing water; leaching experiments.

All the previously proposed work is aimed exclusively at the study of single fracture grouting. Field situations involve grouting fracture networks, and, from a research point of view, in particular the mechanics of grout flow from one fracture into an intersecting one. Although experimental complications, in particular the need for adequate sample preparation and test instrumentation, increase significantly, a conceptual experimental program can readily be visualized. In addition to previously mentioned variables such as stressfield, grout pressure, fracture apertures, grout rheology and particle size, the relative geometry (orientation and width) of intersecting fractures is likely to be a significant factor in grout distribution. Experiments on artificial carefully controlled "fracture networks", designed similarly to the single fracture experiments, should be aimed at clarifying the underlying flow mechanics of the system. Confirmatory experiments on actual rock fractures are needed, particularly to allow identification of fundamental differences, if any, between observations on idealized and on real fracture networks.

Basic difficulties and limitations inherent in laboratory simulations of field grouting require that all critical conclusions and issues identified from laboratory investigations be confirmed by field studies. The most obvious limitations associated with laboratory work are those due to the use of unrepresentative mixes and pumps, typically low-speed, low-volume. Mixing and pumping procedures significantly affect grout properties (e.g. Houlsby, 1982), and it is difficult, therefore, to correctly produce representative field grouts in the laboratory, and hence field grout flow conditions. The second

AVAILABLE

type of fundamental simulation difficulties relate to in-situ rock mass behavior, particularly discontinuity behavior. For these reasons, some field evaluations would be highly desirable, and preferably should be conducted under fairly representative conditions, e.g. around excavations at great depth in jointed rock. It is premature to try to outline a field testing program in detail, in light of the need to first develop a significantly improved understanding of the issues on the basis of systematic laboratory investigations.

As itemized briefly in the introduction to Chapter Three, on grouting, as well as in several of the topical sections in that chapter, considerable and well-recognized uncertainty exists about the actual performance of grouting. Much of the uncertainty is due to a lack of understanding of the detailed mechanics of grout distribution, of the sealing performance subsequent to grouting, and of the various parameters that affect it. It is probable that grouting will be required at various points of the engineered rock barrier, and virtually certain that it will be required at sealing locations. In order for NRC to be able to make an assessment of reasonable assurance with regard to the performance of these grouting barrier components, it would appear highly desirable to develop a significantly improved understanding of grouting of fractured rock.

BEST COPY AVAILABLE

BLANK PAGE

REFERENCES

Albritton, J.A., 1982, "Cement Grouting Practices, U.S. Army Corp of Engineers," Grouting in Geotechnical Engineering, proceedings of the conference on Feb. 10-12, New Orleans, LA, ASCE, pp. 264-278.

American Petroleum Institute, 1977, "Testing Oil Cements and Cement Additives," Twentieth Edition, API, Dallas, Texas, April.

American Petroleum Institute, 1985, "Standard Procedure for Field Testing Drilling Fluids," Eleventh Edition, API, Dallas, Texas, May.

American Society of Civil Engineers, 1962, "Cement Grouting," Progress Report of the Task Committee on Cement Grouting, Journal of the Soil Mechanics and Foundation Division, Paper 3098, Vol. 88, No. SM2, pp. 49-98.

Apps, J.A., C.L. Carnahan, P.C. Lichtner, M.C. Michel, D. Perry, R.J. Silva, O. Weres, and A.F. White, 1983, "Status of Geochemical Problems Relating to the Burial of High-level Radioactive Waste, 1982," NUREG/CR-3062, LBL-15103, Prepared for U.S. Nuclear Regulatory Commission by Lawrence Berkeley Laboratory, University of California, Berkeley.

ASTM C39-83b, "Standard Test Method for Compressive Strength of Cylindrical Concrete Specimens," Annual Book of ASTM Standards, Section 4, Construction, Vol. 04.02, Concrete and Mineral Aggregates, American Society for Testing and Materials, Philadelphia.

ASTM C39-84, "Standard Test Method for Compressive Strength of Cylindrical Concrete Specimens," Annual Book of ASTM Standards, Section 4, Construction, Volume 04.02, Concrete and Mineral Aggregates, American Society for Testing and Materials, Philadelphia.

ASTM C150-85a, "Standard Specification for Portland Cement," Annual Book of ASTM Standards, Section 4, Construction, Volume 04.02, Concrete and Mineral Aggregates, American Society for Testing and Materials, Philadelphia.

ASTM C243-85, "Standard Test Method for Bleeding of Cement Pastes and Mortars," Annual Book of ASTM Standards, Section 4, Construction, Volume 04.01, Cement; Lime; Gypsum, American Society for Testing and Materials, Philadelphia.

ASTM C939-81, "Standard Test Method for Flow of Grout for Preplaced-Aggregate Concrete," Annual Book of ASTM Standards, Section 4, Construction, Volume 04.02, Concrete and Mineral Aggregates, American Society for Testing and Materials, Philadelphia.

BEST COPY AVAILABLE

Auld, F.A., 1983, "Design of Underground Plugs," International Journal of Mining Engineering, Vol. 1, no. 3, pp. 184-228, October.

Baker, W.J., 1955, "Flow in Fissured Formations," Proceedings, Fourth World Petroleum Congress, Rome, Vol. II, Section II/E, Paper 7, pp. 379-393. Carlo Colombo Publishers, Rome.

Ballivy, G. and P. Niemants, 1982, "New Laboratory Techniques to Test Grouted Fractured Rock," Grouting in Geotechnical Engineering, W.H. Baker, editor, proceedings of the conference on Feb. 10-12, New Orleans, LA, pp. 809-821. American Society of Civil Engineers, New York.

Bawden, W.F., J.H. Curran, and J.C. Roegiers, 1980, "Influence of Fracture Deformation on Secondary Permeability - A Numerical Approach," pp. 265-279, Vol. 17, Int. J. Rock Mech. Min. Sci. & Geomech. Abstr.

Black, J.C., C.A. Pollard, and G.P. Daw, 1982, "Hydrogeological Assessment and Grouting at Selby," Grouting in Geotechnical Engineering, W.H. Baker, editor, proceedings of the conference on Feb. 10-12, New Orleans, Louisiana, ASCE, pp. 665-679. American Society of Civil Engineers, New York.

Borden, R. and D.M. Groome, 1984, "Influence of Bentonite Cement on the Pumpability of Compaction Grouts," pp. 115-128, Innovative Cement Grouting, Publication SP-83, American Concrete Institute, Detroit.

Bowen, R., 1981, Grouting in Engineering Practice, Second Edition, Applied Science Publishers, Ltd., London, 285 pp.

Brar, N.S. and R.M. Stesky, 1980, "Permeability of Intact and Jointed Rock," EOS, Vol. 61, No. 46, Abstract T94, p. 1112, November 11.

Burgin, C.R., 1979, "Investigation of the Physical Properties of Cement-Bentonite Grouts for Improvement of Dam Foundations," M.S. Thesis, University of Florida.

Cambefort, H., 1977, "The Principles and Applications of Grouting," Quarterly Journal of Engineering Geology, Vol. 10, The Geological Society, London, pp. 57-95.

Carter, T.G., 1982, "Evaluation of Some Electronically Monitored Grouting Data," pp. 127-135, Vol. 2, Grouting in Geotechnical Engineering, W.H. Baker, ed., ASCE, New York.

Chadwick, W.L., A. Casagrande, H.A. Coombs, M.W. Dowd, E.M. Fucik, R.K. Higginson, T.M. Leps, R.B. Peck, H.B. Seed, and R.B. Jansen, Executive Director, 1976, "Report to U.S. Dept. of the Interior and State of Idaho on Failure of Teton Dam," Supt. Documents, U.S. Govt. Printing Off., Dec. 31, 219 pp., 7 appendices.

COPY AVAILABLE

Chalmers, A., G.P. Daw, and R.A. Scott, 1979, "A Modified Form of Aquifer Depletion/Recovery Test for Assessing Potential Water Makes into Deep Excavations," Proceedings, 4th Congress of the International Society for Rock Mechanics, Vol. 2, pp. 67-72, Vol. 3, p. 225, Sept. 2-8, Montreux, Switzerland. A.A. Balkema, Rotterdam.

Chamber of Mines of South Africa, 1982, "Construction of Underground Plugs and Bulkhead Doors Using Grout Intrusion Concrete, Code of Practice," 10 pp., February.

Clarke, W.J., 1984, "Performance Characteristics of Microfine Cement," Preprint 84-023, Atlanta, Georgia, May. ASCE Meeting.

Cobb, S.L. and J.J.K. Daemen, 1982, "Polyaxial Testing of Borehole Plug Performance," Topical Report to the U.S. Nuclear Regulatory Commission, Contract No. NRC-04-78-271, prepared by the Department of Mining and Geological Engineering, University of Arizona, Tucson.

Consulting Engineer, 1969, "Grouting Design and Practice," The Consulting Engineer, London, Vol. 33, no. 10, October, 40 p. insert.

Crawford, A.M. and G. Groskopf, 1984, "Groutability Ratio for Filter Blocking of Joints in Rock," Rock Mechanics in Productivity and Protection, 25th U.S. Symposium on Rock Mechanics, June 25-27, Evanston, Illinois, Society of Mining Engineers of AIME, pp. 899-906.

Cruickshank, C.V., 1976, "Flow in Fractured Rock Masses," pp. 283-297, Q. 45, R. 17, Vol. IV, Twelfth Congress on Large Dams, Mexico.

Daemen, J.J.K., J.C. Stormont, N.I. Colburn, D.L. South, S.A. Dischler, K. Fuenkajorn, W.B. Greer, G.S. Adisoma, D.E. Miles, B. Kousari, and J. Bertuca, 1983, "Rock Mass Sealing - Experimental Assessment of Borehole Plug Performance, Annual Report, June 1982 - May 1983," NUREG/CR-3473, prepared for U.S. Nuclear Regulatory Commission, Division of Health, Siting and Waste Management, by by the Department of Mining and Geological Engineering, University of Arizona, Tucson.

Daneshy, A.A., 1978, "Numerical Simulation of Sand Transport in Hydraulic Fracturing," pp. 132-140, Journal of Petroleum Technology, January.

Deere, D.U., 1976, "Dams on Rock Foundations - Some Design Questions," Rock Engineering for Foundations and Slopes, Vol. 2, proceedings of a specialty conference on Aug. 15-18, Boulder, Colorado, pp. 55-86. Published by American Society of Civil Engineers, New York.

Deere, D.U., 1982, "Cement-Bentonite Grouting for Dams," Grouting in Geotechnial Engineering, W.H. Baker, editor, proceedings of

BEST COPY AVAILABLE

the conference on Feb. 10-12, New Orleans, LA, pp. 279-300. Published by American Society of Civil Engineers, New York.

Deere, D.U. and G. Lombardi, 1985, "Grout Slurries - Thick or Thin?" pp. 156-164, Issues in Dam Grouting, W.H. Baker, editor. American Soceity of Civil Engineers, New York.

Detournay, E., 1980, "Hydraulic Conductivity of Close Rock Fracture: An Experiment and Analytical Study," pp. 168-173 of Underground Rock Engineering, 13th Canadian Rock Mechanics Symposium (The H.R. Rice Memorial Symposium), Toronto, Ontario, May 28-29. CIM Special Volume 22, The Canadian Institute of Mining and Metallurgy, Montreal, Quebec.

Du Bois, E., 1963, "Injections with High Pressure in Deep Mines," Grouts and Drilling Muds in Engineering Practice, symposium organized by the International Society of Soil Mechanics and Foundation Engineering, May, London, pp. 70-74.

Du Bois, H.L.E., 1978, "High Pressure Grouting in Deep Gold Mines," pp. 391-407, Vol. 1, Water in Mining and Underground Works, SIAMOS-78, Granada, Spain.

Earlougher, R.C., 1977, "Advances in Well Test Analysis," Monograph Volume 5 of the Henry L. Doherty Series, second printing, Society of Petroleum Engineers of AIME, New York, 264 pp.

Elsworth, D. and R.E. Goodman, 1986, "Characterization of Rock Fissure Hydraulic Conductivity Using Idealized Wall Roughness Profiles," Int. J. Rock Mech. Min. Sci. & Geomech. Abstr., Vol. 23, No. 3, pp. 233-243.

Engelder, T. and C.H. Scholz, 1981, "Fluid Flow Along Very Smooth Joints at Effective Pressure up to 200 Megapascals," pp.147-152, Mechanical Behavior of Crustal Rocks, The Handin Volume, Geophysical Monograph 24, American Geophysical Union, Washington, DC.

Ewert, F.-K., 1979, "Zur Vergleichbarkeit von Wasseraufnahmen in WD-Versuchen mit der spaeteren Gebirgsdurchlaessigkeit unter Einstaubedingungen bei Talsperren" (On the comparability of water takes during water pressure tests with the later rock mass permeability underneath dams with filled reservoirs), pp. 81-106, Vol. 49, Muenster Forsch. Geol. Palaeont.

Ewert, F.-K., 1982a, "Sohlwasserdruckabbau unter einer Talsperre ohne Dichtungsschleier" (Reduction of uplift pressure under a dam without sealing curtain), pp. 395-400, No. 9, Wasser und Boden.

Ewert, F.-K., 1982b, "Die Einfluesse oertlicher geologischer Verhaeltnisse und der Injektionsmassnahmen auf den Abbau des Sohlwasserdrucks" (Influence of local geological conditions and of grouting measures on the reduction of uplift pressures), pp. 453-459, No. 10, Wasser und Boden.

BEST COPY AVAILABLE

Ewert, F.-K., 1985, Rock Grouting - with Emphasis on Dam Sites, Springer-Verlag, Berlin.

Farmer, I.W., 1970, "Design of Cement Grouts," Research Report R.17/70, University of Newcastle upon Tyne, England, 69 pp.

Fernandez, J.A., 1985, "Repository Sealing Plan for the Nevada Nuclear Waste Storage Investigations Project Fiscal Years 1984 Through 1990," Sandia Report SAND 84-0910. Prepared by Sandia National Laboratories, Albuquerque, New Mexico 87185.

Fernandez, J.A. and M.D. Freshley, 1984, "Repository Sealing Concepts for the Nevada Nuclear Waste Storage Investigations Project," SAND 83-1778. Prepared by Sandia National Laboratories, Albuquerque, New Mexico 87185.

Franz, R.L., A.D. Frankel, T. Engelder, and C.H. Scholz, 1979, "The Permeability of Whole and Jointed Barre Granite," Int. J. Rock Mech. Min. Sci. & Geomech. Abstr., Vol. 16, pp. 225-234.

Fyfe, W.F., V. Babuska, N.J. Price, E. Schmid, C.F. Tsang, S. Uyeda, and B. Velde, 1984, "The Geology of Nuclear Waste Disposal," pp. 537-540, Nature, Vol. 310, August 16.

Gale, J.E., 1975, "A Numerical, Field and Laboratory Study of Flow in Rocks with Deformable Fractures," Ph.D. Thesis, University of California, Berkeley, 255 pp. Published as Scientific Series 72, Inland Waters Directorate, Environment Canada, Ottawa.

Gale, J.E., 1982a, "The Effects of Fracture Type (Induced Versus Natural) on the Stress-Fracture Closure-Fracture Permeability Relationships," Issues in Rock Mechanics, 23rd Symposium on Rock Mechanics, R. Goodman and F.E. Heuze, eds., Aug. 25-27, Berkeley, California, Society of Mining Engineers of AIME, pp. 290-298.

Gale, J.E., 1982b, "Assessing the Permeability Characteristics of Fractured Rock," pp. 163-182, Recent Trends in Hydrogeology, Special Paper 189, Geological Society of America.

Gale, J.E., 1984, "Changes in Fracture Permeability as a Function of Sample Size, Fracture Type, and Stress History," pp. 43-53, Vol. 1, Proc. Intern. Symp. on Groundwater Utilization and Contaminant Hydrogeology, Vol. 1, Intern. Assoc. of Hydr., Montreal, Quebec, May. Published by Atomic Energy of Canada Limited, Pinawa, Manitoba.

Gale, J.E. and K.G. Raven, 1980, "Effects of Sample Size on the Stress-Permeability Relationship for Natural Fractures," Technical Information Report No. 48, Dept. of Earth Sciences, University of Waterloo, Waterloo, Ontario, Canada, 111 pp.

Gale, J.E. and E.J. Reardon, 1984, "Effects of Groundwater Geochemistry on the Permeability of Grouted Fractures," Canadian Geotechnical Journal, Vol. 21, pp. 8-20.

BEST COPY AVAILABLE

Gale, J.E., A. Rouleau, and L.C. Atkinson, 1985, "Hydraulic Properties of Fractures," pp. 1-16, Vol. XVII, Part 1, Hydrogeology of Rocks of Low Permeability, Memoires, International Association of Hydrogeologists, Tucson, Arizona, Congress.

Gangi, A.F., 1978, "Variation of Whole and Fractured Porous Rock Permeability with Confining Pressure," Int. J. Rock Mech. Min. Sci. & Geomech. Abstr., Vol. 15, pp. 249-257.

Garrett, W.S. and L.T. Campbell Pitt, 1961, "Design and Construction of Underground Bulkheads and Water Barriers," pp. 1283-1299, Discussion pp. 1300-1, Vol. III, Transactions of the Seventh Commonwealth Mining and Metallurgical Congress, South African Institute of Mining and Metallurgy, Johannesburg.

Garrity, P., 1983, "The Effect of Underground Construction on the Geohydrology of Proximate Rocks," a report to the Building Research Establishment of the Dept. of the Environment, Contract No. PECD7/9/075, University of Newcastle upon Tyne, England, 210 pp.

Goodman, R.E. and Y. Ohnishi, 1974, "Results of Laboratory Tests on Water Pressure and Flow in Joints," Advances in Rock Mechanics, Proceedings of the Third Congress of the International Society for Rock Mechanics, Denver, September, Vol. II, Part A, pp. 660-666. National Academy of Sciences, Washington, DC.

Goodman, R.E. and P.N. Sundaram, 1980, "Permeability and Piping in Fractured Rock," Paper 15433, pp. 485-498, Journal of the Geotechnical Engineering Division, Proceedings of the American Society of Civil Engineers, Vol. 106, No. GT5, May.

Gyenge, M., 1980a, "Grouting of Nuclear Waste Vault Shafts," pp. 77-90 in Proceedings of Borehole and Shaft Plugging Workshop, Columbus, Ohio, May 7-9. OECD Nuclear Energy Agency, Paris.

Gyenge, M., 1980b, "Nuclear Waste Vault Sealing," pp. 181-192, Underground Rock Engineering, 13th Canadian Rock Mechanics Symposium (The H.R. Rice Memorial Symposium), Toronto, Ontario, May 28-29. CIM Special Volume 22, The Canadian Institute of Mining and Metallurgy, Montreal, Quebec.

Harr, M.E., 1977, Mechanics of Particulate Media: A Probabilistic Approach, McGraw-Hill, Inc., New York.

Heise, G., 1973, "Zur Injizierbarkeit von klueftigem Gebirge unter Beruecksichtigung der chemisch-physikalischen Eigenschaften von Zementsuspensionen" (On the groutability of jointed rock with consideration of the chemical-physical properties of cement suspensions), Freiberger Forschungsheft A 523. VEB Deutscher Verlag Fuer Grundstoffindustrie, Leipzig, DDR, Germany.

BEST COPY AVAILABLE

Hoek, E. and E.T. Brown, 1980, Underground Excavations in Rock, The Institution of Mining and Metallurgy, London, 527 pp.

Holl, G.W. and N.D. Harte, 1981, "Site Testing of Shafts, Tunnels, and Caverns; The Pregrouting of Excavations with Special Reference to South African Conditions," 1981 Rapid Excavation and Tunneling Conference, Vol. 1, May 3-7, San Francisco, CA, AIME, pp. 34-62.

Houlsby, A.C., 1969, discussion of "Rock Fracture Spacings, Openings and Porosities," by David J. Snow, Journal of the Soil Mechanics and Foundations Division, ASCE, Vol. 95, no. SM 1, pp. 416-7, paper 6324, Jan.

Houlsby, A.C., 1976, "Routine Interpretation of the Lugeon Water Test," Quarterly Journal of Engineering Geology, Vol. 9, The Geological Society, London, England, pp. 303-313.

Houlsby, A.C., 1977, "Engineering of Grout Curtains to Standards," Journal of the Geotechnical Engineering Division, ASCE, Vol. 103, no. GT9, paper 13214, pp. 953-970, Sept. 1977.

Houlsby, A.C., 1982, "Cement Grouting for Dams," Background Talk,. pp. 1-34, Grouting in Geotechnical Engineering, Proceedings of the Conference, New Orleans, Louisiana, February. American Society of Civil Engineers, New York.

Houlsby, A.C., 1985a, "Cement Grouting: Water Minimizing Practices," pp. 34-75, Issues in Dam Grouting, W.H. Baker, ed., American Society of Civil Engineers, New York.

Houlsby, A.C., 1985b, "Design and Construction of Cement Grouted Curtains," pp. 999-1015, Vol. 3, Transactions, Fifteenth International Congress on Large Dams, Lausanne, Switzerland, June 24-28. Published by the International Commission on Large Dams, Paris.

Huitt, J.L., 1956, "Fluid Flow in Simulated Fractures," Journal of the American Institute of Chemical Engineering, Vol. 2, No. 2, pp. 259-264, June.

Iwai, K., 1976, "Fundamental Studies of Fluid Flow Through a Single Fracture," Ph.D. Thesis, University of California, Berkeley, 208 pp.

Jawanski, W., 1970, "Contribution to Correlation of Cement Absorption and Loss of Water in Pressure Tests for Flysch Rocks," Paper 6-16, pp. 241-246, Vol. 3, Proceedings, Second Congress of the International Society for Rock Mechanics, Belgrade, Yugoslavia.

Johnson, B., 1983, "Permeability of a Simulated-Fracture as a Function of Normal Stress," pp. 519-523, Rock Mechanics - Theory - Experiment - Practice, Proceedings, 24th U.S. Symposium on Rock Mechanics, Texas A&M University, June. Published by the Association of Engineering Geologists.

BEST COPY AVAILABLE

Jones, F.O., Jr., 1975, "A Laboratory Study of the Effects of Confining Pressure on Fracture Flow and Storage Capacity in Carbonate Rocks," pp. 21-27, Journal of Petroleum Technology, January.

Jones, G.K., 1963, "Chemistry and Flow Properties of Bentonite Grouts," Grouts and Drilling Muds in Engineering Practice, symposium organized by the International Society of Soil Mechanics and Foundation Engineering, May, London, pp. 22-28.

Jouanna, P., 1972a, "Essais de Percolation au Laboratoire sur des Echantillons de Micaschiste soumis a des Contraintes" (Laboratory tests on the permeability of micaschist samples under applied stresses), Paper T2-F, Symposium Percolation Through Fissured Rock, Proceedings, Stuttgart 1972. Published by Deutsche Gesellschaft fuer Erd-und Grundbau, Essen.

Jouanna, 1972b, "Essais in situ de Percolation sous Contrainte" (In situ permeability tests under applied stress), Paper T2-G, Symposium Percolation Through Fissured Rock, Proceedings, Stuttgart 1972. Published by Deutsche Gesellschaft fuer Erd-und Grundbau, Essen.

Kelsall, P.C., J.B. Case, and C.R. Chabannes, 1982, "A Preliminary Evaluation of the Rock Mass Disturbance Resulting from Shaft, Tunnel, or Borehole Excavation," ONWI-411, prepared by D'Appolonia Consulting Engineers, Inc., for Office of Nuclear Waste Isolation, Battelle Memorial Institute, Columbus, Ohio.

Kelsall, P.C., W.E. Coons, and D. Meyer, 1983, "Repository Sealing Program Plan. Repository in Salt," ONWI-414, prepared by D'Appolonia Consulting Engineers, Inc., for Office of Nuclear Waste Isolation, Battelle Memorial Institute, Columbus, Ohio.

Kelsall, P.C., J.B. Case, D. Meyer, J.G. Franzone, and W.E. Coons, 1985a, "Schematic Designs for Penetration Seals for a Repository in Richton Dome," BMI/ONWI-562, prepared by IT Corporation for Office of Nuclear Waste Isolation, Battelle Memorial Institute, Columbus, Ohio. December.

Kelsall, P.C., D. Meyer, J.B. Case, and W.E. Coons, 1985b, "Schematic Designs for Penetration Seals for a Repository in the Paradox Basin," BMI/ONWI-563, prepared by IT Corporation for Office of Nuclear Waste Isolation, Battelle Memorial Institute, Columbus, Ohio. December.

Kelsall, P.C., J.B. Case, W.E. Coons, J.G. Franzone, and D. Meyer, 1985c, "Schematic Designs for Penetration Seals for a Repository in the Permian Basin," BMI/ONWI-564, prepared by IT Corporation for Office of Nuclear Waste Isolation, Battelle Memorial Institute, Columbus, Ohio. December.

Kennedy, T.B., 1958, "Pressure Grouting Fine Fissures," Journal Soil Mech. Fnd. Engng., ASCE, Vol. 84, no. SM3, Aug. 1958, paper 1731.

BEST COPY AVAILABLE

Koplick, C.M., D.L. Pentz, and R. Talbot, 1979, "Information Base for Waste Repository Design, Vol. 7, Executive Summary," NUREG/CR-0495. Prepared for U.S. Nuclear Regulatory Commission, Division of Waste Management, Office of Nuclear Material Safety and Safeguards, by the Analytical Sciences Corporation, Reading, Massachusetts, NTIS: PB 293407.

Kutzer, C., 1985, "Considerations on Rock Permeability and Grouting Criteria," Q. 58, R. 17, pp. 315-328, Vol. 3, Transactions, Fifteenth International Congress on Large Dams, Lausanne, Switzerland, June. Published by the International Commission on Large Dams, Paris.

Lau, D., and A. Crawford, 1986a, "Grouting for the Underground Containment of Radioactive Waste," a report prepared for Atomic Energy of Canada Limited, Contract Number: A-7635, TIS-85-41, by Department of Civil Engineering, University of Toronto, Toronto, Ontario.

Lau, D., and A. Crawford, 1986b, "The Cement Grouting of Discontinuities in Rock Masses," Chapter 122, pp. 854-861, Proceedings, 27th U.S. Symposium on Rock Mechanics, Rock Mechanics: Key to Energy Production, H.L. Hartman, ed., June 23-25, University of Alabama, Tuscaloosa. Published by Society of Mining Engineers, Inc., Littleton, CO.

Linscott, J.P., 1985, "A Laboratory Study of the Effects of Shear Stress on Fracture Permeability," M.Sc. Thesis, Univ. of Oklahoma, Norman.

Lombardi, G., 1985, "The Role of Cohesion in Cement Grouting of Rock," pp. 253-261, Q. 58, R. 13, Vol. 3, Transactions, Fifteenth International Congress on Large Dams, Lausanne, Switzerland, June. Published by the International Commission on Large Dams, Paris.

Lomize, 1951, Filtratsiya u Treshchinovatyk Porodakh (Flow in fractured rock), Gosenergoizdat, Moscow.

Londe, P. and F. Sabarly, 1966, "La Distribution des permeabilites dans la fondation des barrages voutes en fonction du champ de contrainte" (The distribution of permeabilities in the foundation of arch dams as a function of the stress field), Paper 8.6, pp. 517-521, Vol. 2, Proceedings of the First Congress of the International Society of Rock Mechanics, Lisbon.

Loofbourow, R.L., 1973, "Ground Water and Ground-Water Control," Ch. 26, pp. 26-1/55, Vol. 2, SME Mining Engineering Handbook, Society of Mining Engineers of the American Institute of Mining, Metallurgical, and Petroleum Engineers, Inc., New York, N.Y.

BEST COPY AVAILABLE

Louis, C., 1968, Etude des Ecoulements d'Eau dans les Roches Fissurees et de leurs Influences sur La Stabilite des Massifs Rocheux (Study of Water flows in jointed rocks and of their influence on rock mass stability). Bulletin de la Direction des Etudes et Recherches - Serie A - no. 3, pp. 5-132, Electricite de France, (French translation of a Dissertation presented at the University of Karlsruhe, 1967). English Translation: Imperial College Rock Mechanics Research Report No. 10, London, 1969.

Louis, C., 1976, "Introduction A L'Hydraulique Des Roches" (Introduction to rock hydraulics), Dr. Thesis, University of Pierre et Marie Curie, Paris.

Louis, C. and Y.N. Maini, 1970, "Determination of In Situ Hydraulic Parameters in Jointed Rock," 2nd Congress of the International Society for Rock Mechanics, Vol. 1, Sept. 21-26, Belgrade, Yugoslavia, Paper 1-32, pp. 235-245.

Louis, C. and M. Pernot, 1972, "Analyse Tridimensionnelle des Ecoulements dans le Massif de Fondation du Barrage de Grand Maison" (Three dimensional investigation of flow conditions at Grand Maison damsite), Paper T4-F, Percolation Through Fissured Rock, Proceedings, Symposium, Stuttgart 1972. Published by Deutsche Gesellschaft fuer Erd- und Grundbau, Essen, with Prof. Dr.-Ing. Wittke.

Lowe, D.K. and J.L. Huitt, 1966, "Propping Agent Transport in Horizontal Fractures," pp. 753-764, Journal of Petroleum Technology, June.

Maini, Y.N.T, 1971, "In-situ Hydraulic Parameters in Jointed Rock - Their Measurement and Interpretation," Ph.D. Thesis, University of London, Imp. Coll. of Sci. and Technol.

Maini, Y.N.T., J. Noorishad, and J. Sharp, 1982, "Theoretical and Field Considerations on the Determination of In Situ Hydraulic Parameters in Fractured Rock," Paper T1-E, Percolation Through Fissured Rock, Proceedings, Symposium, Stuttgart 1972. Published by Deutsche Gesellschaft fuer Erd- und Grundbau, Essen, with Prof. Dr.-Ing. Wittke.

Makurat, A., 1985, "The Effect of Shear Displacement on the Permeability of Natural Rough Joints," pp. 99-106, Hydrogeology of Rocks of Low Permeability, Memoires Volume XVII, Part 1, Proceedings, Tucson, Arizona, Congress International Association of Hydrogeologists.

Moller, D.W., H. Minch, J.P. Welsh, and R.M. Rubright, 1983, "Pressure Grouting to Control Ground Water in Fractured Granite Rock, Helms Pumped Storage Project," American Concrete Institute Fall Convention, Kansas City, September 25-30. Published in Innovative Cement Grouting, Publication SP-83, American Concrete Institute, Detroit.

BEST AVAILABLE

Morgenstern, N.R. and P.R. Vaughan, 1963, "Some Observations on Allowable Grouting Pressures," Grouts and Drilling Muds in Engineering Practice, symposium organized by the International Society of Soil Mechanics and Foundation Engineering, May, London, pp. 36-42.

Morrow, C., D.A. Lockner, D.E. Moore, and J.D. Byerlee, 1980, "Fluid Flow through Granite in a Temperature Gradient: I. Permeability," EOS, Vol. 61, No. 46, Abstract T95, p. 1112, November 11.

Mott, Hay, and Anderson, 1984, "The Backfilling and Sealing of Radioactive Waste Repositories," EUR 9115 EN, Commission of the European Communities, Luxembourg.

National Coal Board, 1982, "The Treatment of Disused Mine Shafts and Adits," Mining Department, National Coal Board, London, 88 pp.

Nelson, R., 1975, "Fracture Permeability in Porous Reservoirs: Experimental and Field Approach," Ph.D. Dissertation, Texas A&M University, College Station, Texas.

Nelson, R.A. and J.W. Handin, 1977, "Experimental Study of Fracture Permeability in Porous Rock," Bull. Am. Ass. Petrol. Geol., Vol. 61, No. 2, pp. 227-236.

Neuzil, C.E. and J.V. Tracy, 1981, "Flow Through Fractures," Water Resources Research, Vol. 17, no. 1, Feb., pp. 191-199.

Nonveiller, E. and M. Habekovic, 1961, "Properties of Clay-Cement Suspensions for Grouting," pp. 593-606, Question No. 25-R.86, Seventh Congress on Large Dams, Rome.

Obert, L. and W.I. Duvall, 1967, "Rock Mechanics and the Design of Structures in Rock," John Wiley & Sons, New York, 650 pp.

Ohnishi, Y., 1973, "Laboratory Measurement of Induced Water Pressures in Jointed Rock," Ph.D. Thesis, University of California, Berkeley.

Osende, J., 1985, "The Durability of Cement Grouts," pp. 759-766, Q. 58, R. 43, Volume 3, Transactions, Fifteenth Congress on Large Dams, Lausanne, Switzerland, June. Published by the International Commission on Large Dams, Paris.

Parrish, D.R., 1963, "Fluid Flow in Rough Fractures," Paper SPE 563, Production Research Symposium, Norman, Oklahoma, April 29-30.

Pratt, H.R., H.S. Swolfs, W.F. Brace, A.D. Black, and J.W. Handin, 1977, "Elastic and Transport Properties of an In Situ Jointed Granite," pp. 35-45, Vol. 14, Int. J. Rock Mech. Min. Sci. & Geomech. Abstr.

BEST COPY AVAILABLE

Pyrak, L.J., L.R. Myer, and N.G.W. Cook, 1985, "Determination of Fracture Void Geometry and Contact Area at Different Effective Stress," (Abstract), Transactions, American Geophysical Union, Vol. 66, No. 46, p. 903, November 12.

Raven, K.G. and J.E. Gale, 1985, "Water Flow in a Natural Rock Fracture as a Function of Stress and Sample Size," Int. J. Rock Mech. Min. Sci. & Geomech. Abstr., Vol. 22, No. 4, pp. 251-261.

Rayneau, C., 1972, "Contribution a L'Etude des Ecoulements Autour d'un Forage en Milieu Fissure" (Contribution to the study of flow around a borehole in a fractured medium), Doctor of Engineering Thesis, University of Montpellier, France.

Reda, D.C. and G.R. Hadley, 1985, "Saturated Permeability Measurements on Pumice and Welded-Tuffaceous Materials," pp. 87-98, Hydrogeology of Rocks of Low Permeability, Memoires Volume XVII, Part 1, Proceedings, Tucson, Arizona, Congress International Association of Hydrogeologists.

Rissler, 1978, "Determination of the Water Permeability of Jointed Rock," English edition of Vol. 5, Publications of the Institute for Foundation Engineering, Soil Mechanics, Rock Mechanics and Water Ways Construction RWTH (University) Aachen, FRG, Germany.

Roko, R.O., 1987, "Effect of Discontinuity Roughness on Strength and on Deformation Behavior of Rocks," Ph.D. Dissertation, Dept. of Mining and Geological Engineering, University of Arizona, Tucson (In preparation).

Roko, R.O., G.S. Adisoma, and J.J.K. Daemen, 1986, "A New Approach in Direct Shear Testing to Obtain the 'True' Residual Properties of Rock Joints," pp. 33-39, Ch. 5, Rock Mechanics: Key to Energy Production, 27th U.S. Symposium on Rock Mechanics, H.L. Hartman, Editor. Society of Mining Engineers, Inc., Littleton, Colorado.

Romm, E.S., 1966, "Filtratsionnye Suoistva Treshchinonavtykh Gornyx Porod" (Filtration properties of fractured mine rocks), Izdat Nedra, Moscow.

Ruiz, M.D. and P.C. Leone, 1970, "The Importance of Grout Properties in Grouting Jointed Rock Masses," 1st International Congress of the International Association of Engineering Geology, Sept. 8-11, Paris, Vol. 1, pp. 616-635.

Sabarly, F., 1972, Contribution to the Discussion, D1-7, Percolation Through Fissured Rock, Proceedings, Symposium, Stuttgart 1972. Published by Deutsche Gesellschaft fuer Erd- und Grundbau, Essen, with Prof. Dr.-Ing. Wittke.

COPY AVAILABLE

Sabarly, F., 1968, "Les Injections et les drainages de fondation de barrages" (Injections and drainage of dam foundations), pp. 229-249, Vol. 18, Geotechnique.

Sato, K., K. Watanabe, and N. Kotajima, 1984, "Fundamental Study on Flow Resistance in Rock Fissures," Soils and Foundations, Vol. 24, No. 1, pp. 1-8, March.

Schrauf, T.W. and D.D. Evans, 1984, "Relationship Between the Gas Conductivity and Geometry of a Natural Fracture," NUREG/CR-3680, prepared for Division of Health, Siting, and Waste Management, U.S. Nuclear Regulatory Commission, by Department of Hydrology and Water Resources, University of Arizona, Tucson.

Schrauf, T.W. and D.D. Evans, 1986, "Laboratory Studies of Gas Flow Through a Single Natural Fracture," Water Resources Research, Vol. 22, No. 7, pp. 1038-1050, July.

Scott, R.A., 1969, discussion of "Rock Fracture Spacings, Openings, and Porosities," by David J. Snow, Journal of the Soil Mechanics and Foundations Division, ASCE, Vol. 95, no. SM1, paper 6324, January.

Settari, A. and H.S. Price, 1984, "Simulation of Hydraulic Fracturing in Low-Permeability Reservoirs," pp. 141-152, Society of Petroleum Engineers Journal, April.

Sharp, J.C., 1969, Contribution to the Discussion, Theme 6, Vol. 4 pp. 519-521, Proceedings of the Second Congress of the International Society for Rock Mechanics, Belgrade, Yugoslavia, September.

Sharp, J.C., 1970, "Fluid Flow Through Fissured Media," Ph.D. Thesis University of London, Imp. Coll. of Sci. and Technol.

Sharp, J.C. and Y.N.T. Maini, 1972, "Fundamental Considerations on the Hydraulic Characteristics of Joints in Rock," Paper T1-F, Percolation Through Fissured Rock, Proceedings, Symposium, Stuttgart 1972. Published by Deutsche Gesellschaft fuer Erd- und Grundbau, Essen, with Prof. Dr.-Ing. Wittke.

Shimoda, M. and H. Ohmori, 1982, "Ultra Fine Grouting Material," Grouting in Geotechnical Engineering, W.H. Baker, editor, proceedings of the conference on Feb. 10-12, New Orleans, LA, Vol. 1, pp. 77-91. Published by American Society of Civil Engineers, New York.

Shimooka, K., T. Yamamoto, H. Nakamura, Y. Wadachi, N. Tsunoda, T. Murano, and T. Mauo, 1983, "Pilot Research Projects for Underground Disposal of Radioactive Waste in Japan," pp. 339-350, Radioactive Waste Management, Proceedings of an International Conference, Seattle, May 16-20. Published by International Atomic Energy Agency, Vienna, 1984.

BEST COPY AVAILABLE

Sims, G.P. and T.P. Rainey, 1985, "Gitaru Dam Grouting," pp. 1143-1166, Q. 58, R. 69, Vol. 3, Transactions, Fifteenth Congress on Large Dams, Lausanne, Switzerland. Published by the International Commission on Large Dams, Paris.

Snow, D.T., 1968, "Rock Fracture Spacings, Openings, and Porosities," Journal of Soil Mechanics and Foundations Division, ASCE, Vol. 94, no. SM1, paper 5736, pp. 73-91, January.

Snow, D.T., 1970, "The Frequency and Apertures of Fractures in Rock," International Journal of Rock Mechanics and Mining Sciences, Vol. 7, pp. 23-40.

Summers, R., K. Winkler, and J. Byerlee, 1978, "Permeability Changes During the Flow of Water through Westerly Granite at Temperatures of 100°-400°C," Journal of Geophysical Research, Vol. 83, No. B1, pp. 339-344, January 10.

Sundaram, P.N. and D. Fink, 1983, "Electrical Analogy of Hydraulic Flow Through Rock Fractures," Geotechnical Testing Journal, Vol. 6, No. 1, pp. 3-9, March.

Thiers, G.R., L.W. Lobdell, and B.M. Mihalcin, 1976, "Foundation Treatment for Little Blue Run Dam," Rock Engineering for Foundations and Slopes, Vol. 1, proceedings of a specialty conference on Aug. 15-18, Boulder, Colorado, ASCE, pp. 283-308.

Trimmer, D., 1982, "Laboratory Measurements of Ultralow Permeability of Geologic Materials," Rev. Sci. Instrum., Vol. 53, No. 8, pp. 1246-54, August.

Trimmer, D., B. Bonner, H.C. Heard, and A. Duba, 1980a, "Effect of Pressure and Stress on Water Transport in Intact and Fractured Gabbro and Granite," Journal of Geophysical Research, Vol. 85, No. B12, pp. 7059-71, December 10.

Trimmer, D., B. Bonner, H.C. Heard, and A. Duba, 1980b, "Effect of Pressure and Stress on Water Transport in Intact and Fractured Gabbro and Granite," UCRL Preprint 83932, Lawrence Livermore Laboratory, February.

Tsang, C.F., J. Noorishad, and P.A. Witherspoon, 1985, "The Effect of Deformability on Fluid Flow through a Fractured-Porous Medium," pp. 473-485, Part 2, Proceedings, Hydrogeology of Rocks of Low Permeability, Memoires Vol. XVII, International Association of Hydrogeologists, Tucson, Arizona, Congress.

Tsang, Y.W., 1984, "The Effect of Tortuosity on Fluid Flow Through a Single Fracture," Water Resources Research, Vol. 20, No. 9, pp. 1209-15, September.

Tsang, Y.W. and P.A. Witherspoon, 1981, "Hydromechanical Behavior of a Deformable Rock Fracture Subject to Normal Stress," Journal of Geophysical Research, Vol. 86, No. B10, pp. 9287-98, October 10.

COPY AVAILABLE

Tsang, Y.W. and P.A. Witherspoon, 1983, "The Dependence of Fracture Mechanical and Fluid Flow Properties on Fracture Roughness and Sample Size," Journal of Geophysical Research, Vol. 88, No. B3, pp. 2359-66, March 10.

Tsang, Y.W. and P.A. Witherspoon, 1985, "Effects of Fracture Roughness on Fluid Flow through a Single Deformable Fracture, pp. 683-694, Part 2, Proceedings, Hydrogeology of Rocks of Low Permeability, Memoires Vol. XVII, International Association of Hydrogeologists, Tucson, Arizona, Congress.

U.S. Army Corps of Engineers, 1956, "Pressure Grouting Fine Fissures," Technical Report No. 6-437, Waterways Experiment Station, Vicksburg, Mississippi.

U.S. Environmental Protection Agency, 1986, "Environmental Standards and Federal Radiation Protection Guidance for Management and Disposal of Spent Nuclear Fuel, High-Level and Transuranic Radioactive Wastes," 40 CFR 191, Federal Register, Final Rule.

U.S. Nuclear Regulatory Commission, 1983, "Disposal of High-Level Radioactive Wastes: Licensing Procedures," Title 10, Chapter 1, Code of Federal Regulations - Energy. Part 60. June 30.

U.S. Nuclear Regulatory Commission, 1983, "Disposal of High-Level Radioactive Wastes in Geologic Repositories," Final Rule 10 CRF 60, Federal Register, Vol. 48, No. 120, June 30.

U.S. Nuclear Regulatory Commission, 1985, "Disposal of High-Level Radioactive Wastes in Geologic Repositories," 10 CFR Part 60, Federal Register, Vol. 50, No. 140, pp. 29641-8. Monday, July 22.

U.S. Nuclear Regulatory Commission, 1985, "Disposal of High-Level Radioactive Wastes in Geologic Repositories," Final Rule, Unsaturated Zone Amendment, Federal Register, Vol. 50, No. 140, pp. 29641-8, Monday, July 22.

Vaughan, P.R., 1963, discussion of "Some Observations on Allowable Grouting Pressures," Grouts and Drilling Muds in Engineering Practice, symposium organized by the International Society of Soil Mechanics and Foundation Engineering, May, London, pp. 54-55.

Wallner, M., 1976, "Propagation of Sedimentation Stable Cement Pastes in Jointed Rock," pp. 49-165, English edition of Volume 2, Publications of the Institute for Foundation Engineering, Soil Mechanics, Rock Mechanics and Water Ways Construction RWTH (University) Aachen, FRG, Germany.

Wallner, M. and W. Wittke, 1974, "Theorie und Experiment zu einem neuen Injektionsverfahren" (Theory and experiment of a new grouting procedure), pp. 744-750, Vol. II, Part B, Advances in Rock Mechanics, Proceedings of the Third Congress of the

BEST COPY AVAILABLE

International Society for Rock Mechanics, Denver. Published by National Academy of Sciences, Washington, DC.

Walsh, J.B., 1981, "Effect of Pore Pressure and Confining Pressure on Fracture Permeability," Int. J. Rock Mech. Min. Sci. & Geomech. Abstr., Vol. 18, pp. 429-435.

Water Resources Commission, N.S.W., 1978, "Manual of Grouting Techniques for Anchor Tendons," First Edition, North Sydney, Australia.

Water Resources Commission, N.S.W., 1981, "Grouting Manual," fourth edition, North Sydney, Australia.

Witherspoon, P.A., 1981, "Effect of Size on Fluid Movements in Rock Fractures," Geophysical Research Letters, Vol. 8, No. 7, pp. 659-661, July.

Witherspoon, P.A., C.H. Amick, and J.E. Gale, 1977, "Stress-flow Behavior of a Fault Zone with Fluid Injection and Withdrawal," Report No. 77-1, Dept. of Materials Science and Mineral Engineering, University of California, Berkeley.

Witherspoon, P.A., C.H. Amick, J.E. Gale, and K. Iwai, 1979, "Observations of a Potential Size Effect in Experimental Determination of the Hydraulic Properties of Fractures," Water Resources Research, Vol. 15, no. 5, October, pp. 1142-1146.

Witherspoon, P.A., J.S.Y. Wang, K. Iwai, and J.E. Gale, 1980, "Validity of the Cubic Law for Fluid Flow in a Deformable Rock Fracture," Water Resources Research, Vol. 16, no. 6, December, pp. 1016-1024.

Witherspoon, P.A., D.J. Watkins, and Y.W. Tsang, 1981, "Theoretical and Laboratory Investigations of Flow Through Fractures in Crystalline Rock," pp. 65-83, The Technology of Nuclear Waste Disposal, DOE/TIC-4621 (Vol. 1), P.L. Hofmann, editor. Technical Information Center, U.S. Department of Energy.

Wittke, W., 1968, "Zur Reichweite von Injektionen in klueftigen Fels" (Concerning the extent of penetration of grout in fissured rock), Felsmechanik und Ingenieurgeologie, Suppl. IV, pp. 79-89.

Wittke, W., 1969, "Neues Verfahren zum Verpressen von klueftigem Fels mit Pasten auf der Basis von Zement" (New method for grouting jointed rock with pastes based on cement), VDI Zeitschrift, Vol. III, No. 22, pp. 1568-1573, November (II).

Wittke, W., 1973, "Anwendung der Finite-Element-Methode auf den Entwurf von untertagigen Dammen," (Application of the Finite Element Method to the Design of Underground Dams) Erzmetall, Vol. 26, pp. 66-74.

AVAILABLE

Wittke, W. and C. Louis, 1968, "Modellversuche zur Durchstroemung klueftiger Medien" (Model tests on flow through fissured media), Felsmechanik und Ingenieurgeologie - Rock Mechanics and Engineering Geology, Supplementum IV, pp. 57-78.

Wittke, W., B. Pierau, and B. Plischke, 1978, "Erfahrungen mit Zementpasten bei Injektionsarbeiten in flueftigem Fels" (Experience with cement pastes during injections of jointed rock), pp. 75-166, Vol. 7, Veroeffentlichungen des Institutes fuer Grundbau, Bodenmechanik, Felsmechanik und Verkehrswasserbau der RWTH Aachen, Aachen.

Wong, H.Y. and I.W. Farmer, 1973, "Hydrofracture Mechanisms in Rock During Pressure Grouting," Rock Mechanics, journal of the International Society for Rock Mechanics, Vol. 5, Springer-Verlag, New York, pp. 21-41.

Yuen, C.M.K. and J.M. Boyd, 1982, "A Conceptual Design Study for an Underground Research Laboratory," TR-160, by Golder Associates for Atomic Energy of Canada Limited, Pinawa, Manitoba.

Zeigler, T.W., 1976, "Determination of Rock Mass Permeability," U.S. Army Engr. Waterways Expt. Station, Technical Report S-76-2.

BEST COPY AVAILABLE

BLANK PAGE

APPENDIX A

GROUT COMPOSITION AND

UNIAXIAL COMPRESSIVE STRENGTH TEST RESULTS

Table A.1 Grout Mix Compositions

Grout Mix	Composition
1	Ideal Class A (Tijeras Canyon) 10% D53 1% D65 64% H_2O
2	Ideal Class A (Tijeras Canyon) 10% D53 1% D65 133% H_2O 2.67% Bentonite
3	Ideal Class A (Tijeras Canyon) 10% D53 1% D65 200% H_2O 5% Bentonite
4	Ideal Class A (Tijeras Canyon) 10% D53 1% D65 133% H_2O
5	Ideal Class A (Tijeras Canyon) 10% D53 1% D65 200% H_2O

Cement and additives D53 and D65 provided by Dowell, Tulsa, Oklahoma.
D53 is an expansive agent.
D65 is a dispersant.
Bentonite - American Colloid C/S Granular.

BEST COPY AVAILABLE

Table A.2 Uniaxial Compressive Strength and Unit Weight of Grout Mix 1.

Sample	Diameter (in)	Length (in)	Unit Wt. (pcf)	Failure Load (lbs)	Axial Stress at Failure (psi)
			8 Days Curing Time:		
1	1.135	2.338	111.0	2640	2609
2	1.132	2.353	111.7	2620	2603
3	1.122	2.273	114.3	2520	2549
4	1.127	2.318	113.5	2400	2513
5	1.121	2.346	115.1	2480	2513
Average:			113.1		2536
Standard Deviation:			1.73		82.8
Coefficient of Variation:			1.5%		3.3%
			28 Days Curing Time:		
1	1.128	2.265	113.5	3820	3823
2	1.125	2.343	114.4	4080	4105
3	1.128	2.355	113.2	4120	4123
4	1.129	2.368	114.0	4060	4056
Average:			113.8		4027
Standard Deviation:			0.53		138.8
Coefficient of Variation:			0.5%		3.5%

NOTE: All samples cured under water at room temperature and atmospheric pressure.

COPY AVAILABLE

Table A.3 Uniaxial Compressive Strength and Unit Weight of Grout Mix 2.

Sample	Diameter (in)	Length (in)	Unit Wt. (pcf)	Failure Load (lbs)	Axial Stress at Failure (psi)
			8 Days Curing Time:		
1	1.129	2.317	-	480	479
2	1.133	1.871	-	520	504*
3	1.127	2.220	92.8	480	481
4	1.127	2.206	91.7	460	461
Average:			92.2		481
Standard Deviation:			0.78		17.6
Coefficient of Variation:			0.8%		3.7%
			28 Days Curing Time:		
1	1.130	2.413	91.2	680	678
2	1.131	2.470	93.6	780	776
3	1.132	2.417	93.9	800	795
4	1.134	2.434	92.9	800	792
5	1.134	2.251	92.1	800	792
Average:			92.7		767
Standard Deviation:			1.11		50.1
Coefficient of Variation			1.2%		6.5%

*Failure stress corrected to length/diameter = 2 after Obert and Duvall (1967, p. 332).

NOTE: All samples cured under water at room temperature and atmospheric pressure.

BEST COPY AVAILABLE

Table A.4 Uniaxial Compressive Strength and Unit Weight of Grout Mix 3

Sample	Diameter (in)	Length (in)	Unit Weight (pcf)	Failure Load (lbs)	Axial Stress at Failure (psi)
			8 Days Curing Time:		
1	1.125	2.512	82.3	145	146
2	1.125	2.424	82.9	139	140
3	1.128	2.377	81.7	141	141
4	1.129	2.322	81.9	146	146
5	1.123	2.316	82.1	145	146
6	1.125	2.258	82.2	133	134
Average:			82.2		142
Standard Deviation:			0.41		4.8
Coefficient of variation:			0.5%		3.4%
			28 Days Curing Time:		
1	1.124	2.533	83.3	225	227
2	1.127	2.511	83.6	232	232
3	1.126	2.500	82.6	223	224
4	1.128	2.461	82.8	227	227
5	1.127	2.489	82.0	202	202
6	1.130	2.495	81.4	234	233
Average:			82.6		224
Standard Deviation:			0.82		11.4
Coefficient of Variation:			1.0%		5.1%

NOTE: All samples cured under water at room temperature and atmospheric pressure.

BEST COPY AVAILABLE

Table A.5 Uniaxial Compressive Strength and Unit Weight of Grout Mix 4

Sample	Diameter (in)	Length (in)	Unit Weight (pcf)	Failure Load (lbs)	Axial Stress at Failure (psi)
			8 Days Curing Time:		
1	1.129	2.475	96.0	311	311
2	1.131	2.466	95.3	276	275
3	1.128	2.491	96.3	315	315
4	1.133	2.485	94.9	311	308
5	1.130	2.437	95.0	307	306
Average:			95.5		303
Standard Deviation:			0.62		16.0
Coefficient of variation:			0.6%		5.3%
			28 Days Curing Time:		
1	1.129	2.512	100.6	540	539
2	1.132	2.485	111.1	1100	1093
3	1.130	2.471	102.6	660	658
4	1.130	2.458	98.5	520	518
Average:			103.2		702
Standard Deviation:			5.54		267.9
Coefficient of Variation:			5.4%		38.2%

NOTE: All samples cured under water at room temperature and atmospheric pressure.

BEST COPY AVAILABLE

Table A.6 Uniaxial Compressive Strength and Unit Weight of Grout Mix 5

Sample	Diameter (in)	Length (in)	Unit Weight (pcf)	Failure Load (lbs)	Axial Stress at Failure (psi)
			8 Days Curing Time:		
1	1.126	2.421	86.8	54	54
2	1.129	2.462	88.0	104	104
3	1.125	2.485	87.8	123	124
4	1.128	2.494	87.8	101	101
5	1.128	2.500	89.9	123	123
Average:			88.1		101
Standard Deviation:			1.13		28.4
Coefficient of variation:			1.3%		28.1%
			28 Days Curing Time:		
1	1.131	2.483	90.0	165	164
2	1.131	2.500	86.9	152	151
3	1.130	2.440	88.8	151	151
4	1.130	2.385	88.5	147	147
5	1.132	2.098	91.4	198	195
Average:			89.1		162
Standard Deviation:			1.68		19.9
Coefficient of Variation:			1.9%		12.3%

NOTE: All samples cured under water at room temperature and atmospheric pressure.

...Y AVAILABLE

Table A.7 28 Day Uniaxial Compressive Strength and Unit Weight of Grout Mix 2.

Sample	Diameter (in)	Length (in)	Unit Wt. (pcf)	Failure Load (lbs)	Axial Stress at Failure (psi)
			900 psi Grout Injection Pressure:		
1	1.129	2.257	91.0	420	420
2	1.131	2.309	90.2	420	418
3	1.132	2.449	89.6	400	397
Average:			90.3		412
Standard Deviation:			0.70		12.7
Coefficient of Variation:			0.8%		3.1%
			180 psi Grout Injection Pressure:		
1	1.127	2.515	91.1	560	561
2	1.128	2.434	91.5	600	600
Average:			91.3		580.5
Standard Deviation:			0.14		27.6
Coefficient of Variation:			0.2%		4.8%

NOTE: All samples cured under water at room temperature and atmospheric pressure.

BEST COPY AVAILABLE

Table A.8 28-Day Uniaxial Compressive Strength and Unit Weight of Grout Mix 3

Sample	Diameter (in)	Length (in)	Unit Weight (pcf)	Failure Load (lbs)	Axial Stress at Failure (psi)
		300 psi Grout Injection Pressure:			
1	1.127	2.472	81.4	162	162
2	1.129	2.450	81.0	---	---
3	1.131	2.450	82.0	181	180
Average:			81.5		171
Standard Deviation:			0.39		
Coefficient of Variation:			0.5%		

NOTE: All samples cured under water at room temperature and atmospheric pressure.

BEST COPY AVAILABLE

Figure A.1 Grout mix 1 specimens failed in uniaxial compression. Top row, specimens tested after 8 days curing; bottom row, specimens tested after 28 days curing.

Figure A.2 Grout mix 2 specimens failed in uniaxial compression. Top row, specimens tested after 8 days curing; bottom row, specimens tested after 28 days curing.

AVAILABLE

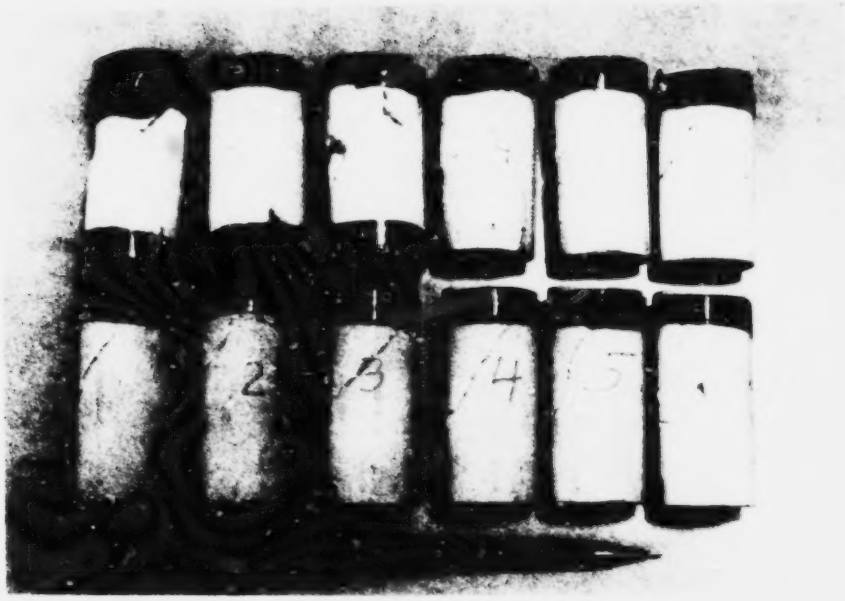

Figure A.3 Grout mix 3 specimens failed in uniaxial compression. Top row, specimens tested after 8 days curing; bottom row, specimens tested after 28 days curing.

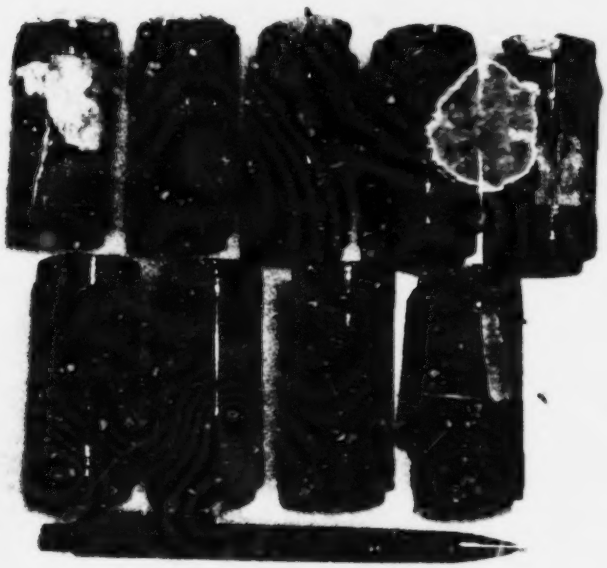

Figure A.4 Grout mix 4 specimens failed in uniaxial compression. Top row, specimens tested after 8 days curing; bottom row, specimens tested after 28 days curing.

AVAILABLE COPY

Figure A.5 Grout mix 5 specimens failed in uniaxial compression. Top row, specimens tested after 8 days curing; bottom row, specimens tested after 28 days curing.

Figure A.6 Specimens of pumped grout mix 2 failed in uniaxial compression after 28 days curing time. Top row, specimens subjected to 900 psi grout injection pressure; bottom row, specimens subjected to 180 psi grout injection pressure.

BEST COPY AVAILABLE

Figure A.7 Specimens of pumped grout mix 3 failed in uniaxial compression after 28 days curing time. Specimens subjected to 300 psi grout injection pressure.

COPY NOT AVAILABLE

APPENDIX B

BLEED TEST RESULTS

Table B.1 Bleed Test for Grout Mix 1

Time (min)	Total Volume (ml)	Cement Volume (ml)	Bleed Volume (ml)	Bleed Volume / Total Volume (%)
0	997	997	0	0
20	997	994	3	0.3
40	994	991	3	0.3
60	993	990	3	0.3
80	993	990	3	0.3
100	993	990	3	0.3
120	992	989	3	0.3
140	991	988	3	0.3

BEST COPY AVAILABLE

Table B.2 Bleed Test for Grout Mix 2

Time (min)	Total Volume (ml)	Cement Volume (ml)	Bleed Volume (ml)	Bleed Volume / Total Volume (%)
0	1000	1000	0	0
30	1000	998	2	0.2
60	998	994	4	0.4
90	996	991	5	0.5
120	995	990	5	0.5
150	995	989	6	0.6
180	994	988	6	0.6
210	993	987	6	0.6
240	991	985	6	0.6

Table B.3 Bleed Test for Grout Mix 3

Time (min)	Total Volume (ml)	Cement Volume (ml)	Bleed Volume (ml)	Bleed Volume / Total Volume (%)
0	1005	1005	0	0
30	1001	1000	1	0.1
60	1000	998	2	0.2
90	999	995	4	0.4
120	996	992	4	0.4
150	995	990	5	0.5
180	994	989	5	0.5
210	994	989	5	0.5

Table B.5 Bleed Test for Grout Mix 5

Time (min)	Total Volume (ml)	Cement Volume (ml)	Bleed Volume (ml)	Bleed Volume / Total Volume (%)
		Test 1		
0	1005	1005	0	0
30	995	944	51	5
60	994	900	94	9
90	992	846	146	15
120	991	780	211	21
150	990	660	330	33
180	990	645	345	35
210	990	640	350	35
240	990	640	350	35
		Test 2		
0	1000	1000	0	0
20	990	954	36	4
50	988	905	83	8
80	987	853	134	14
110	985	791	194	20
140	984	683	301	31
170	984	637	347	35
200	984	630	354	36
230	984	621	363	37
240	984	619	365	37

BEST COPY AVAILABLE

Table B.4 Bleed Test for Grout Mix 4

Time (min)	Total Volume (ml)	Cement Volume (ml)	Bleed Volume (ml)	Bleed Volume / Total Volume (%)
		Test 1		
0	1000	1000	0	0
10	999	988	11	1
20	997	975	22	2
40	993	950	43	4
60	991	925	66	7
80	990	900	90	9
100	989	867	122	12
120	989	810	179	18
140	988	782	206	21
160	988	776	212	21
180	988	772	216	22
200	987	770	217	22
220	987	770	217	22
		Test 2		
0	1000	1000	0	0
10	998	990	8	0.8
20	995	977	18	2
40	993	954	39	4
60	990	930	60	6
80	990	908	82	8
100	989	883	106	11
120	988	851	136	14
140	988	805	182	18
160	988	774	214	22
180	987	762	225	23
200	987	756	231	23
220	987	755	231	23

BEST COPY AVAILABLE

Figure B.1 Grout mix 1 after bleed testing.

BEST COPY AVAILABLE

BEST COPY AVAILABLE

Figure B.2 Grout mix 2 after bleed testing.

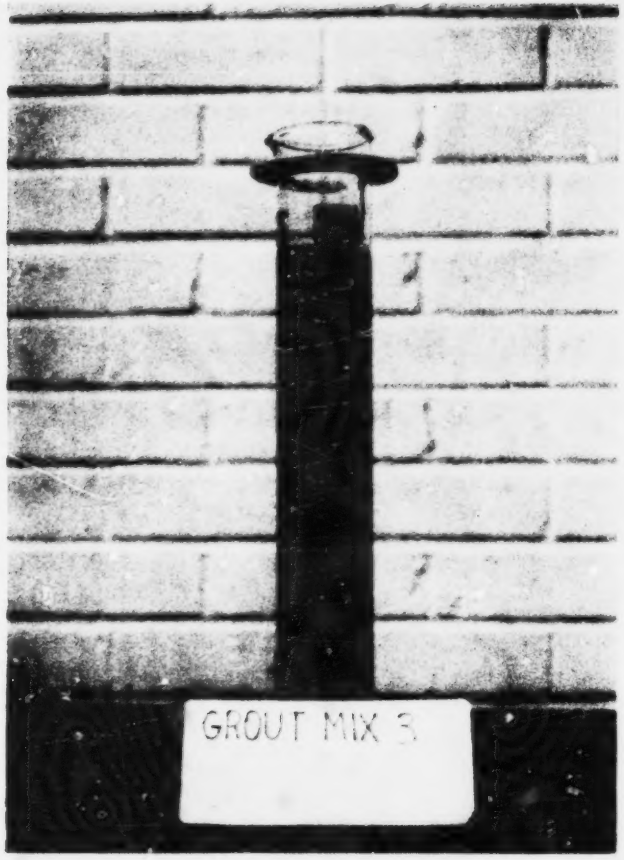

Figure B.3 Grout mix 3 after bleed testing

BEST COPY AVAILABLE

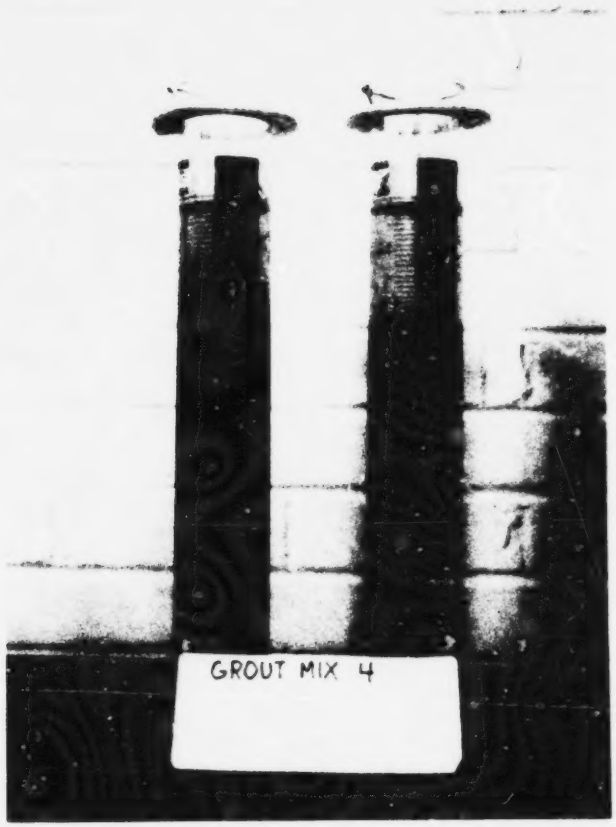

Figure B.4 Grout mix 4 after bleed testing.

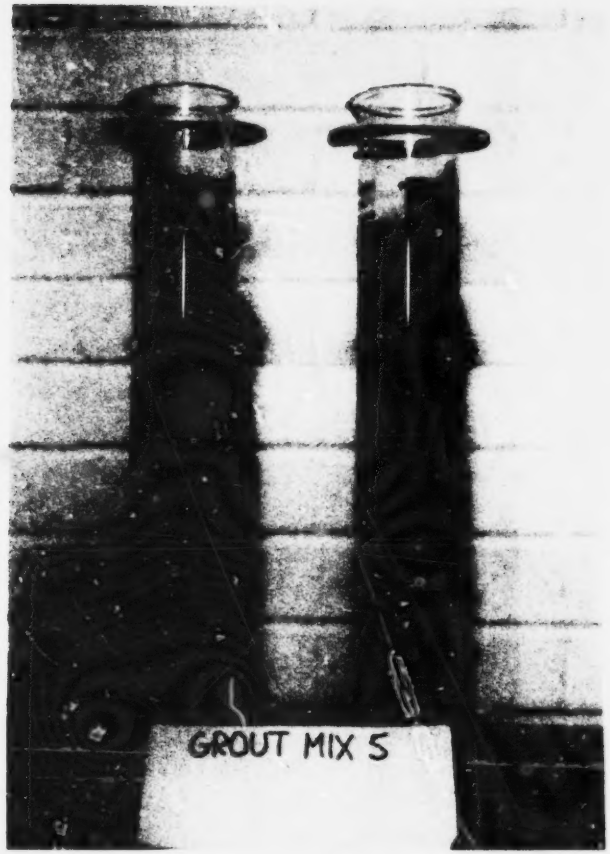

Figure B.5 Grout mix 5 after bleed testing

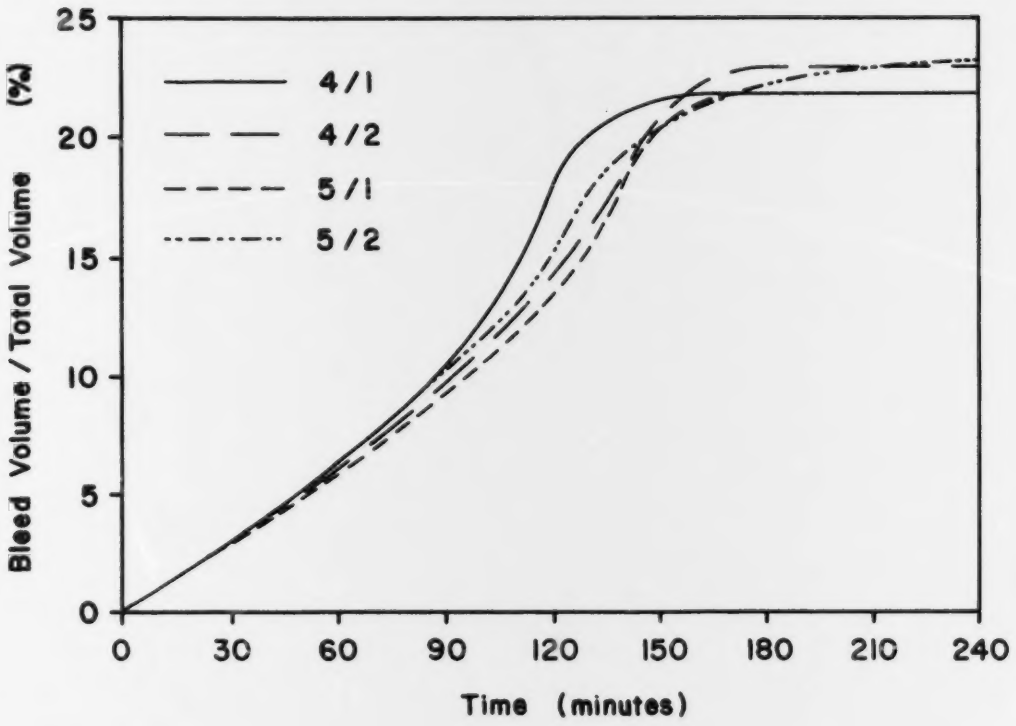

Figure B.6 Bleed rate for grout mixes 4 and 5

4/1: grout mix 4/test 1
4/2: grout mix 4/test 2
5/1: grout mix 5/test 1
5/2: grout mix 5/test 2

BEST COPY AVAILABLE

APPENDIX C

FRACTURE FLOW

STRESS-PERMEABILITY TEST RESULTS

Table C.1.1 Permeability Test Results for a Sawcut in Charcoal Granite, Sample 1

Normal Stress MPa (psi)	Time (sec)	Initial Height (cm)	Final Height (cm)	Aperture (cm)	Hydraulic Conductivity (cm/sec)
3.448 (500)	26.98	127.48	95.08	72.6×10^{-4}	$.391 \times 10^{0}$
6.895 (1000)	30.36	127.48	95.08	69.8×10^{-4}	$.361 \times 10^{0}$
13.790 (2000)	35.12	127.48	95.08	66.5×10^{-4}	$.328 \times 10^{0}$
6.895 (1000)	31.84	127.48	95.08	68.7×10^{-4}	$.350 \times 10^{0}$
3.448 (500)	28.63	127.48	95.08	71.2×10^{-4}	$.376 \times 10^{0}$
0.0138 (2*)	22.96	127.48	95.08	76.6×10^{-4}	$.435 \times 10^{0}$
3.448 (500)	27.90	127.48	95.08	71.8×10^{-4}	$.382 \times 10^{0}$
6.895 (1000)	30.34	127.48	95.08	69.8×10^{-4}	$.362 \times 10^{0}$
13 790 (2000)	34.97	127.48	95.08	66.6×10^{-4}	$.329 \times 10^{0}$
6.985 (1000)	31.26	127.48	95.08	69.1×10^{-4}	$.354 \times 10^{0}$

Buret radius = .54 cm
Ratio of sample radius to drillhole radius = 6.00.

Initial Height and Final Height refer to water level in falling head permeameter buret.

*Estimated, e.g. for exponential curve fitting. Otherwise 0.

BEST COPY AVAILABLE

Table C.1.2 Hydraulic Conductivity - Normal Stress Equations for a Sawcut in Granite. Sample 1.

Equation	Load Cycle-Step (L: Loading U: Unloading)	Best Fit Equation	(r^2)
$K_f = K_1(P^{-\alpha})$ (5.3)	1-L	$0.459(P^{-0.127})$	0.997
(5.3)	1-U	$0.375(P^{-0.037})$	0.914
(5.3)	2-L	$0.380(P^{-0.034})$	0.861
$K_f = K_o(e^{-cP})$ (5.1)	1-L	$0.410(e^{-0.017\ P})$	0.981
(5.1)	1-U	$0.416(e^{-0.019\ P})$	0.873
(5.1)	2-L	$0.421(e^{-0.019\ P})$	0.933
$K_f = K_m(P/P_m)^{-\alpha}1$ (5.4)	1-L	$0.789(P/0.0138)^{-0.127}$	0.997
(5.4)	1-U	$0.439(P/0.0138)^{-0.037}$	0.914
(5.4)	2-L	$0.440(P/0.0138)^{-0.034}$	0.861
(5.4)	1-L	$1.11207(P/0.001)^{-0.128}$	0.998
(5.4)	1-U	$0.43846(P/0.001)^{-0.026}$	0.882
(5.4)	2-L	$0.4379(P/0.001)^{-0.024}$	0.834
(5.4)	1-L	$0.6141(P/0.1)^{-0.127}$	0.997
(5.4)	1-U	$0.4394(P/0.1)^{-0.054}$	0.9535
(5.4)	2-L	$0.4407(P/0.1)^{-0.0508}$	0.9108

AVAILABLE

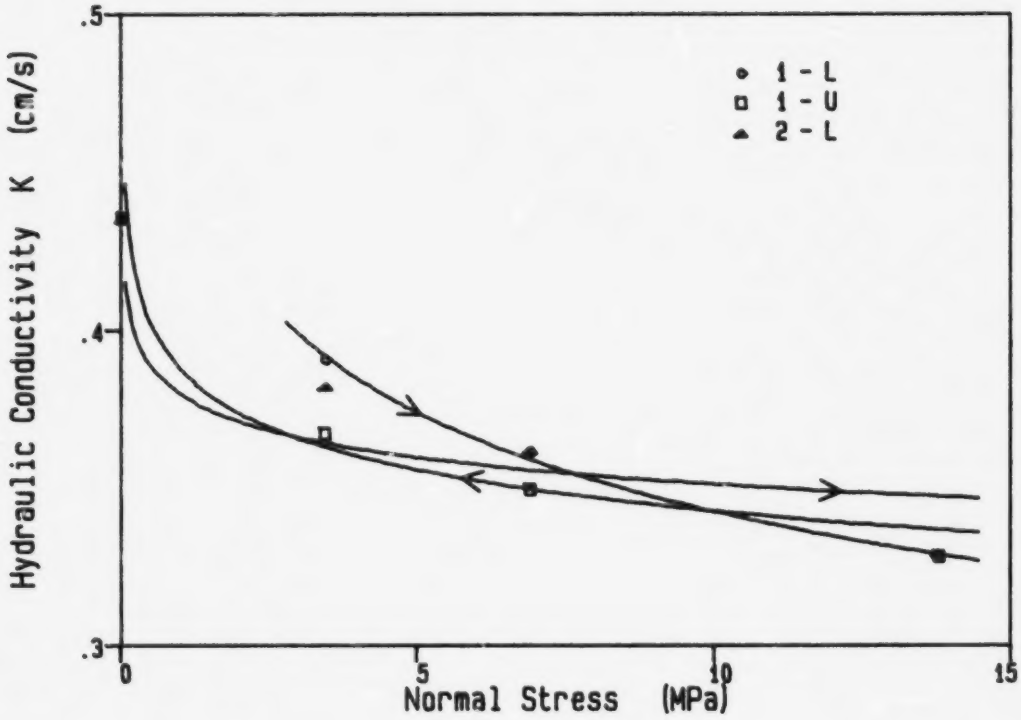

Figure C.1.1 Hydraulic conductivity K_f as a function of total normal stress P for a sawcut in Charcoal granite Sample 1.

Curves plotted:

1-L: $K_f = 0.45864(P^{-0.12675})$ (Eqtn. 5.3)

1-U: $K_f = 0.4394(P/0.1)^{-0.054}$ (Eqtn. 5.4)

2-L: $K_f = 0.43997(P/0.0138)^{-0.03424}$ (Eqtn. 5.4)

1-L: cycle 1, loading; 1-U: cycle 1, unloading.

2-L: cycle 2, loading

BEST COPY AVAILABLE

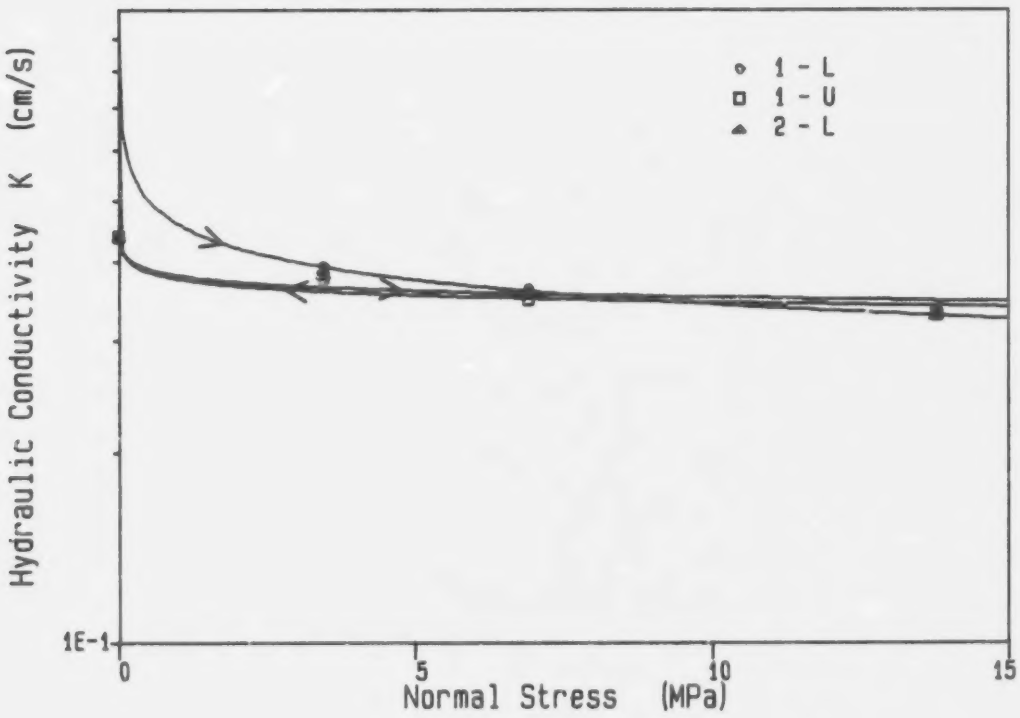

Figure C.1.2 Hydraulic conductivity as a function of normal stress for a sawcut in Charcoal granite Sample 1. Arrows indicate loading path.

Power Law Fit. Equation (5.3), Table C.1.2.

AVAILABLE

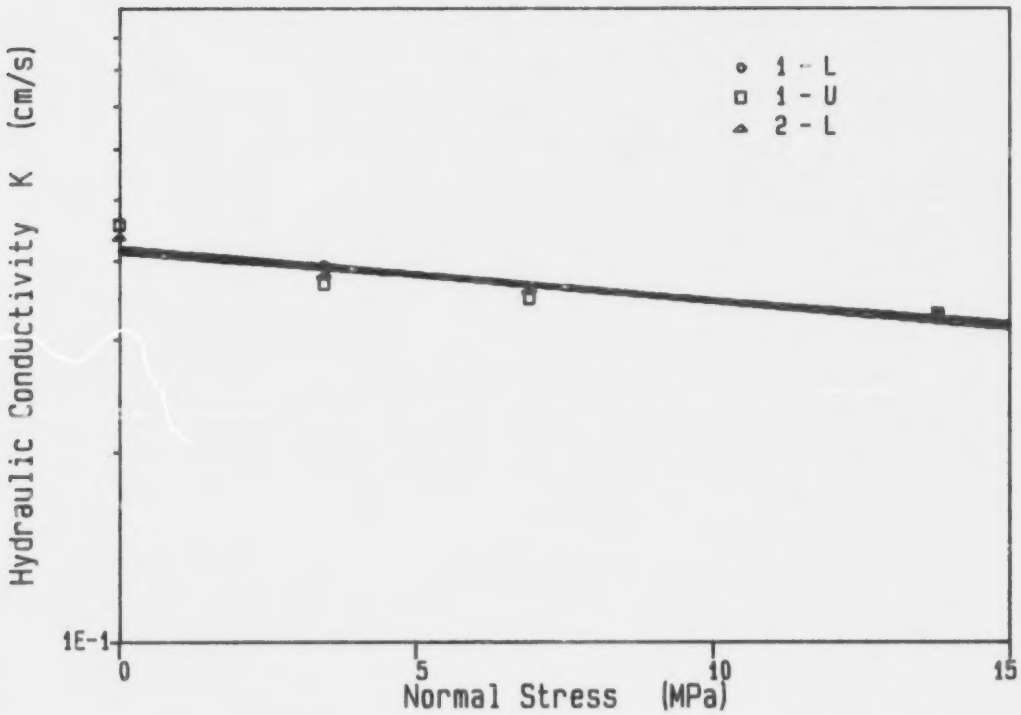

Figure C.1.3 Hydraulic conductivity as a function of normal stress for a sawcut in Charcoal granite Sample 1.

Exponential Fit. Equation (5.1), Table C.1.2.

BEST COPY AVAILABLE

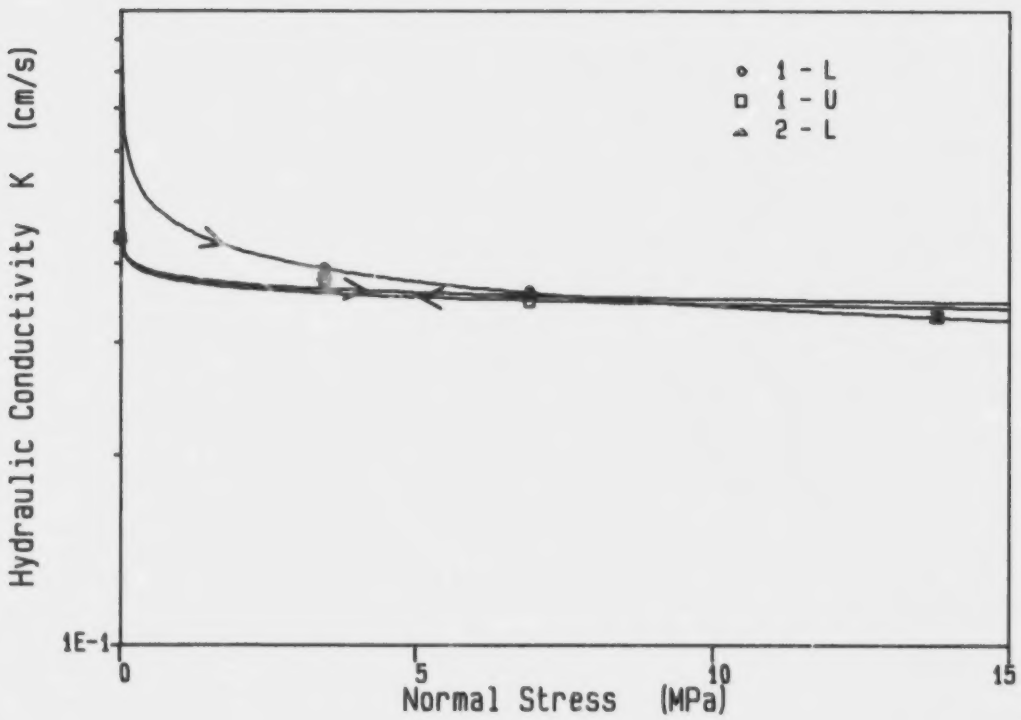

Figure C.1.4 Hydraulic conductivity as a function of normal stress for a sawcut in Charcoal granite Sample 1. Arrows indicate loading path.

Modified Power Law. Equation (5.4), with P_m = 0.0138 MPa, Table C.1.2.

BEST COPY AVAILABLE

Table C.2.1 Permeability Test Results for a Sawcut in Charcoal Granite, Sample 2

Normal Stress MPa (psi)	Time (sec)	Initial Height (cm)	Final Height (cm)	Aperture (cm)	Hydraulic Conductivity (cm/sec)
0.0 (0)	353	127.48	116.68	20.7×10^{-4}	$.317 \times 10^{-1}$
3.448 (500)	9480	130.50	129.64	2.91×10^{-4}	$.629 \times 10^{-3}$
6.895 (1000)	9960	134.39	133.96	2.25×10^{-4}	$.375 \times 10^{-3}$
13.790 (2000)	9540	132.23	132.02	1.82×10^{-4}	$.246 \times 10^{-3}$
6.895 (1000)	11820	131.91	131.48	2.14×10^{-4}	$.339 \times 10^{-3}$
3.448 (500)	6360	134.28	133.85	2.61×10^{-4}	$.506 \times 10^{-3}$
2.069 (300)	3300	133.64	132.34	4.70×10^{-4}	$.164 \times 10^{-2}$
0.690 (100)	577	129.42	128.56	7.42×10^{-4}	$.409 \times 10^{-2}$
0.0 (0)	1340	127.48	116.68	13.3×10^{-4}	$.130 \times 10^{-1}$
0.690 (100)	795	128.78	127.91	6.68×10^{-4}	$.331 \times 10^{-2}$
2.069 (300)	11520	131.80	130.83	2.83×10^{-4}	$.593 \times 10^{-3}$
3.448 (500)	11340	135.04	134.61	2.15×10^{-4}	$.343 \times 10^{-3}$
6.895 (1000)	14820	132.77	132.45	1.80×10^{-3}	$.240 \times 10^{-3}$

Buret radius: .54 cm
Ratio of sample radius to drillhole radius: 6.00.

Initial Height and Final Height refer to water level in falling head permeameter buret.

BEST COPY AVAILABLE

Table C.2.2 Hydraulic Conductivity - Normal Stress Equations for a Sawcut in Granite. Sample 2.

Equation		Load Cycle-Step (L: Loading U: Unloading)	Best Fit Equation	(r^2)
$K_f = K_1(P^{-\alpha})$	(5.3)	1-L	$0.00152(P^{-0.708})$	0.9998
(5.3)		1-U	$0.00149(P^{-0.594})$	0.890
(5.3)		1-L	$0.00105(P^{-0.653})$	0.908
$K_f = K_o(e^{-\epsilon P})$	(5.1)	1-L	$0.0072(e^{-0.3018P})$	0.630
(5.1)		1-U	$0.00375(e^{-0.2465P})$	0.670
(5.1)		2-L	$0.00465(e^{-0.528\ P})$	0.731
$K_f = K_m(P/P_m)^{-\alpha}1$	(5.4)	1-L	$0.03155(P/0.0138)^{-0.708}$	0.9998
(5.4)		1-U	$0.0190(P/0.0138)^{-0.594}$	0.890
(5.4)		2-L	$0.0172(P/0.0138)^{-0.653}$	0.907

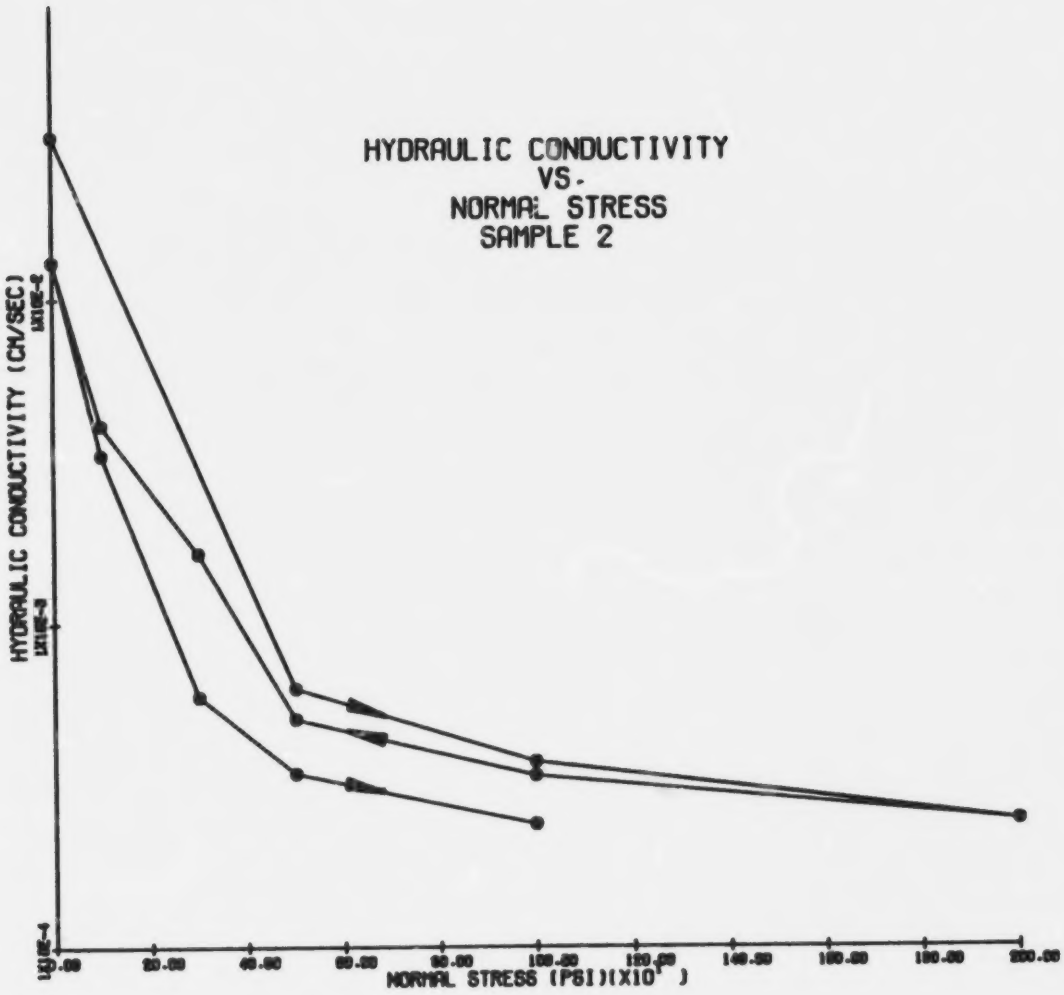

Figure C.2.1 Hydraulic conductivity as a function of normal stress for a sawcut in Charcoal granite, sample 2. Arrows indicate loading sequence.

BEST COPY AVAILABLE

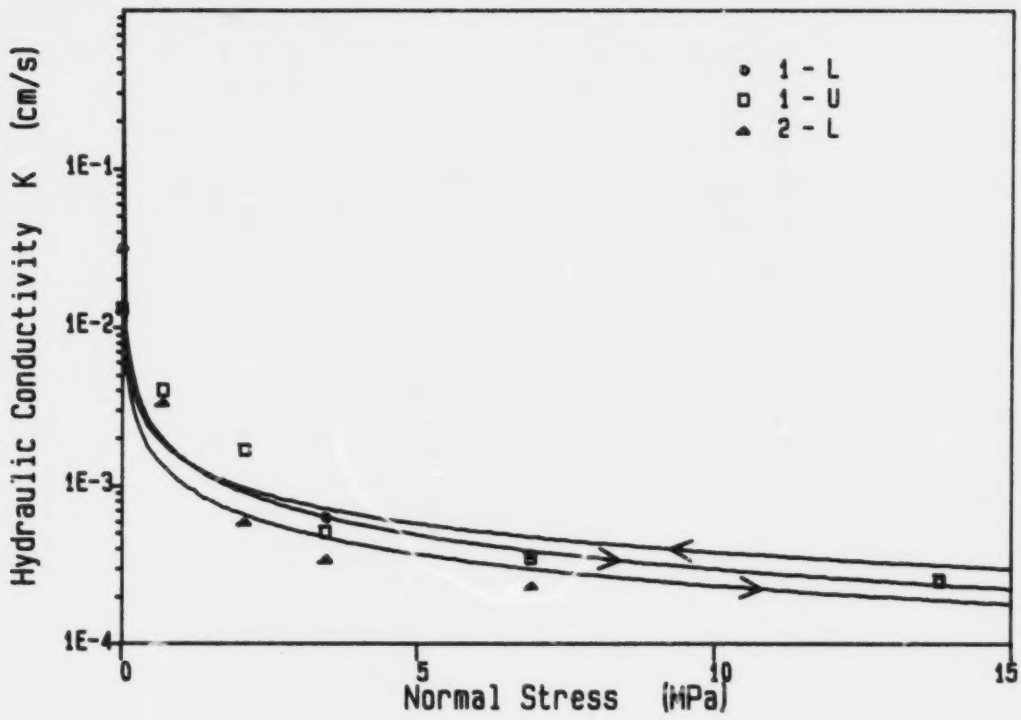

Figure C.2.2 Hydraulic conductivity as a function of normal stress for a sawcut in Charcoal granite Sample 2. Arrows indicate loading sequence.

Power Law Fit. Equation (5.3), Table C.2.2.

BEST COPY AVAILABLE

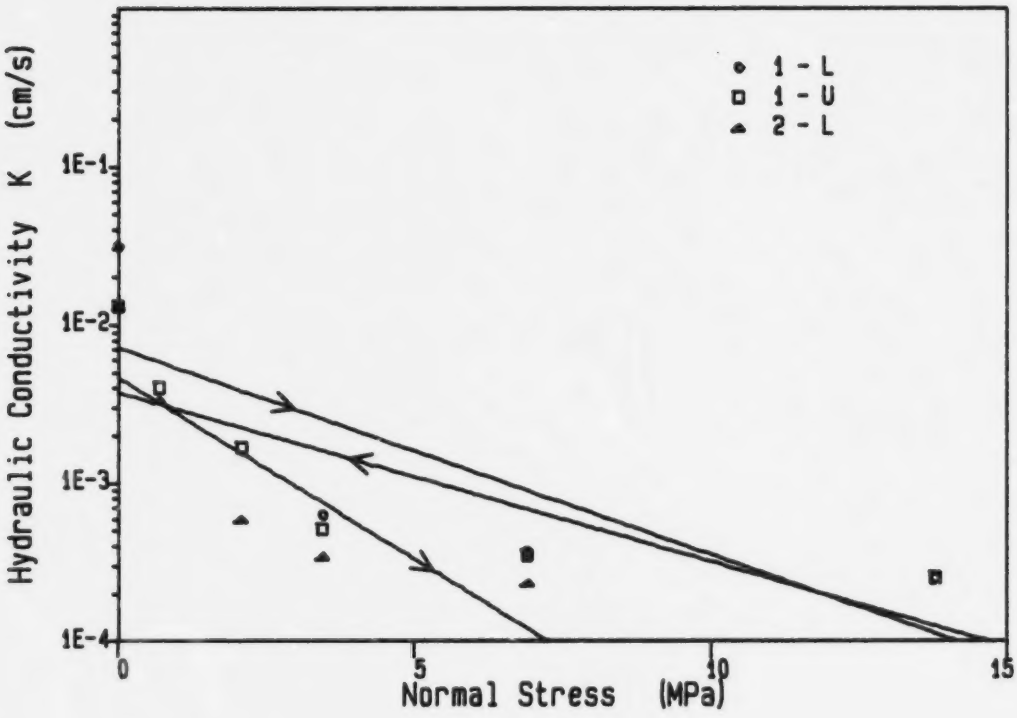

Figure C.2.3 Hydraulic conductivity as a function of normal stress for a sawcut in Charcoal granite Sample 2. Arrows indicate loading sequence.

Exponential Law. Equation (5.1), Table C.2.2.

BEST COPY AVAILABLE

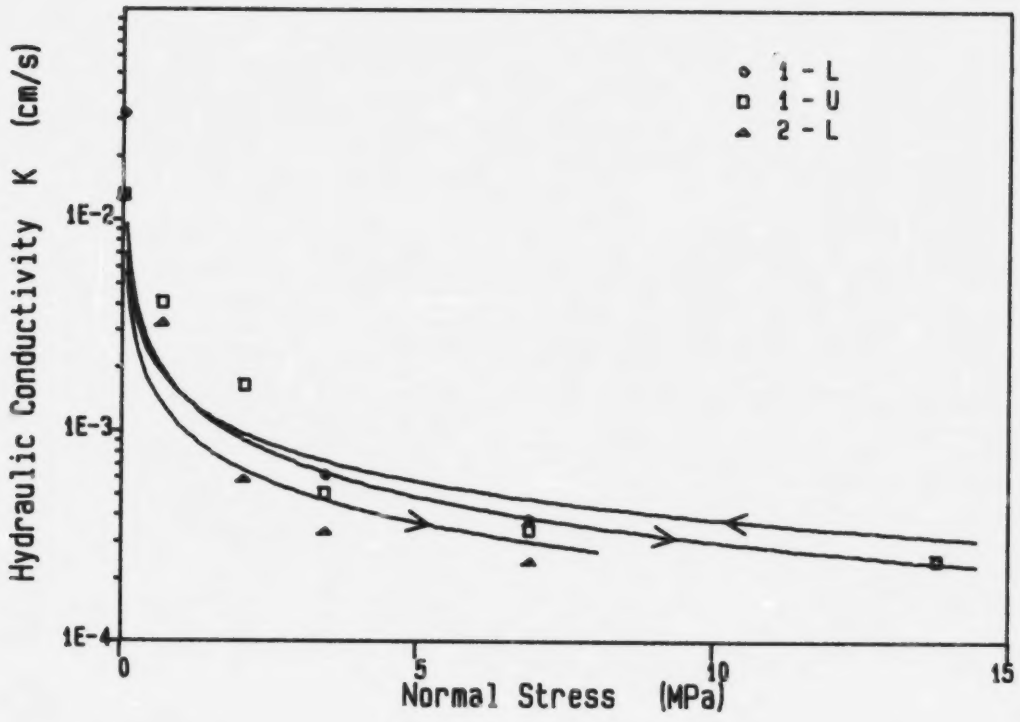

Figure C.2.4 Hydraulic conductivity as a function of normal stress for a sawcut in Charcoal granite Sample 2. Arrows indicate loading sequence.

Modified Power Law. Equation (5.4), Table C.2.2.

BEST COPY AVAILABLE

Table C.3.1 Permeability Test Results for a Sawcut in Charcoal Granite, Sample 3

Normal Stress MPa (psi)	Time (sec)	Initial Height (cm)	Final Height (cm)	Aperture (cm)	Hydraulic Conductivity (cm/sec)
0.0 (0)	39	137.61	106.11	62.7×10^{-2}	$.291 \times 10^{0}$
3.448 (500)	1346	137.61	134.46	8.57×10^{-3}	$.544 \times 10^{-2}$
6.895 (1000)	4740	142.65	140.02	5.23×10^{-3}	$.203 \times 10^{-2}$
13.790 (2000)	8460	140.02	136.67	4.72×10^{-3}	$.165 \times 10^{-2}$
6.895 (1000)	8400	141.71	138.13	4.81×10^{-3}	$.171 \times 10^{-2}$
3.448 (500)	2626	138.24	136.14	5.97×10^{-3}	$.265 \times 10^{-2}$
1.379 (200)	2477	146.85	144.43	6.25×10^{-3}	$.290 \times 10^{-2}$
0.0 (0)	84	137.61	106.11	48.4×10^{-2}	$.174 \times 10^{0}$
1.379 (200)	1369	139.18	135.09	9.27×10^{-3}	$.638 \times 10^{-2}$
3.448 (500)	2728	144.33	142.65	5.39×10^{-3}	$.216 \times 10^{-2}$
6.895 (1000)	7260	143.91	142.02	4.05×10^{-3}	$.122 \times 10^{-2}$
13.790 (2000)	10140	133.51	131.42	3.85×10^{-3}	$.110 \times 10^{-2}$

Buret radius: .55 cm
Ratio of sample radius to drillhole radius: 6.00.

Initial Height and Final Height refer to water level in falling head permeameter buret.

BEST COPY AVAILABLE

Table C.3.2 Hydraulic Conductivity - Normal Stress Equations for a Sawcut in Granite. Sample 3.

Equation		Load Cycle-Step (L: Loading U: Unloading)	Best Fit Equation	(r^2)
$K_f = K_1(P^{-\alpha})$	(5.3)	1-L	$0.01137(P^{-0.76062})$	0.9936
(5.3)		1-U	$0.00673(P^{-0.7089})$	0.9596
(5.3)		2-L	$0.00665(P^{-0.76434})$	0.9007
$K_f = K_o(e^{-cP})$	(5.1)	1-L	$0.06184(e^{-0.3281P})$	0.6415
(5.1)		1-U	$0.01588(e^{-0.2190P})$	0.3708
(5.1)		2-L	$0.02042(e^{-0.2745P})$	0.5175
$K_f = K_m(P/P_m)^{-\alpha}1$	(5.4)	1-L	$0.29554(P/0.0138)^{-0.7605}$	0.9936
(5.4)		1-U	$0.14023(P/0.0138)^{-0.7089}$	0.9596
(5.4)		2-L	$0.17572(P/0.0138)^{-0.7643}$	0.9907

BEST COPY AVAILABLE

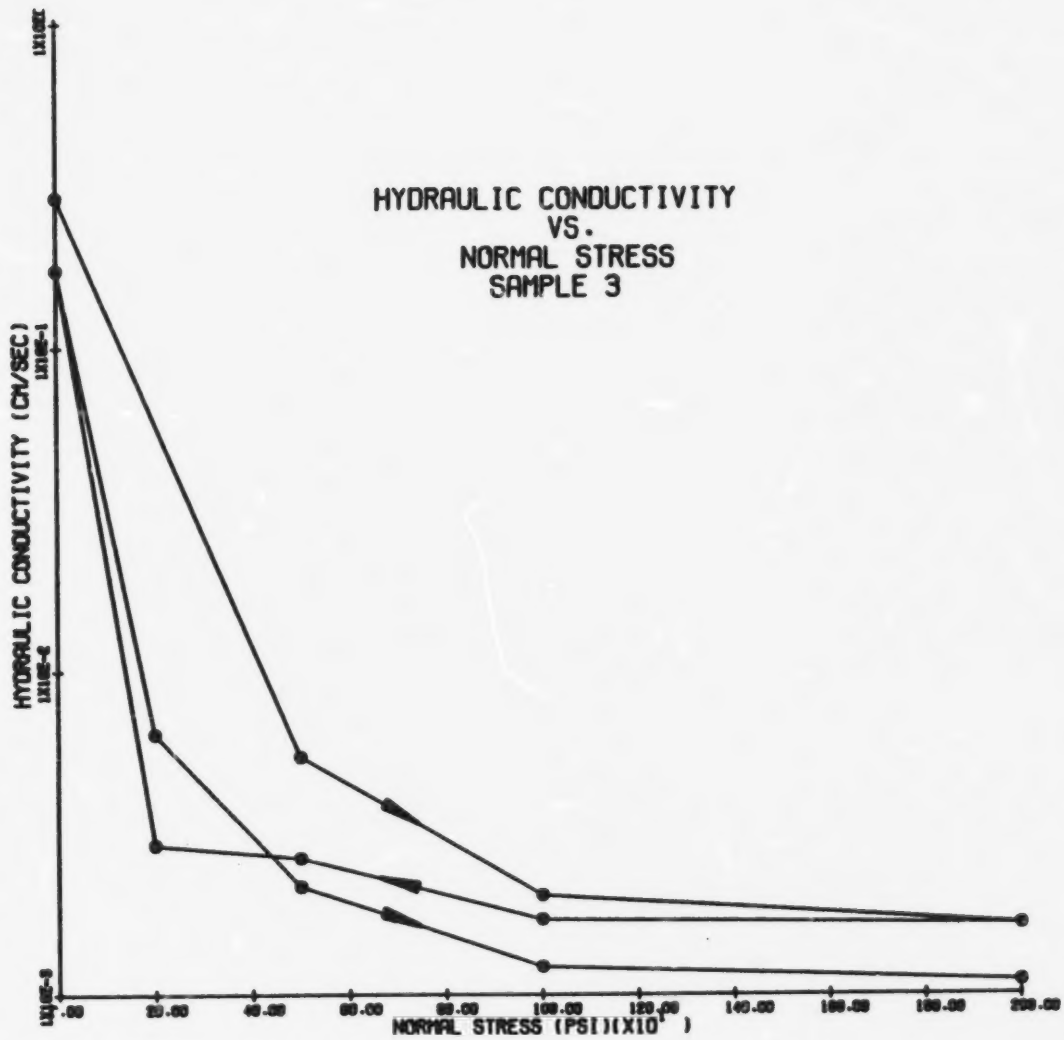

Figure C.3.1 Hydraulic conductivity as a function of normal stress for a sawcut in Charcoal granite Sample 3. Arrows indicate normal stress (loading) sequence.

BEST COPY AVAILABLE

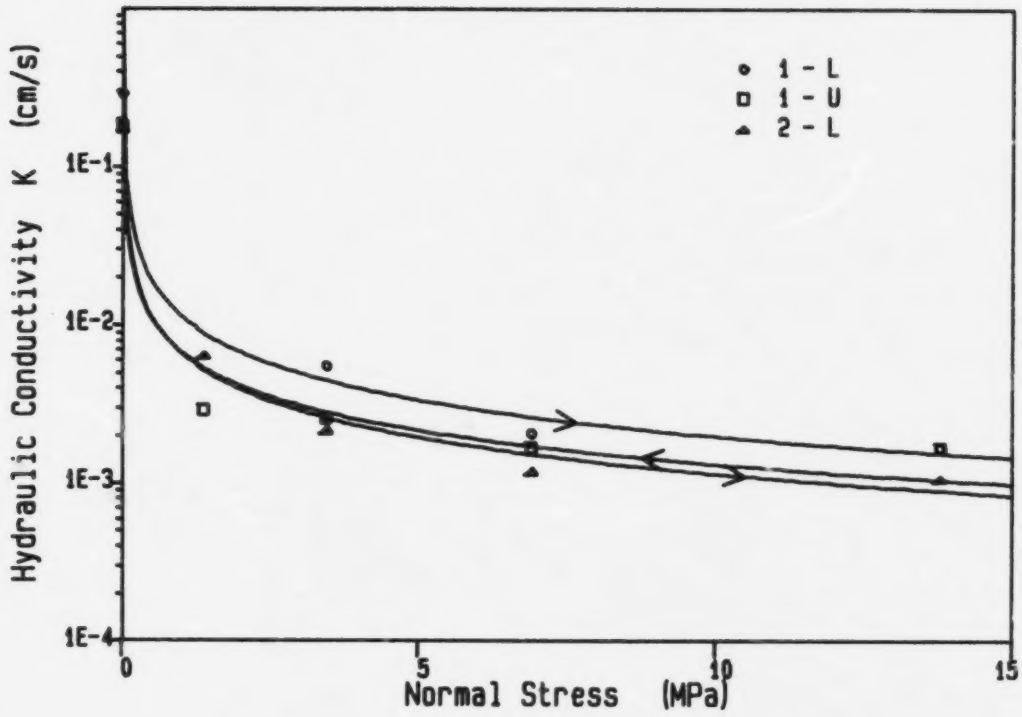

Figure C.3.2 Hydraulic conductivity as a function of normal stress for a sawcut in Charcoal granite Sample 3. Arrows indicate normal stress (loading) sequence.

Power Law. Equation (5.3), Table C.3.2.

BEST COPY AVAILABLE

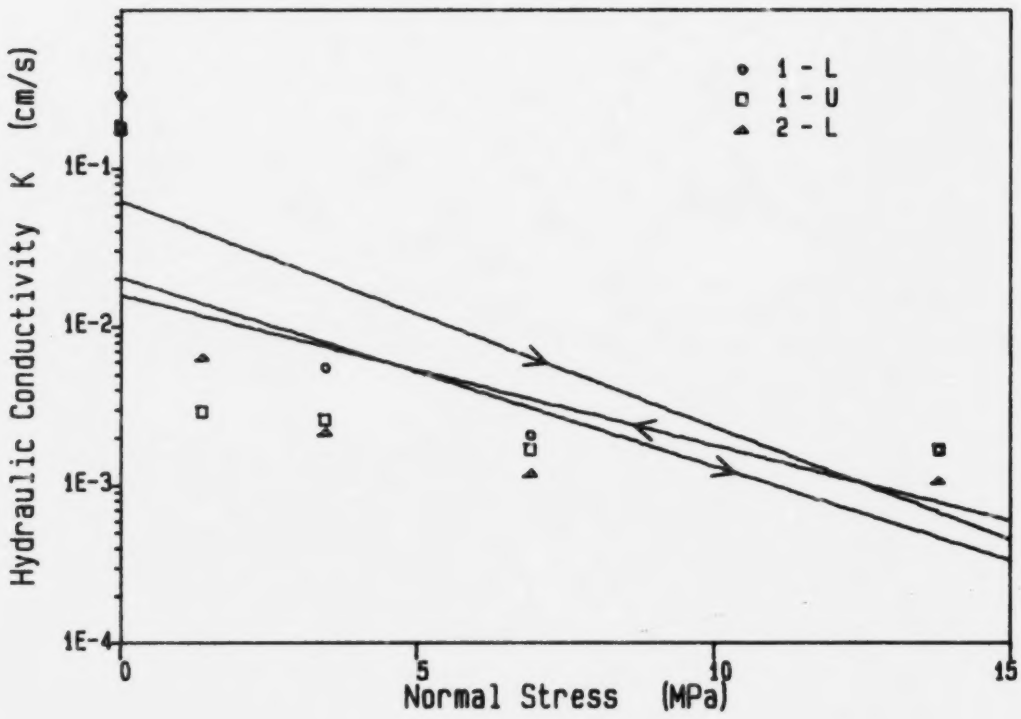

Figure C.3.3 Hydraulic conductivity as a function of normal stress for a sawcut in Charcoal granite Sample 3. Arrows indicate normal stress (loading) sequence.

Exponential Law. Equation (5.1), Table C.3.2.

BEST COPY AVAILABLE

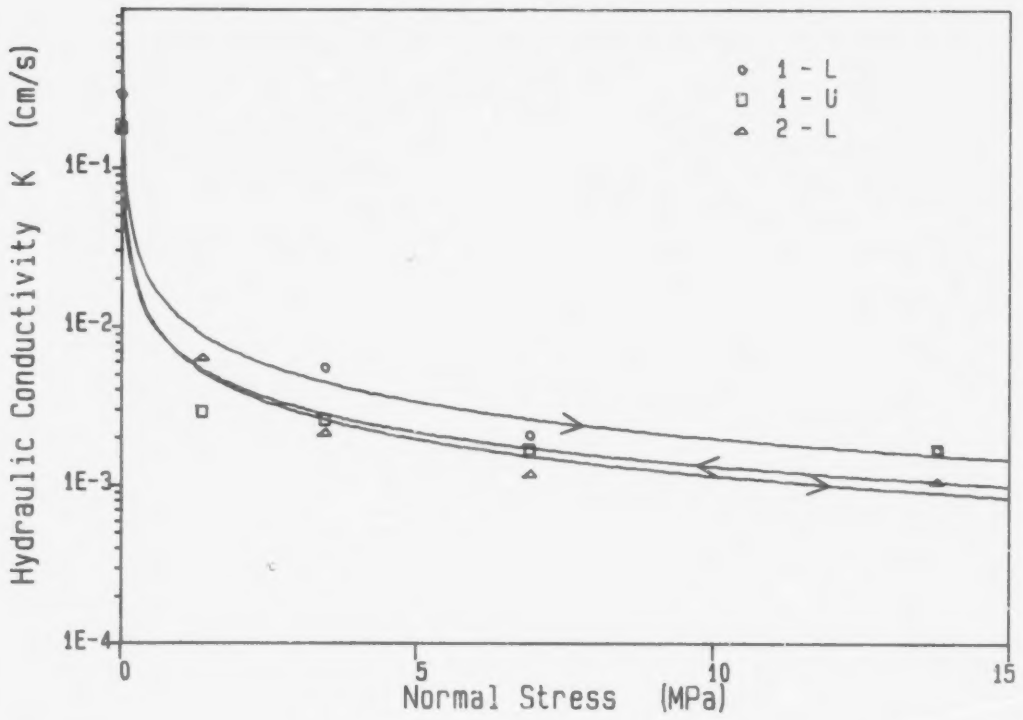

Figure C.3.4 Hydraulic conductivity as a function of normal stress for a sawcut in Charcoal granite Sample 3. Arrows indicate normal stress (loading) sequence.

Modified Power Law. Equation (5.4), Table C.3.2.

Table C.4.1 Permeability Test Results for a Single Fracture in Oracle Ridge Marble, Sample 4

Normal Stress MPa (psi)	Time (sec)	Initial Height (cm)	Final Height (cm)	Aperture (cm)	Hydraulic Conductivity (cm/sec)
0.0 (0)	41	140.01	107.61	60.9×10^{-4}	$.275 \times 10^{0}$
1.379 (200)	91	140.01	107.61	46.8×10^{-4}	$.162 \times 10^{0}$
3.448 (500)	182	140.01	107.61	37.1×10^{-4}	$.102 \times 10^{0}$
6.895 (1000)	139	140.01	129.21	27.3×10^{-4}	$.553 \times 10^{-1}$
3.448 (500)	258	140.01	129.21	22.2×10^{-4}	$.366 \times 10^{-1}$
1.379 (200)	514	140.01	134.61	13.9×10^{-4}	$.144 \times 10^{-1}$
0.0 (0)	51	140.01	107.61	56.6×10^{-4}	$.238 \times 10^{0}$
1.379 (200)	92	140.01	129.21	31.3×10^{-4}	$.728 \times 10^{-1}$

Buret radius: .54 cm
Ratio of sample radius to drillhole radius: 6.00.

Initial Height and Final Height refer to water level in falling head permeameter buret.

Table C.4.2 Hydraulic Conductivity - Normal Stress Equations for a Fracture in an Oracle Ridge Marble Cylinder, Sample 4.

Equation		Load Cycle-Step (L: Loading U: Unloading)	Best Fit Equation	(r^2)
$K_f = K_1(P^{-\alpha})$	(5.3)	1-L	$0.1206(P^{-0.2172})$	0.7961
$K_f = K_o(e^{-cP})$	(5.1)	1-L	$0.24332(e^{-0.2246P})$	0.97227
$K_f = K_m(P/P_m)^{-\alpha}1$	(5.4)	1-L	$0.30569(P/0.0138)^{-0.21713}$	0.796

BEST COPY AVAILABLE

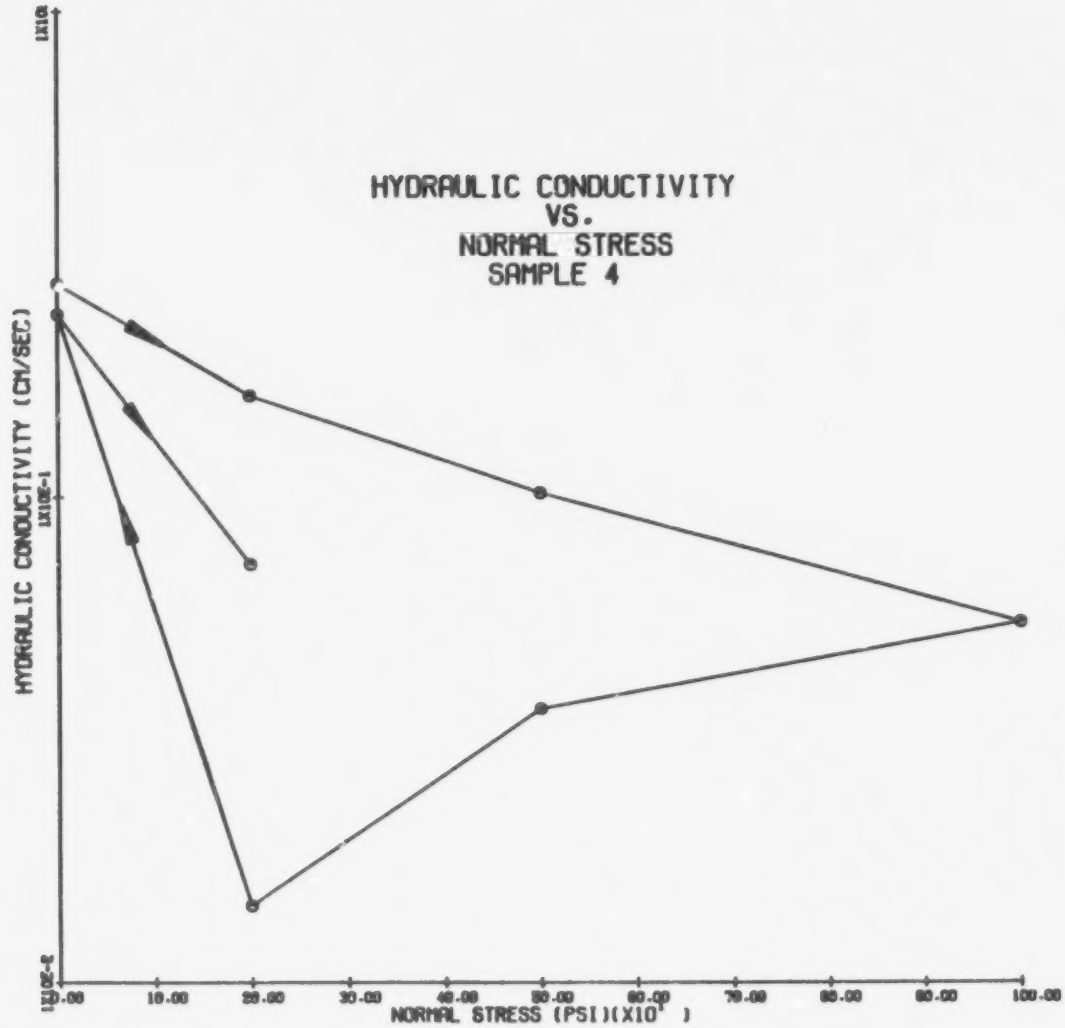

Figure C.4.1 Hydraulic conductivity as a function of normal stress for a natural fracture in Oracle Ridge marble Sample 4. Arrows indicate normal stress (loading) sequence.

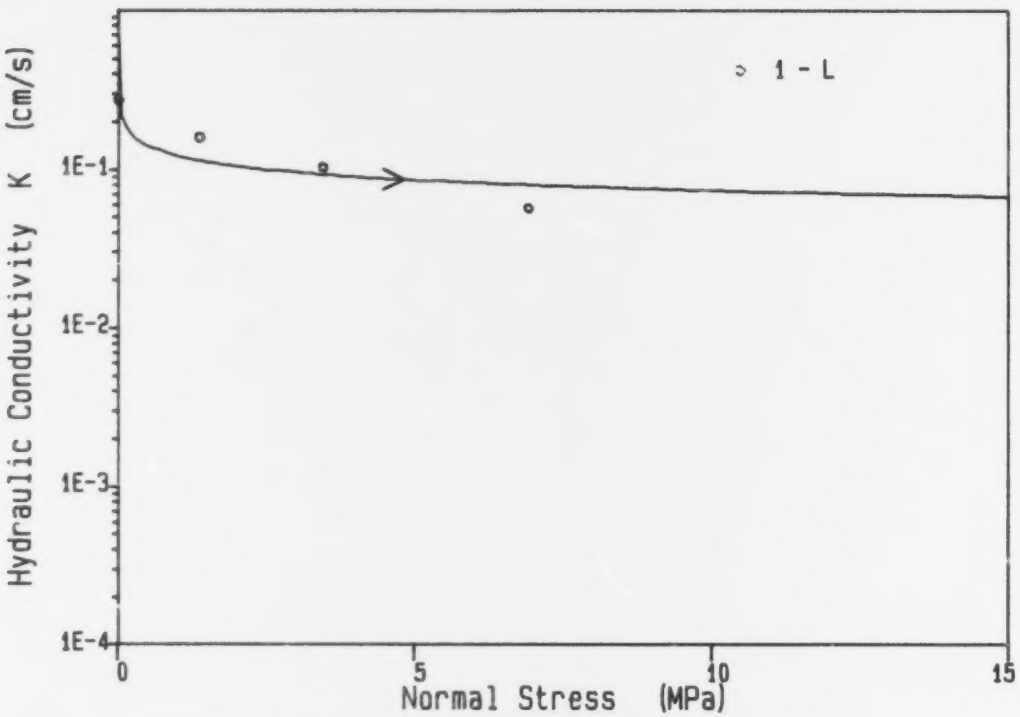

Figure C.4.2 Hydraulic conductivity as a function of normal stress for the first loading cycle on a natural fracture in Oracle Ridge marble Sample 4. Power law fit, equation (5.3), Table C.5.2.

BEST COPY AVAILABLE

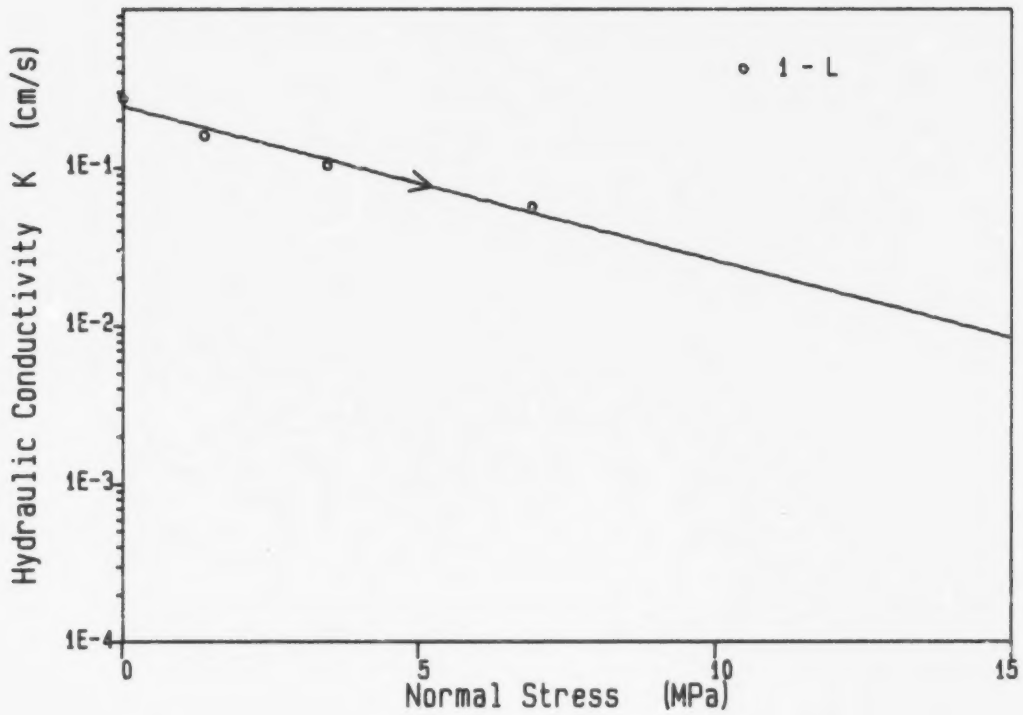

Figure C.4.3 Hydraulic conductivity as a function of normal stress for the first loading cycle on a natural fracture in Oracle Ridge marble Sample 4. Exponential fit, equation (5.1), Table C.5.2.

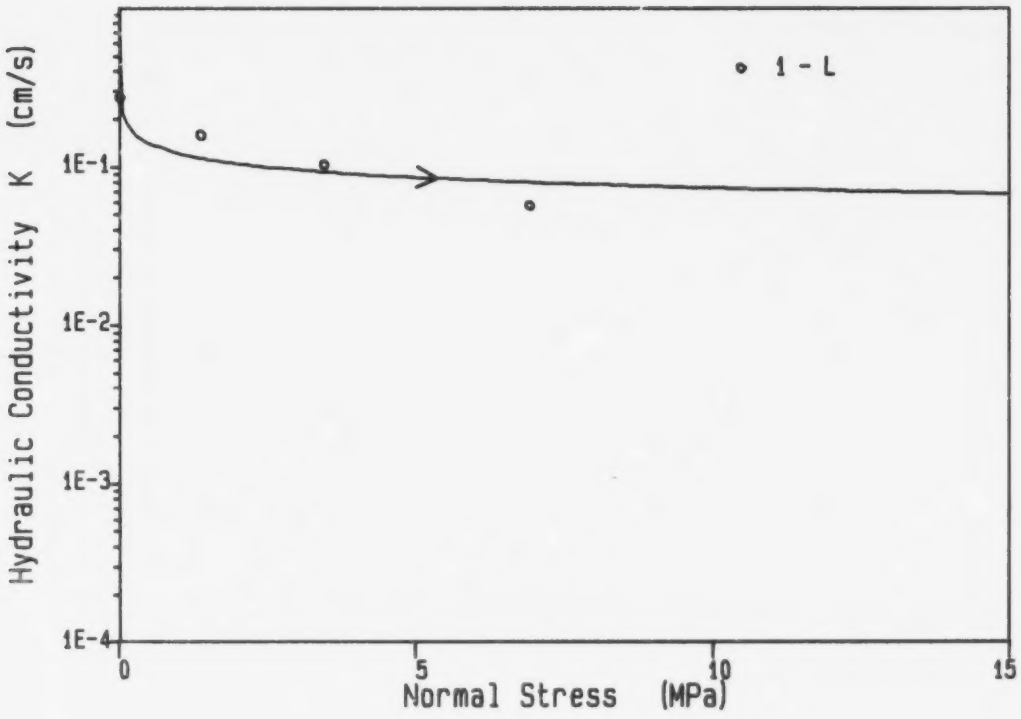

Figure C.4.4 Hydraulic conductivity as a function of normal stress for the first loading cycle on a natural fracture in Oracle Ridge marble Sample 4. Modified power law fit, equation (5.4), Table C.5.2.

BEST COPY AVAILABLE

Table C.5.1 Permeability Test Results for a Single Fracture in Grande Basaltic Andesite, Sample 5

Normal Stress MPa (psi)	Time (sec)	Initial Height (cm)	Final Height (cm)	Aperture (cm)	Hydraulic Conductivity (cm/sec)
0.0 (0)	101	140.01	107.61	48.3×10^{-4}	$.173 \times 10^{0}$
1.379 (200)	229	138.93	137.85	11.4×10^{-4}	$.960 \times 10^{-2}$
3.448 (500)	6720	131.37	127.70	5.67×10^{-4}	$.238 \times 10^{-2}$

Buret radius: .54 cm
Ratio of sample radius to drillhole radius: 9.00

Initial Height and Final Height refer to water level in falling head permeameter buret

Table C.5.2 Hydraulic Conductivity - Normal Stress Equations for a Point Load Fracture in Grande Basaltic Andesite, Sample 5

Equation		Load Cycle-Step (L: Loading U: Unloading)	Best Fit Equation	(r^2)
$K_f = K_1(P^{-\alpha})$	(5.3)	1-L	$0.00816(P^{-0.7284})$	0.9717
$K_f = K_o(e^{-cP})$	(5.1)	1-L	$0.10989(e^{-1.2015P})$	0.90299
$K_f = K_m(P/P_m)^{-\alpha}1$	(5.4)	1-L	$0.18477(P/0.0138)^{-0.7283}$	0.9717

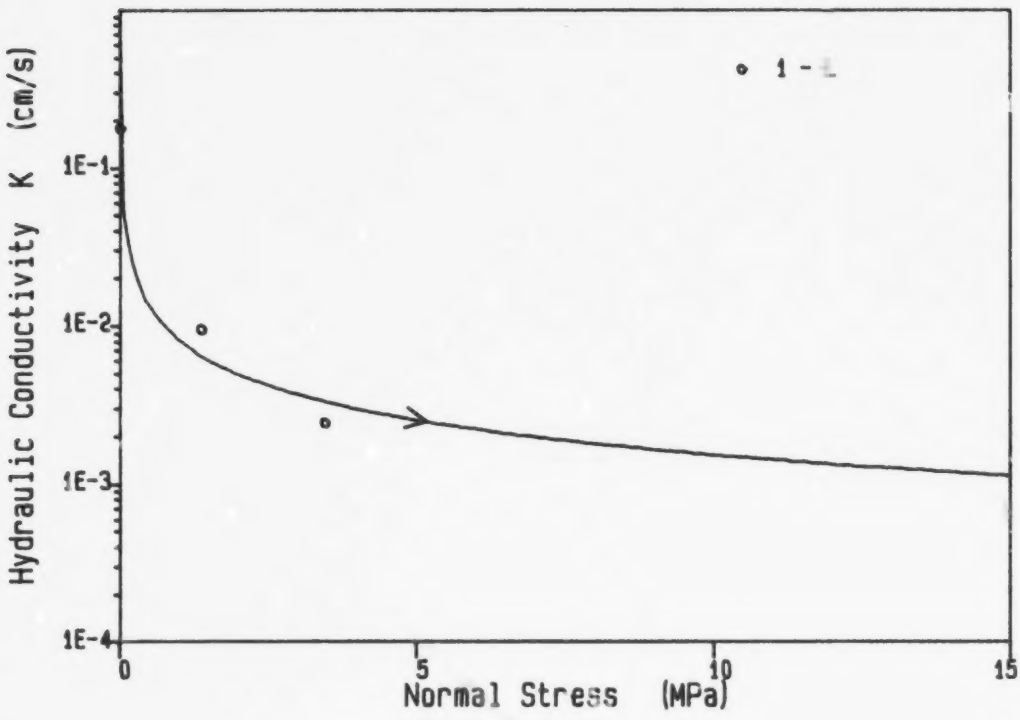

Figure C.5.1 Hydraulic conductivity as a function of normal stress for a point load induced tension fracture in Grande basaltic andesite. Sample 5.

Power Law Fit. Equation (5.3), Table C.5.2.

AVAILABLE

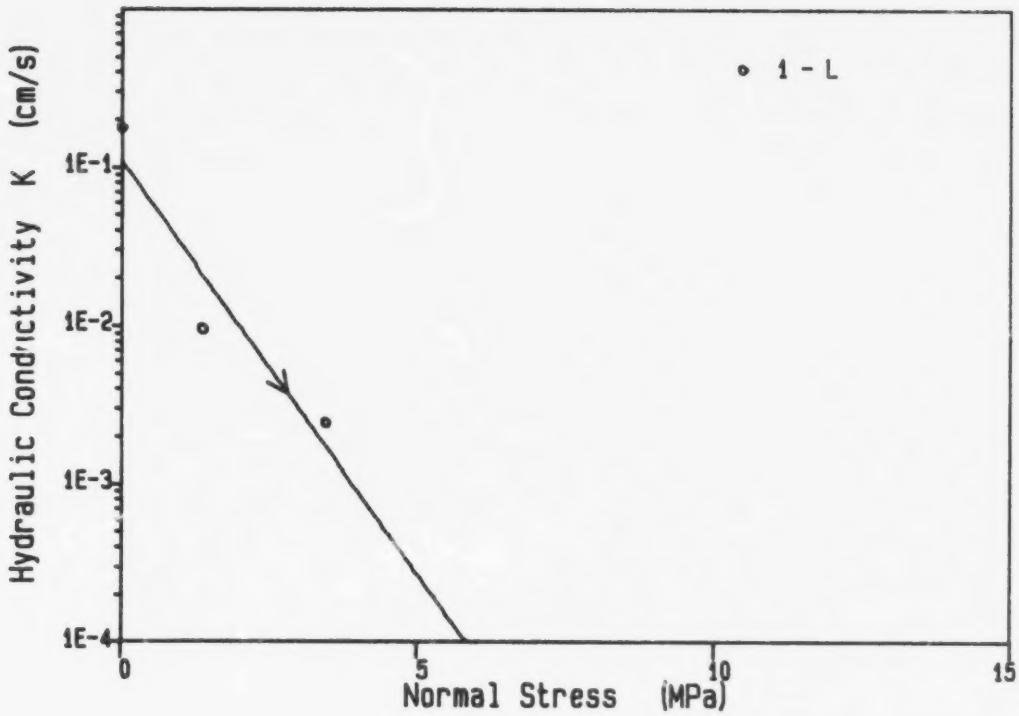

Figure C.5.2 Hydraulic conductivity as a function of normal stress for a point load induced tension fracture in Grande basaltic andesite. Sample 5.

Exponential Fit. Equation (5.1), Table C.5.2.

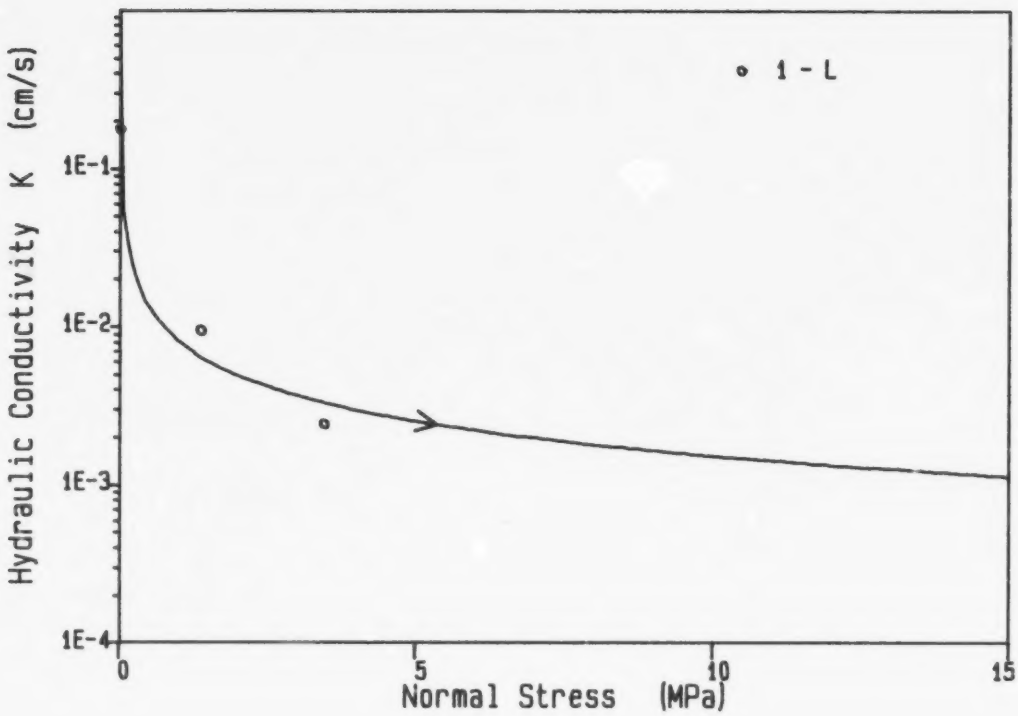

Figure C.5.3 Hydraulic conductivity as a function of normal stress for a point load induced tension fracture in Grande basaltic andesite. Sample 5.

Modified Power Law. Equation (5.4), Table C.5.2.

ST COPY AVAILABL

Table C.6.1 Permeability Test Results for a Single Fracture in Grande Basaltic Andesite, Sample 6

Normal Stress MPa (psi)	Time (sec)	Initial Height (cm)	Final Height (cm)	Aperture (cm)	Hydraulic Conductivity (cm/sec)
0.0 (0)	60	140.01	107.61	57.4×10^{-4}	$.245 \times 10^{0}$
1.379 (200)	7260	149.62	126.40	10.0×10^{-4}	$.743 \times 10^{-2}$
3.448 (500)	4800	141.95	138.28	6.18×10^{-4}	$.283 \times 10^{-2}$
6.895 (1000)	7200	138.93	136.88	4.47×10^{-4}	$.148 \times 10^{-2}$
10.343 (1500)	8800	137.42	135.69	3.96×10^{-4}	$.116 \times 10^{-2}$
6.895 (1000)	10740	148.43	146.06	4.02×10^{-4}	$.120 \times 10^{-2}$
3.448 (500)	8280	136.34	134.29	4.29×10^{-4}	$.137 \times 10^{-2}$
1.379 (200)	3720	145.41	142.82	5.93×10^{-4}	$.261 \times 10^{-2}$
0.0 (0)	92	140.01	137.85	19.4×10^{-4}	$.279 \times 10^{-1}$
1.379 (200)	5940	145.41	141.20	5.98×10^{-4}	$.265 \times 10^{-2}$
3.448 (500)	7320	144.22	141.85	4.61×10^{-4}	$.158 \times 10^{-2}$
6.895 (1000)	11940	139.25	136.99	3.90×10^{-4}	$.113 \times 10^{-2}$
10.343 (1500)	10020	139.90	138.50	3.52×10^{-4}	$.917 \times 10^{-3}$

Buret radius: .54 cm
Ratio of sample radius to drillhole radius: 9.00

Initial Height and Final Height refer to water level in falling head permeameter buret.

Table C.6.2 Hydraulic Conductivity - Normal Stress Equations for a Point Load Fracture in Grande Basaltic Andesite. Sample 6.

Equation		Load Cycle-Step (L: Loading U: Unloading)	Best Fit Equation	(r^2)
$K_f = K_1(P^{-\alpha})$	(5.3)*	1-L	$0.00791(P^{-0.81321})$	0.9972
(5.3)*		1-U	$0.00313(P^{-0.50131})$	0.98952
(5.3)*		2-L	$0.00206(P^{-0.51670})$	0.99987
(5.3)**		1-L	$0.00456(P^{-0.4443})$	0.96867
(5.3)**		1-U	$0.00222(P^{-0.2776})$	0.9877
(5.3)**		2-L	$0.00215(P^{-0.2838})$	0.98179
(5.3)***		1-L	$0.0141(P^{-1.1756})$	0.9908
(5.3)***		1-U	$0.0044(P^{-0.7144})$	0.9554
(5.3)***		2-L	$0.0044(P^{-0.7428})$	0.9824
$K_f = K_o(e^{-\epsilon P})$	(5.1)*	1-L	$0.03865(e^{-0.41604P})$	0.64419
(5.1)*		1-U	$0.00752(e^{-0.23355P})$	0.5301
(5.1)*		2-L	$0.00815(e^{-0.25793P})$	0.61499
(5.1)**		1-L	$0.03861(e^{-0.41604P})$	0.645301
(5.1)**		1-U	$0.00752(e^{-0.2336P})$	0.531255
(5.1)**		2-L	$0.008146(e^{-0.25795P})$	0.61613
(5.1)***		1-L	$0.0389(e^{-0.4160P})$	0.6372
(5.1)***		1-U	$0.0075(e^{-0.2332P})$	0.5228
(5.1)***		2-L	$0.0082(e^{-0.2578P})$	0.6078

COPY AVAILABL

Table C.6.2 Hydraulic Conductivity - Normal Stress Equations for a Point Load Fracture in Grande Basaltic Andesite. Sample 6.--Continued

Equation		Load Cycle-Step (L: Loading U: Unloading)	Best Fit Equation	(r^2)
$K_f = K_m(P/P_m)^{-\alpha_1}$	(5.4)*	1-L	$0.25763(P/0.0138)^{-0.81321}$	0.99716
(5.4)*		1-U	$0.02680(P/0.0138)^{-0.50131}$	0.96252
(5.4)*		2-L	$0.02799(P/0.0138)^{-0.5167}$	0.99987
(5.4)**		1-L	$0.27172(P/0.001)^{-0.56599}$	0.98162
(5.4)**		1-U	$0.02830(P/0.001)^{-0.35211}$	0.99204
(5.4)**		2-L	$0.02920(P/0.001)^{-0.36091}$	0.99141
(5.4)***		1-L	$0.2112(P/0.1)^{-1.1756}$	0.9908
(5.4)***		1-U	$0.0230(P/0.1)^{-0.7144}$	0.9554
(5.4)***		2-L	$0.0244(P/0.1)^{-0.7428}$	0.9824
$K_f = K_o[1 - (P/P_1)^m]^3$	(5.6)#	1-L	$0.03861[1 - (P/39.742)^{0.2456}]^3$	0.9542
(5.6)#		1-U	$0.00752[1 - (P/1.60438)^{0.02828}]^3$	0.30161
(5.6)#		2-L	$0.008146[1 - (P/130.2067)^{0.25035}]^3$	0.97798

*Fit with an assumed minimum ("zero") normal stress of 0.0138 MPa (2 psi).

**Assumed minimum ("zero") normal stress of 0.001 MPa (0.145 psi).

***Assumed minimum ("zero") normal stress of 0.1 MPa (14.5 psi).

#K_o treated as a curve-fitting parameter.

Table C.6.3 Example of Sensitivity of a Hydraulic Conductivity-Normal Stress Equation to "Best Fit" Parameters. Sample 6 (Point Load Fracture in Grande Basaltic Andesite), Unloading Cycle 1.

$$K = K_o[1 - (P/P_1)^m]^3 \qquad (5.6)$$

$\sum d_i^2(10^7)$

P_1 / m	40	300	400	500	600	700	800
0.085							4.8
0.090					4.4	2.8	2.0
0.095				3.3	1.9	1.8	6.8
0.1			3.0	1.7	2.3	4.2	
0.105		3.7	1.8	3.1			
0.11		2.0	3.3				
0.115		2.6					
0.18	12.0						
0.185	11.28						
0.19	11.3						

P_1: asperity modulus

m: empirical constant

K_o: zero stress conductivity

d_i: difference between measured and calculated permeability

COPY AVAILABLE

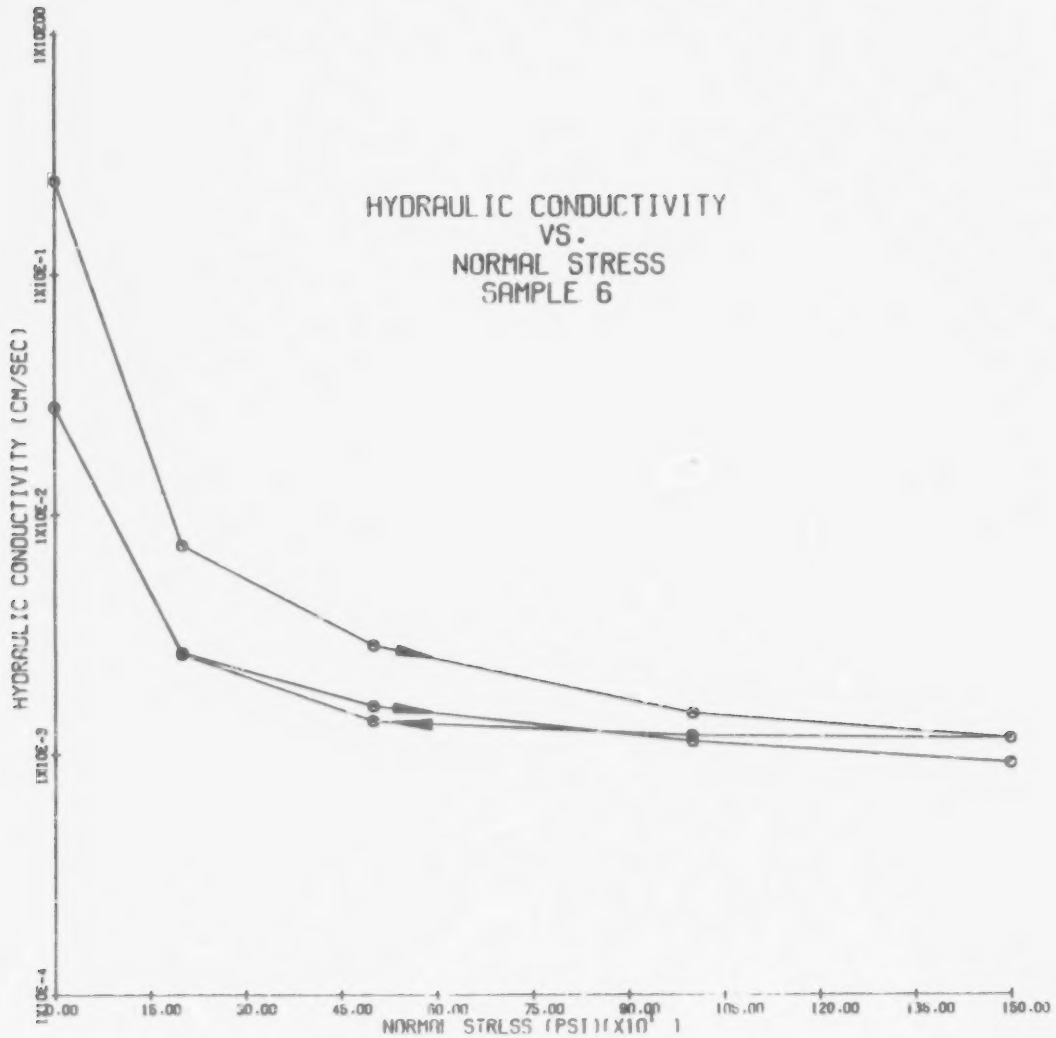

Figure C.6.1 Hydraulic conductivity as a function of normal stress for a tension fracture in Grande basaltic andesite Sample 6. Arrows indicate normal stress loading path.

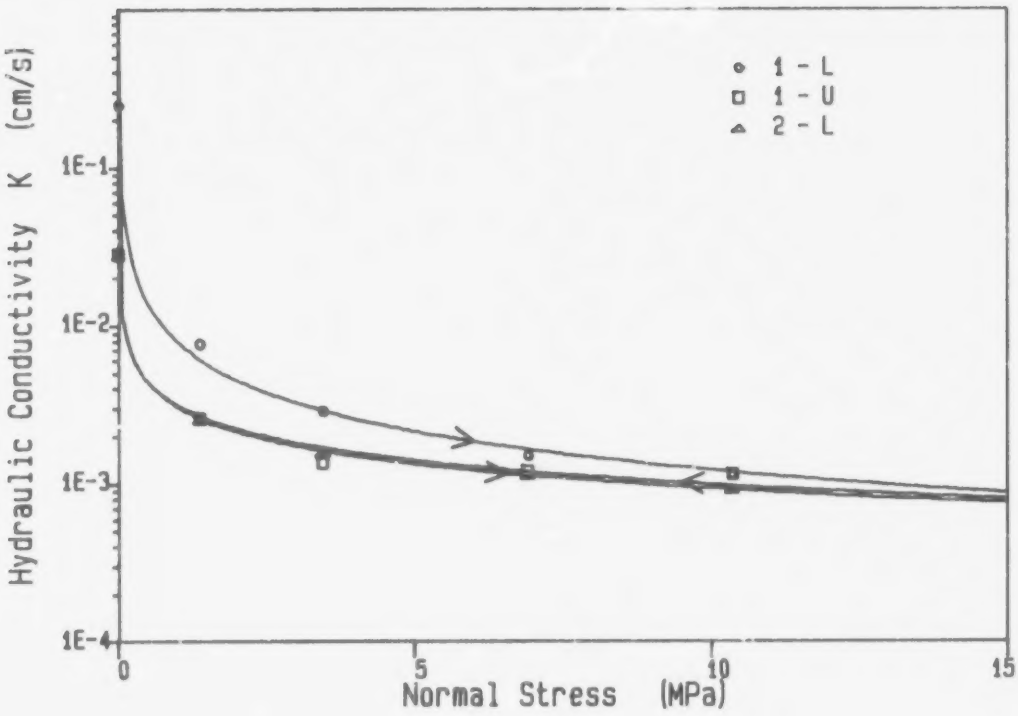

Figure C.6.2 Hydraulic conductivity as a function of normal stress for a point load fracture in Grande basaltic andesite Sample 6.

Power Law Fit. Equation (5.3)*, Table C.6.2.

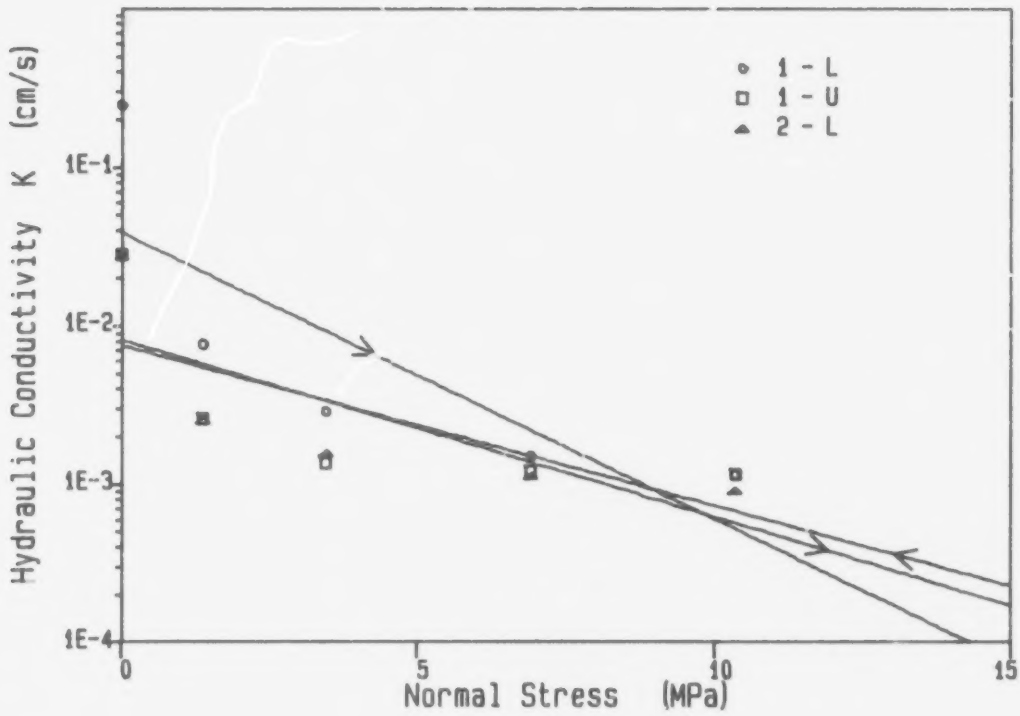

Figure C.6.3 Hydraulic conductivity as a function of normal stress for a point load fracture in Grande basaltic andesite Sample 6.

Exponential Fit. Equation (5.1)*, Table C.6.2.

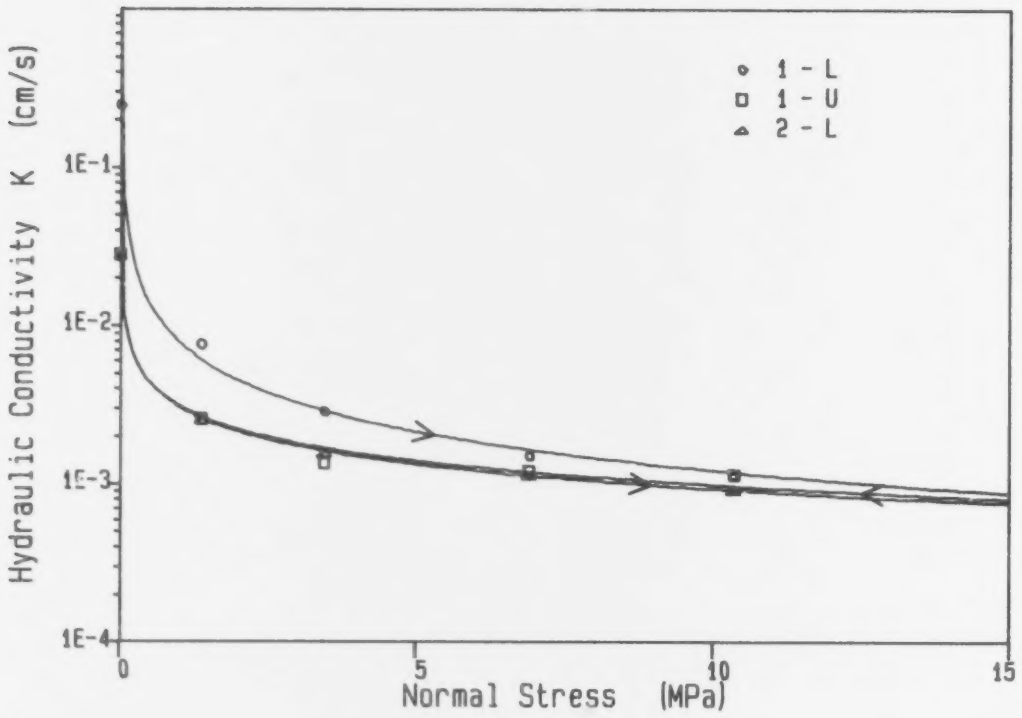

Figure C.6.4 Hydraulic conductivity as a function of normal stress for a point load fracture in Grande basaltic andesite Sample 6.

Modified Power Law. Equation (5.4)*, Table C.6.2.

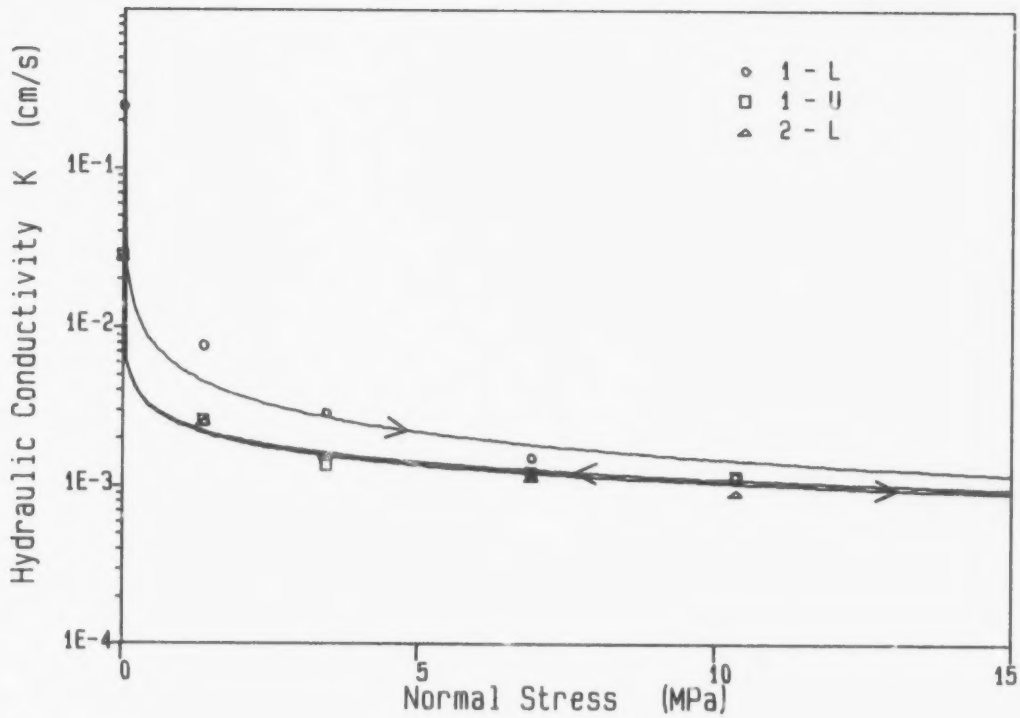

Figure C.6.5 Hydraulic conductivity as a function of normal stress for a point load fracture in Grande basaltic andesite Sample 6.

Modified Power Law. Equation (5.4)**, Table C.6.2.

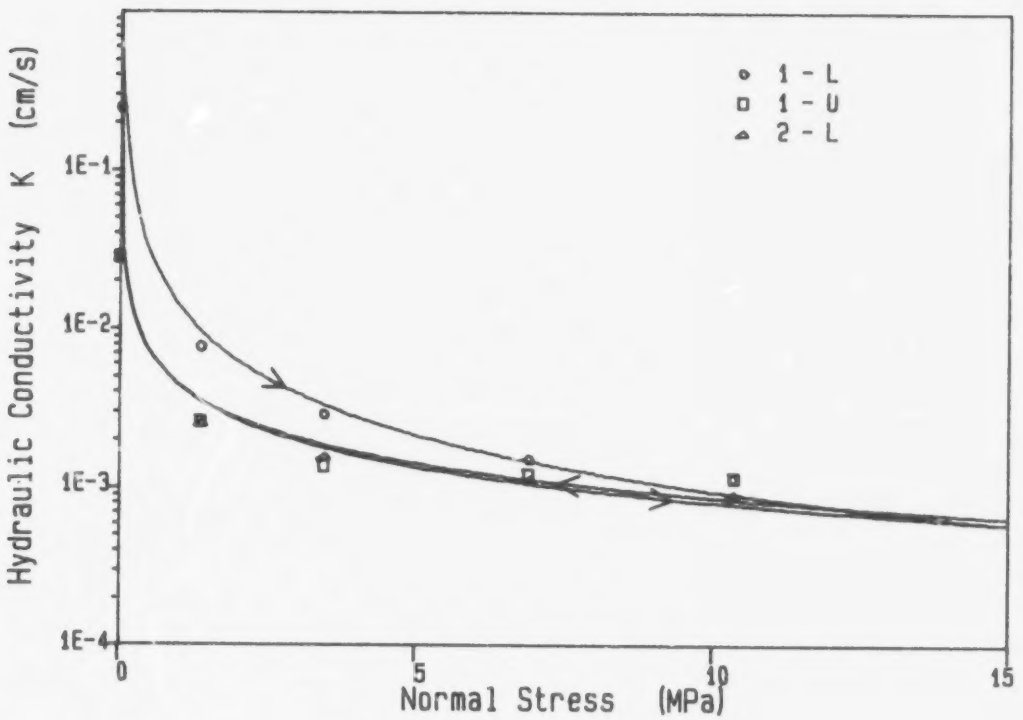

Figure C.6.6 Hydraulic conductivity as a function of normal stress for a point load fracture in Grande basaltic andesite Sample 6.

Modified Power Law. Equation (5.4)***, Table C.6.2.

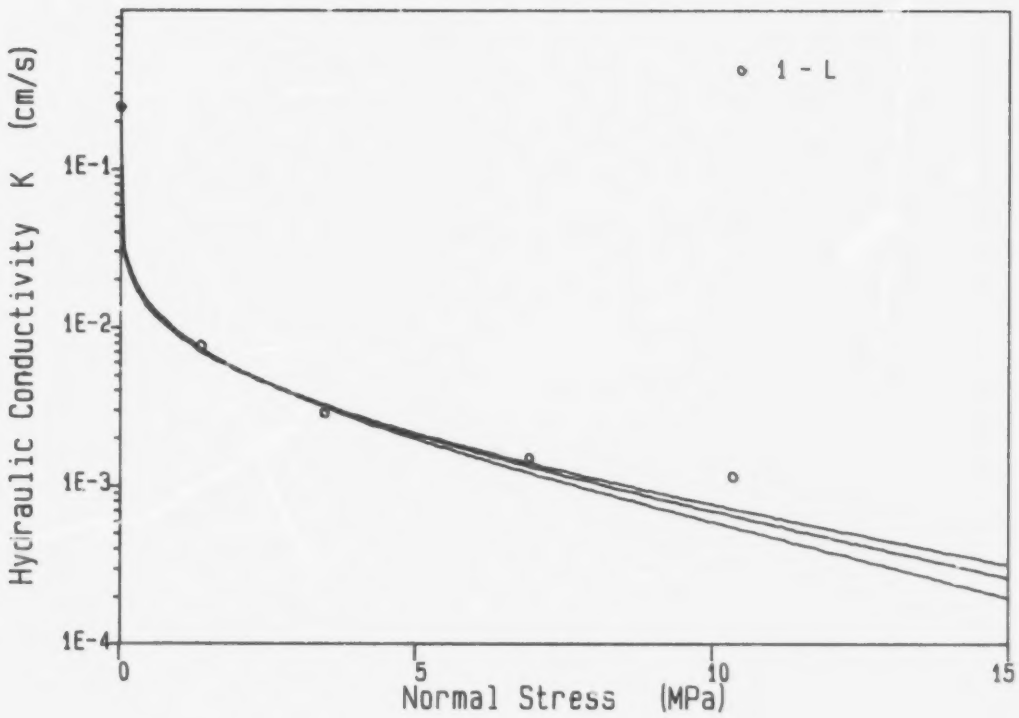

Figure C.6.7 "Bed of nails" (Gangi, 1978) fit for hydraulic conductivity as a function of normal stress. Point load fracture in Grande basaltic andesite, Sample 6. Loading, cycle 1.

Equation (5.6) with K_{01} = 0.245 cm/s

Upper curve: m = 0.105, P_1 = 45 MPa

Middle curve: m = 0.110, P_1 = 40 MPa

Lower curve: m = 0.115, P_1 = 35 MPa

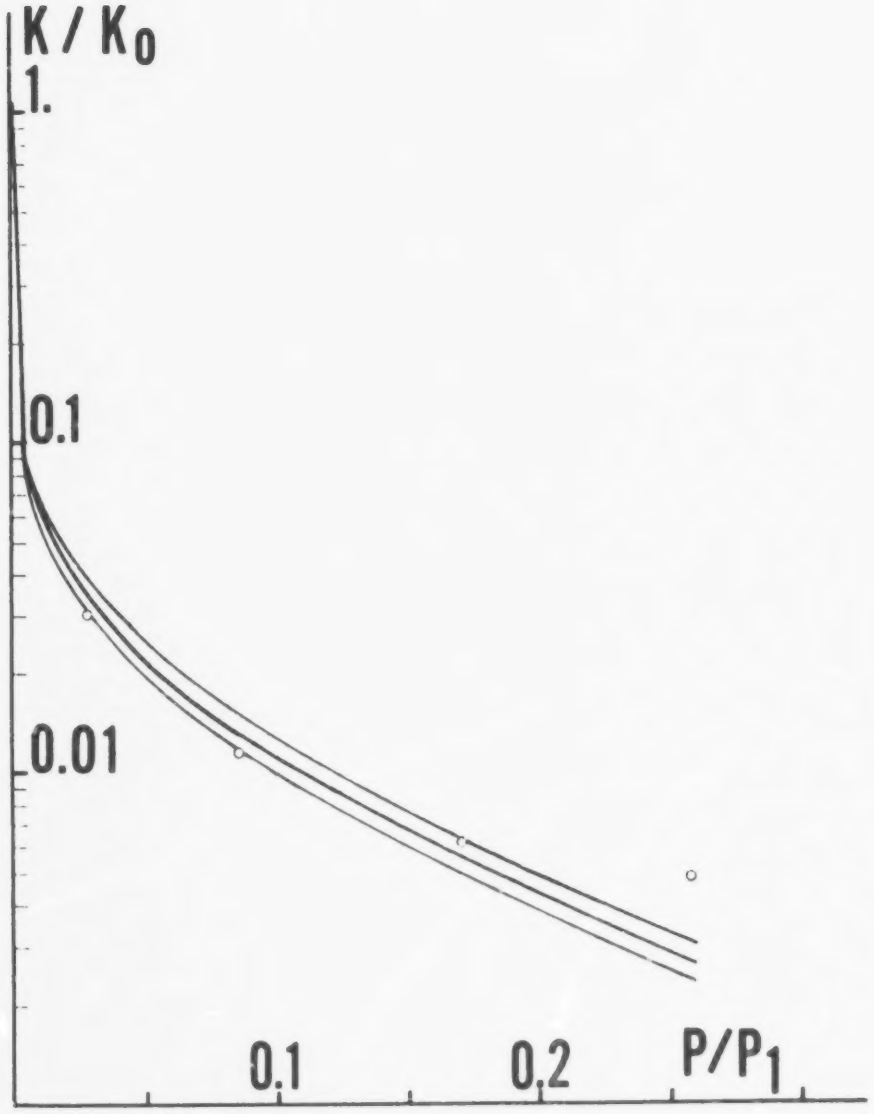

Figure C.6.8 Dimensionless fracture conductivity as a function of normalized normal stress across the fracture. Point load fracture in Grande basaltic andesite. Sample 6. Cycle 1, Loading.

Equation (5.6) with K_{01} = 0.0245 cm/s, P_1 = 40 MPa

Upper curve: m = 0.115,
Middle curve: m = 0.110,
Lower curve: m = 0.105,

BEST AVAILABLE

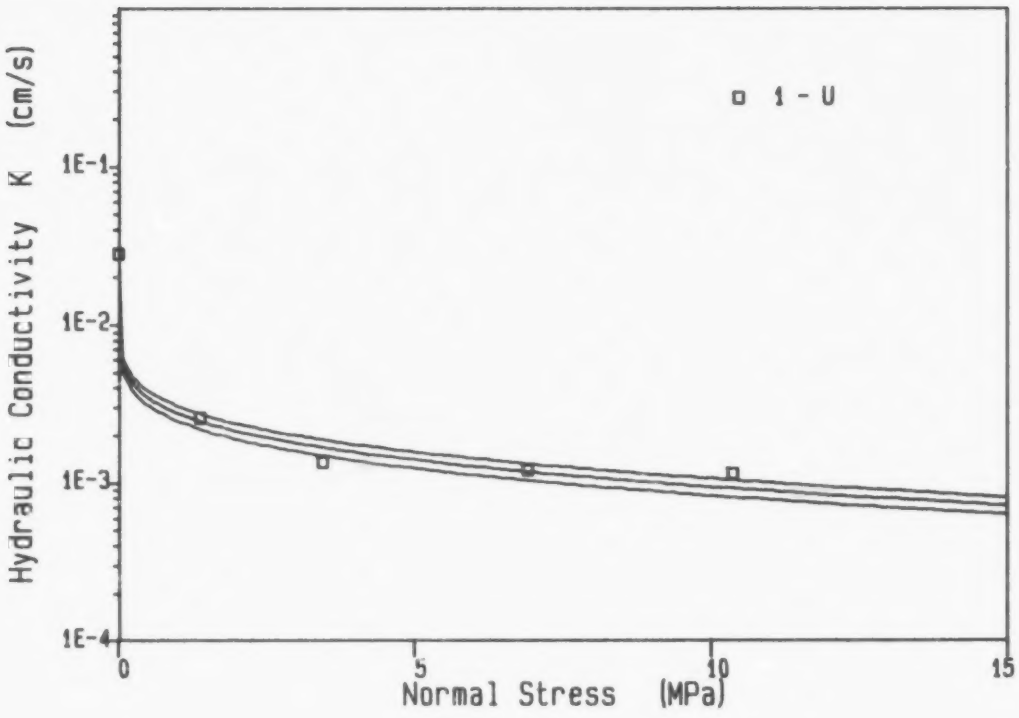

Figure C.6.9 "Bed of nails" (Gangi, 1978) fit for hydraulic conductivity as a function of normal stress. Point load fracture in Grande basaltic andesite, Sample 6. Unloading, cycle 1.

Equation (5.6) with K_{01} = 0.0279 cm/s, P_1 = 500 MPa

Upper curve: m = 0.095,
Middle curve: m = 0.1,
Lower curve: m = 0.105,

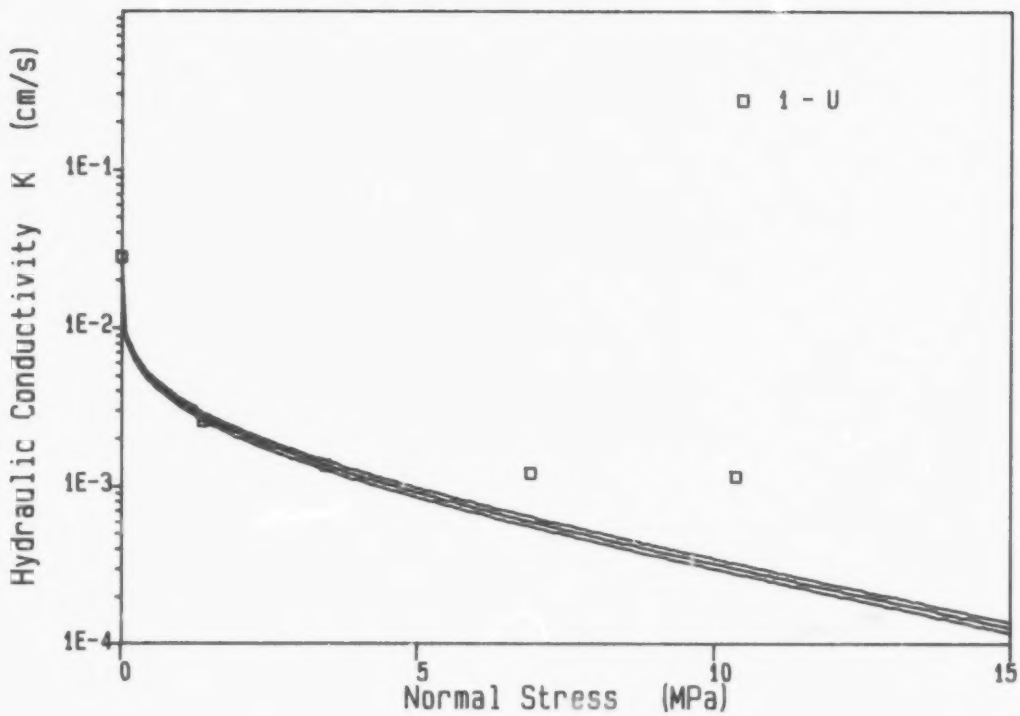

Figure C.6.10 "Bed of nails" (Gangi, 1978) fit for hydraulic conductivity as a function of normal stress. Point load fracture in Grande basaltic andesite, Sample 6. Unloading, cycle 1.

Equation (5.6) with K_{01} = 0.0279 cm/s, P_1 = 40 MPa

Upper curve: m = 0.190,
Middle curve: m = 0.185,
Lower curve: m = 0.180,

BEST AVAILABLE

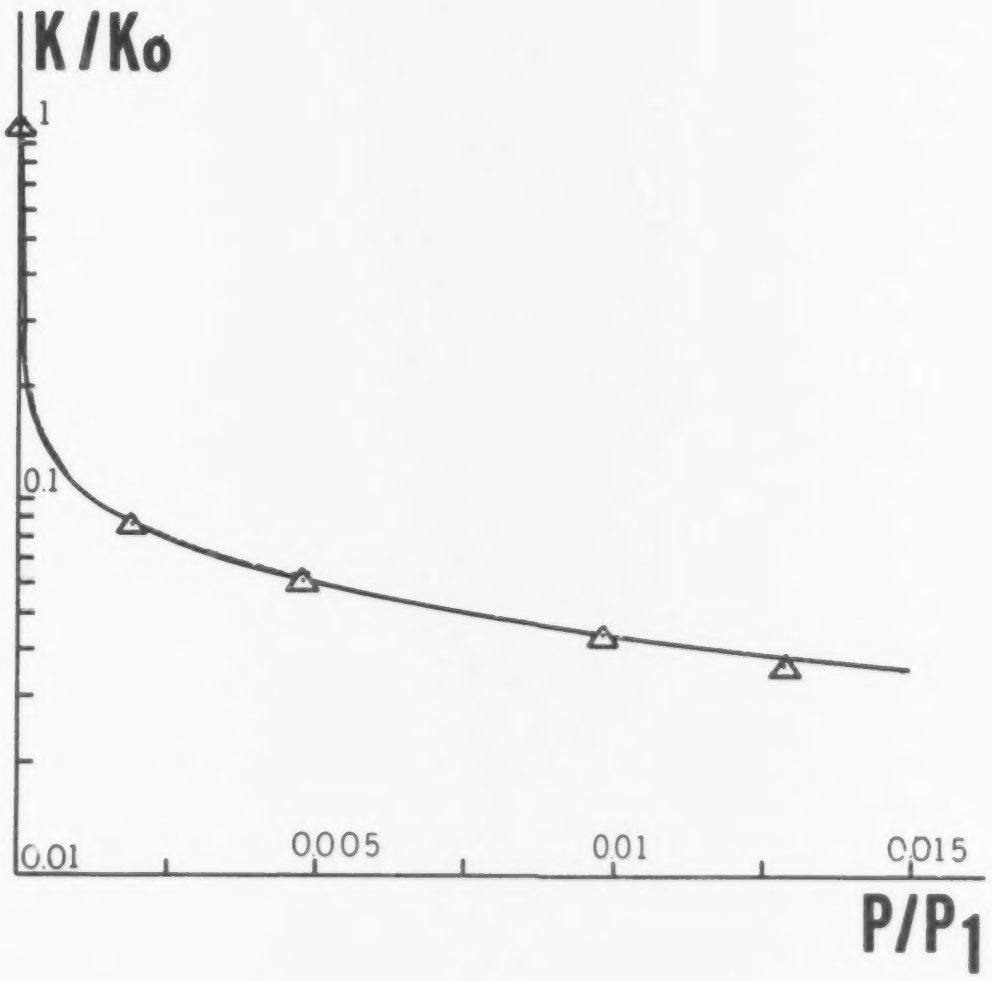

Figure C.6.11 Dimensionless fracture conductivity as a function of normalized normal stress across the fracture. Point load fracture in Grande basaltic andesite. Sample 6. Cycle 1, Loading.

Equation (5.6) with K_{01} = 0.0279 cm/s, P_1 = 900 MPa, and m = 0.09.

BEST COPY AVAILABLE

APPENDIX D

BIBLIOGRAPHIES, TEXTBOOKS, AND PROCEEDINGS OF MEETINGS ON GROUTING

The literature on grouting is voluminous, and widely dispersed. The authors have found the availability of published bibliographies, textbooks, and conference proceedings devoted exclusively to the subject of considerable help in locating information and information sources.

____, 1963, Grouts and Drilling Muds in Engineering Practice, Symposium organized by the British National Society of the International Society of Soil Mechanics and Foundation Engineering at the Institution of Civil Engineers held in May. Butterworths, London.

American Society of Civil Engineers, 1962, "Cement Grouting," Progress Report of the Task Committee on Cement Grouting, Journal of the Soil Mechanics and Foundation Division, Paper 3098, Vol. 88, No. SM2, pp. 49-98.

Anonymous, 1978, Bibliography on Grouting, Miscellaneous Paper C-78-8, Technical Information Center and Concrete Laboratory, U.S. Army Engineer Waterways Experiment Station, Vicksburg, MS.

Baker, W.H., editor, 1982, Grouting in Geotechnical Engineering, Proceedings of the Conference, New Orleans, February 10-12, published by the American Society of Civil Engineers, New York.

Baker, W.H., editor, 1985, Issues in Dam Grouting, Proceedings of the session sponsored by the Geotechnical Engineering Division of the American Society of Civil Engineers in Conjunction with the ASCE Convention in Denver, Colorado, April 30, 1985, published by the American Society of Civil Engineers, New York.

Bowen, R., 1975, Grouting in Engineering Practice, Applied Science Publishers Ltd, London.

Bowen, R., 1981, Grouting in Engineering Practice, Second Edition, Applied Science Publishers Ltd, London.

Committee on Grouting of the Geotechnical Engineering Division, 1980, "Preliminary Glossary of Terms Relating to Grouting," Paper 15581, pp. 803-815, Journal of the Geotechnical Engineering Division, Proceedings of the American Society of Civil Engineers, Vol. 106, No. GT7, July.

Ewert, F.-K., 1985, Rock Grouting with Emphasis on Dam Sites, Springer-Verlag, Berlin.

International Commission on Large Dams, 1985, Transactions, Fifteenth International Congress on Large Dams, Lausanne, Switzerland, June, Vol. 3, Question 58: Foundation treatment for control of seepage. ICOLD, Paris.

U.S. Grout Corporation, 1983, Grouting Handbook, Second Edition, Fairfield, Connecticut.

Wallner, M., 1976, Propagation of Sedimentation Stable Cement Pastes in Jointed Rock, English edition of Volume 2, pp. 49-165, Publications of the Institute for Foundation Engineering, Soil Mechanics, Rock Mechanics and Water Ways Construction, RWTH (University), Aachen, FRG, Germany.

Water Resources Commission, N.S.W. Australia, 1981, Grouting Manual, Fourth Edition, 624.159.4G/WAT/16.

Welsh, J.P., editor, 1984, Innovative Cement Grouting, Publication SP-83, American Concrete Institute, Detroit.

Weyermann, W.J., 1977, Rock Conditions Improved Through Pressure Grouting, A Publication of Rodio, Zurich.

NRC FORM 335 (7.77)

U.S. NUCLEAR REGULATORY COMMISSION

BIBLIOGRAPHIC DATA SHEET

1. REPORT NUMBER (Assigned by DDC)
NUREG/CR-4541

4. TITLE AND SUBTITLE (Add Volume No., if appropriate)
Experimental Assessment of the Sealing Effectiveness of Rock Fracture Grouting

2. (Leave blank)

3. RECIPIENT'S ACCESSION NO

7. AUTHOR(S)
A. Schaffer and J.J.K. Daemen

5. DATE REPORT COMPLETED
MONTH December YEAR 1986

9. PERFORMING ORGANIZATION NAME AND MAILING ADDRESS (Include Zip Code)
Department of Mining and Geological Engineering
University of Arizona
Tucson, AZ 85721

DATE REPORT ISSUED
MONTH March YEAR 1987

6. (Leave blank)

8. (Leave blank)

12. SPONSORING ORGANIZATION NAME AND MAILING ADDRESS (Include Zip Code)
Division of Engineering Safety
Office of Nuclear Regulatory Research
U.S. Nuclear Regulatory Commission
Washington, DC 20555

10. PROJECT/TASK/WORK UNIT NO

11. CONTRACT NO
NRC-04-78-271
FIN B6627

13. TYPE OF REPORT
Technical Report

PERIOD COVERED (Inclusive dates)
1983 - 1985

15. SUPPLEMENTARY NOTES

14. (Leave blank)

16. ABSTRACT (200 words or less)

The objective of this investigation is to determine the effectiveness of cement grouts as sealants of fractures in rock. Laboratory experiments have been conducted on seven 15-cm granite cubes containing saw cuts, three 23-cm diameter andesite cores containing induced tension cracks, and one 15-cm diameter marble core containing a natural fracture. Prior to grouting, the hydraulic conductivity of the fractures is determined under a range of normal stresses, applied in the loading and unloading cycles, from 0 to 14 MPa (2000 psi). Grout is injected through an axial borehole, at a pressure of 1.2 to 8.3 MPa (180 to 1200 psi), pressure selected to provide a likely groutable fracture aperture, while the fracture is stressed at a constant normal stress. The fracture permeability is measured after grouting. Flow tests on the ungrouted samples confirm the inverse relation between normal stress and fracture permeability. The equivalent aperture determined by these tests is a reliable indicator of groutability. Post-grouting permeability measurements as performed here, and frequently in practice, can be misleading, since incomplete grouting of fractures can result in major apparent reductions in permeability. The apparent permeability reduction is caused by grouting of a small area of a highly preferential flowpath directly adjacent to the hole used for grouting and for permeability testing. Experimental results confirm claims in the literature that ordinary portland cement inadequately penetrates fine fractures.

17. KEY WORDS AND DOCUMENT ANALYSIS

17a. DESCRIPTORS

Grouting
Cement grout
Grout testing
Fracture permeability
Fracture grouting
Repository sealing
Falling head test
Permeability test
Bleed test
Grouts
Grout bleeding

17b. IDENTIFIERS/OPEN-ENDED TERMS

18. AVAILABILITY STATEMENT
Unlimited

19. SECURITY CLASS (This report)
Unclassified

21. NO. OF PAGES

20. SECURITY CLASS (This page)
Unclassified

22. PRICE
$

NRC FORM 335 (7.77)

*U.S. GOVERNMENT PRINTING OFFICE: 1987-181-582:50006

BEST COPY AVAILABLE

179